NOVEL FORMULATIONS AND MECHANISTIC INSIGHTS INTO GASTRORESISTANT DOSAGE FORMS

João Alberto Cunha Barbosa

February 2020

A thesis submitted to the University of Huddersfield in partial fulfilment of the requirements for the degree of Doctor of Philosophy

The University of Huddersfield

COPYRIGHT STATEMENT

1. The author of this thesis (including any appendices and/or schedules to this thesis) owns any copyright in it (the “Copyright”) and he has given The University of Huddersfield the right to use such copyright for any administrative, promotional, educational and/or teaching purposes.

2. Copies of this thesis, either in full or in extracts, may be made only in accordance with the regulations of the University Library. Details of these regulations may be obtained from the Librarian. This page must form part of any such copies made.

3. The ownership of any patents, designs, trademarks and any and all other intellectual property rights except for the Copyright (the “Intellectual Property Rights”) and any reproductions of copyright works, for example graphs and tables (“Reproductions”), which may be described in this thesis, may not be owned by the author and may be owned by third parties. Such Intellectual Property Rights and Reproductions cannot and must not be made available for use without the prior written permission of the owner(s) of the relevant Intellectual Property Rights and/or Reproductions.

DECLARATION OF AUTHORSHIP

I, João Alberto Cunha Barbosa, declare that the work presented in this thesis entitled “Novel Formulations and Mechanistic Insights into Gastroresistant Dosage Forms”, is my own. I confirm that:

• This work was done wholly or mainly while in candidature for a research degree at this University.

• Where any part of this thesis has previously been submitted for a degree or any other qualification at this University or any other institution, this has been clearly stated.

• Where I have consulted the published work of others, this is always clearly attributed.

• Where I have quoted from the work of others, the source is always given. With the exception of such quotations, this thesis is entirely my own work.

• I have acknowledged all main sources of help.

• Where the thesis is based on work done by myself jointly with others, I have made clear exactly what was done by others and what I have contributed myself.

Signed:

Date: 20.02.2020

PUBLICATIONS ARISING FROM THIS WORK

Sections of this thesis have already been published in the following articles:

Barbosa, J. A. C., Conway, B. R., & Merchant, H. A. (2017). Going Natural: Using polymers from nature for gastroresistant applications. *British Journal of Pharmacy*, *2*(1), 14–30. https://doi.org/10.5920/bjpharm.2017.01

Barbosa, J. A. C., Abdelsadig, M. S. E., Conway, B. R., & Merchant, H. A. (2019). Using zeta potential to study the ionisation behaviour of polymers employed in modified-release dosage forms and estimating their pKa. *International Journal of Pharmaceutics: X*, *1*, 100024. https://doi.org/10.1016/j.ijpx.2019.100024

Barbosa, J. A. C., Al-Kauraishi, M. M., Smith, A. M., Conway, B. R., & Merchant, H. A. (2019). Achieving gastroresistance without coating: Formulation of capsule shells from enteric polymers. *European Journal of Pharmaceutics and Biopharmaceutics*, *144*, 174–179. https://doi.org/10.1016/j.ejpb.2019.09.015

Additionally, following manuscript is also under preparation at the time of this thesis submission, which includes the work described in Chapter 4:

Barbosa, J. A. C., Abdelsadig, M. S. E., Ghori, M. U., Conway, B. R., & Merchant, H. A. (2020). A mechanistic insight into ionisation and dissolution of commonly used hypromellose polymers in formulating gastroresistant dosage forms.

ACKNOWLEDGMENTS

First of all, I would like to thank my supervisor, Dr. Hamid Merchant, for having accepted me as his student. As his first PhD student I feel this has been a new and enriching experience for the both of us. It was a true roller-coaster but, in the end, a true success. Thank you for allowing me this spectacular "ride". I also want to truly thank Prof. Barbara Conway for all her support and motivation during the darkest periods of this journey. Also, a word of appreciation to Dr. Alan Smith, whom was always available to help and provide me with the best advice for my work. A special thank you for Hayley and Jack, the two technicians who were always there to help us. At last, an appreciation to Prof. Abdul Basit, from University College London, whom has so kindly welcomed me in his lab, greatly contributing to my PhD experience. Thank you for all your help and your kind conversations.

I want to thank all my colleagues and friends who in a way or another, contributed to my journey as a PhD student. Firstly, Suhail, my day one desk/lab mate who became a great friend, always there for the good and the bad. Thank you for all the lifts, all the gym sessions, all the lunches, all the complaining, all the celebrations! To Alessandro, my friend/housemate, thank you for always being the most enthusiastic of us, for the good and for the bad! Thank you for all the laughter, and essentially thank you for with me inventing the best steak sauce ever!! To all my office mates, a great thank you for all the tea breaks, the nonsense chatting, the listening; You are too many to enumerate, but I will remember all of you. A special word to Claire, for always being the cheeriest among us, always there for a chat, always offering lifts, always cheering us up. It was great to have met you and your family! Finally, a word for Malaz. the MSc student who grew to become a great scientist and do a great PhD. It was a pleasure to watch you grow, although sometimes somewhat strangely! haha Thank you for all the help, all the talks, the discussions! You also made me a better scientist and person. I am truly grateful to you.

To Marina and Dulce, the only other Tugas I knew for a while. Obrigado meninas por tudo: os risos, os desabafos, os cafés, as tainadas! Vocês foram um cantinho de Casa, em Huddersfield. Also, a word to Rita and Simão, who later joined the group. Obrigado a ambos pela companhia, pelos momentos de conversa, pelos serões, pela risota! Simão, obrigado especialmente por seres um labrego-nerd, sabe tão bem poder ser estupido e nos compreenderem! To Diana, who was not in Huddersfield, but who listened time and time again to my complaints throughout this PhD. Thank you for still being a friend!

A word for everyone back home – in Portugal. To all my friends, who had to watch me go back to the UK countless times, to whom I had to say "no" so many times. Obrigado Ursos, e desculpem-me a ausência. To my parents and my sister, thank you for all your unconditional support! I am sorry for being away for so long.

Lastly, an indefinable thank you to Filipa! Tão rápido te tornaste a minha âncora enquanto estava longe. Obrigado por todos os momentos racionais quando eu panicava, pelos mimos enquanto eu escrevia, por estares aqui comigo, por seres e ajudares a criar a nossa Casa. You are truly my Mew. (Thank you also to Chinchy, for being our special cat-dog and especially for keeping me company during long nights.)

"...Journey before Destination."

Code of the Knights Radiant – The Stormlight Archive

"To love the journey is to accept no such end.
I have found, through painful experience,
that the most important step a person can take
is always the next one."

Dalinar Kholin – in Oathbringer, The Stormlight Archive

ABSTRACT

The oral route is still the preferred route for the administration of active substances, being drugs, nutraceuticals or food supplements. Capsules are the simplest oral dosage forms, allowing the administration of different substances without the need of extensive formulation development. Nevertheless, an additional coating step is normally necessary to provide gastroresistance to solid dosage forms, which means added materials, equipment, time and consequently, costs. This thesis shows the successful development of enteric hard capsules which do not require additional enteric coating and subsequent mechanistic insights into polymer dissolution. The produced capsules are fabricated using gastroresistant polymers, guaranteeing their efficacy in bypassing the stomach without disintegration. The *in-vitro* success of these capsules may however not warrant *in-vivo* efficacy. This occurs due to the clear differences between the commonly used *in-vitro* dissolution media and the gastrointestinal fluids. During this thesis the mechanics of enteric polymer dissolution was studied, alongside their ionisation proprieties and the effect of different buffers in their dissolution. The pK_a of synthetic and natural polymers was estimated using a novel application of electrophoretic light scattering technique, through the study of zeta potential. Both the type and the number of functional groups have shown to impact the estimated pK_a, with phthalyl showing opposite effects to succinoyl groups on polymer dissolution pH and pK_a. A new technique was developed for the quantification of HPMC-based polymers, adapted from the conventional phenol-sulfuric acid assay for carbohydrates. Using this technique, the dissolution rate of enteric polymers was measured in compendial phosphate and physiological bicarbonate buffers with varying buffer capacities. The microenvironmental pH of the dissolving polymers was also measured on the surface of the dissolving films using the same buffers. A link was observed between buffer capacity, buffer type and polymer dissolution rate, hinting at possible reasons for the observed poor *in-vitro/in-vivo* correlation. The wettability of enteric polymeric films was also studied using contact angle kinetics under different dissolution media, tracking contact angle, drop volume and basal area over a period of time. Ultimately, the data from polymer dissolution rate, microenvironmental pH, ionisation, pK_a and wettability were correlated to better understand the mechanics of enteric polymer dissolution under *in-vitro* physiological conditions.

Keywords: *Enteric; Capsules; Zeta potential; pK_a; Polymer dissolution rate; microenvironmental pH; buffer capacity; contact angle.*

TABLE OF CONTENTS

LIST OF FIGURES

LIST OF TABLES

LIST OF ABBREVIATIONS

A^-	Unprotonated weak acid
AS-HF	HPMC-AS HF
AS-LF	HPMC-AS LF
CAP	Cellulose acetate phthalate
DpHT	Dissolution pH threshold
ELS	Electrophoretic Light Scattering
EP	European Pharmacopoeia
EUD L100	EUDRAGIT® L100
EUD S100	EUDRAGIT® S100
FaSSGF	Fasted State Simulated Gastric Fluid
FaSSIF	Fasted State Simulated Intestinal Fluid
FDA	Food and Drug Administration
FeSSGF	Fed State Simulated Gastric Fluid
FeSSIF	Fed State Simulated Intestinal Fluid
G'	Storage modulus
G''	Loss modulus
GI	Gastrointestinal
HA	Weak acid
HP-50	HPMC-P 50
HP-55	HPMC-P 55
HPMC	Hydroxypropyl methylcellulose
HPMC-AS	HPMC acetate succinate
HPMC-P	HPMC phthalate
IVIVC	*In-vitro/In-vivo* correlation
LOD	Limit of detection
LOQ	Limit of quantification
pH_m	Microenvironmental pH
PVAP	Polyvinyl acetate phthalate
SGF	Simulated Gastric Fluid
SLS	Sodium lauryl sulphate
TEC	Triacetyl citrate
USP	United States Pharmacopoeia
$Zeta_{max}$	Maximum zeta potential
$Zeta_{min}$	Minimum zeta potential
θ_0	Contact angle at first contact
θ_{30}	Contact angle after 30 seconds
β	Buffer capacity

Chapter 1

INTRODUCTION:
CURRENT STATE OF GASTRORESISTANT DOSAGE FORMS & FUTURE PROSPECTS

Parts of this chapter have been published as follows:

Barbosa, J. A. C., Conway, B. R., & Merchant, H. A. (2017). Going Natural: Using polymers from nature for gastroresistant applications. *British Journal of Pharmacy*, *2*(1), 14–30. https://doi.org/10.5920/bjpharm.2017.01

1.1. Capsules: a simpler formulation for *per os* administration

The bioavailability of an active ingredient is greatly dependent on the route by which it is administered. All administration routes offer advantages and disadvantages, however, from all the possibilities the oral route is still preferred over others, with over eighty percent of the 50 most-sold pharmaceutical products in the USA and Europe being administered *per os* (Lennernäs and Abrahamsson, 2005).

Capsules are one of the most common solid dosage forms employed for oral administration of active ingredients. With a global market valued at US$1.4bn in 2016 and an expected annual growth rate of 7.3%, the empty capsule market is predicted to worth roughly US$2.9bn in 2026 (Future Market Insights, 2016). Capsules are relatively simple to use compared to tablets which need more formulation development and take longer comparatively to capsules to manufacture and quality control. Hard capsules present a more convenient delivery system for pharmaceuticals and nutraceuticals, allowing for both liquid and powder form, without the need to develop a complex formulation. Also, for drugs undergoing animal or clinical trials, capsules are often employed due to their simplicity and quick formulation turnaround for early stages of drug development (Murachanian, 2010). Using capsules as dosage forms for preclinical studies in animals ensures that no time-consuming formulation development is needed, with the test substance being readily loaded and administered as a capsule. Bespoke capsules are also available for various species for use in pre-clinical studies. The availability of specialised dosing kits aids the administration of capsules directly to the stomach, or to the colon through rectum (Torpac®, 2016a). Additionally, capsules pose a great aid not just in pre-clinical studies, but also in animal health, with veterinary use of capsules being a growing market. In animals, capsules may be used to accurately and more conveniently dose a range of materials for animal health, ensuring the entirety of the dose is ingested by the animal. These may be administered orally, vaginally or post-partum intrauterinally to cattle, horses, sheep, goats, pigs and dogs (Torpac®, 2016b).

Hard capsules can be manufactured in different sizes and materials, depending on their purpose and encapsulated material (Figure 1.1). Even though other materials are used, the large majority of capsules are still produced using gelatine (type A, type B) from the skin/bones of pigs, cows or

the fish bones (Murachanian, 2010). Other materials were also developed to meet the demand for non-animal-origin capsules which would address a growing need for Halal, Kosher and vegetarian/vegan markets (Future Market Insights, 2016). The most common alternatives currently used are hydroxypropyl methyl cellulose (HPMC), pullulan and starch-based capsules (Capsugel, 2019a; Qualicaps, 2019; Roxlor, 2019). Although these capsules produce a very good immediate release dosage form, they pose some limitations when intended for modified release applications, in particular gastroresistant formulations.

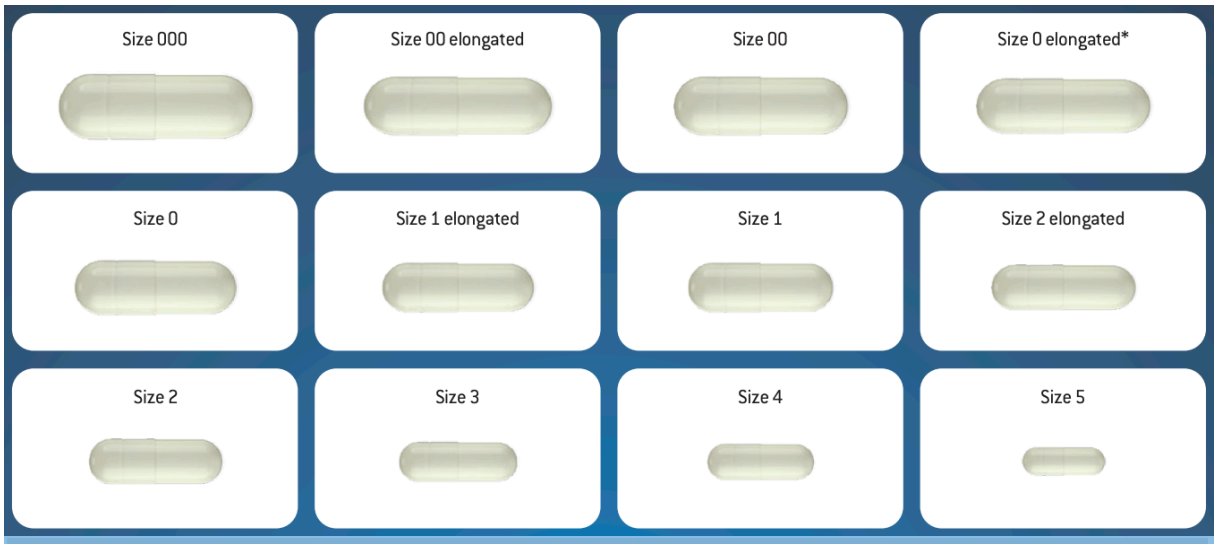

Size	000	00el	00	0el	0	1el	1	2el	2	3	4	5
Capsule volume (ml)	1.37	1.02	0.91	0.78	0.68	0.54	0.50	0.41	0.37	0.30	0.21	0.13
Powder tapped density	Capsule capacity (mg)											
0.6g/ml	822	612	546	468	408	324	300	246	222	180	126	78
0.8g/ml	1096	816	728	624	544	432	400	308	296	240	168	104
1.0g/ml	1370	1020	910	780	680	540	500	410	370	300	210	130
1.2g/ml	1644	1224	1092	936	816	648	600	492	444	360	252	156

Figure 1.1: Examples of capsule shapes and sizes, with corresponding volumes and powder capacities. Adapted from Murachanian (2010) *and Capsugel®* (2019).

1.1.1. Capsules as gastroresistant formulations

To protect acid sensitive substances from being degraded in the stomach, the pharmaceutical industry typically uses gastro resistant polymers to coat oral solid dosage forms. These coatings are composed of one or more polymers which behave as weak acids, being insoluble at low pH typically (pH 1–4), while dissolving once the pH of the media rises above 5.5 to 7, depending on the polymer used. The rationale behind the most common gastroresistant oral formulations is

therefore based on the pH changes occurring throughout the gastrointestinal (GI) tract, from the stomach to the colon. To resist the highly acidic pH of the stomach, a gastroresistant formulation has to be practically insoluble in these conditions, maintaining its integrity in stomach, yet soluble at intestinal pH to release the drug in proximal small intestine. The first attempt to create a gastroresistant formulation, exploiting the insolubility of materials in the stomach, is attributed to a German physician who reported clinical use of keratin coated carbolic acids pills in 1884 (Unna, 1884). After the first glimpse of a gastroresistant solid dosage form by Unna (1884), very distinct approaches have been designed aiming to provide gastric protection to oral formulations.

Typically, when a gastroresistant formulation is required, the most conventional and common practice is to coat the dosage forms such as tablets or pellets with gastro-resistant polymers. Several synthetic materials have been developed and used in the last decades for gastroresistant purposes, of particular importance are acrylic acid derivatives, cellulose derivatives (HPMC-P, HPMC-AS) and polyvinyl derivatives (PVAP), as being the most common (Cole et al., 2002). The most used examples of each category and their primary characteristics are summarised in Table 1.1.

In addition to their application in pharmaceutical industry, gastroresistant dosage forms are also sought after by the nutraceutical market, which is ever more demanding to include natural substances in the dosage form design. Hence, the industry-standard synthetic materials used to formulate gastroresistant pharmaceuticals cannot be used for nutraceutical applications, therefore creating an exceptional demand for the natural materials with gastroresistant proprieties. A critical review of various natural materials was performed during this project (Barbosa et al., 2017), and a summary is shown in Table 1.2.

Table 1.1: Summary table of the most commonly used commercially available synthetic enteric polymers.

Polymer	Brand name	Grade	DpHT	% ionisable groups	Particle size	M_w (g/mol)	Observations	Manufacturer/ supplier	Ref.
Acrylic acid derivatives				**Methacrylic acid**					
Methacrylic Acid - Ethyl Acrylate Copolymer (1:1)	EUDRAGIT®	L100-55	≥5.5	46.0 - 50.6	<0.25mm (95%)	320.000	All grades are available as dispersions: - L100-55 – 30% (w/w) aqueous dispersion; - L100 and S100 – 12.5% (w/w) in aqueous isopropyl alcohol, containing 3% (w/w) of water.	Evonik GmbH, Darmstadt, Germany	1
Methacrylic Acid - Methyl Methacrylate Copolymer (1:1)		L100	≥6.0	46.0 - 50.6	<0.25mm (95%)	125.000			2
Methacrylic Acid - Methyl Methacrylate Copolymer (1:2)		S100	≥7.0	27.6 - 30.7	<0.25mm (95%)	125.000			2
Cellulose derivatives				**Succinoyl**					
HPMC acetate succinate (HPMC-AS)	Aqoat®	LF / LG	≥5.5	14.0 – 18.0	5μm / 1mm	18.000	F (fine) grade is the micronized version of G (granule) grade. F grade can be used as aqueous dispersion in coating, G grade demands organic solvents	Shin-Etsu Chemical Co., Ltd., Chiyoda, Japan	3
		MF / MG	≥6.0	10.0 – 14.0	5μm / 1mm	18.000			3
		HF / HG	≥6.8	4.0 – 8.0	5μm / 1mm	18.000			3
				Phthalyl					
HPMC phthalate (HPMC-P)	HPMCP	HP-50	≥5.0	21.0 – 27.0	<800μm	78.000			4
		HP-55	≥5.5	27.0 – 35.0	<800μm	84.000			4
Cellulose acetate phthalate (CAP)	Aquacoat CPD	-	≥6.0	30.0–36.0%	0.2 μm			FMC Biopolymer, Flintshire, United Kingdom	5
Polyvinyl derivatives				**Phthalyl**					
Polyvinyl acetate phthalate (PVAP)	Phthalavin	-	≥5.0	55.0–62.0%	100–125 μm			Colorcon Ltd., Dartford Kent, United Kingdom	6

***DpHT**: dissolution pH threshold; **M_w**: Weight-average molecular weight;*
1: Evonik Industries (2018)*; 2: Evonik Industries* (2012)*; 3: Shin-Etsu Chemical Co.* (2018)*; 4: Shin-Etsu Chemical Co. (2002); 5: Smith, (2019); 6: Rajabi-siahboomi et al., (2018)*

Table 1.2: Summary of natural based products for gastroresistant applications.

Material	Product and formulation	Description	Ref
1. **CELLULOSE**			
Hydroxypropyl methylcellulose (HPMC)+ gellan gum	**DRCaps™** (Capsules)	Claimed to provide protection for acid sensitive ingredients using a delayed-release mechanism. Prone to significant inter- and intra-subject variability in gastric emptying affecting its effectiveness.	1
Ethylcellulose (EC) + sodium alginate (SA)	**Nutrateric ®** coated tablets	Comprises EC coating containing SA, which dissolves at intestinal pH and forms pores in the coating layer, enabling drug release. Although coated tablets remain intact in 0.1M HCl (pH≤1.2) for 2h, the coating is not robust to resist gastric conditions pH >2.0, possibly leading to premature drug release in the stomach.	2-4
2. **STARCH**			
Maize starch	**Eudraguard® Natural** coated tablets or pellets	Based on maize starch and claimed to provide taste-masking proprieties and acid-resistance. However, no further information is available on coating composition and on mechanisms of gastroresistance achieved using maize starch. It is not clear if this is also a delayed release approach, as in DRCaps™, or is a pH sensitive coating.	5,6
High amylose corn starch (HACS)	Coated glass beads	HACS is highly resilient to both gastric (0.1M, pH1.6, 2h) and neutral (pH 7.0. 0.1M phosphate buffer, 3h) conditions. However, it is shown to dissolve in a medium containing pancreatic amylases.	7
3. **SHELLAC**			
Shellac succinate	Cast films	Chemically modified shellac, where esterification with succinic anhydride and manipulation of annealing time allows the tailoring of the polymer's dissolution pH. However, due to chemical modification, it potentially loses its GRAS status.	8
Shellac + inulin	Coated tablets	Coating resisted 0.1M HCl for 2 h, yet drug release was initiated when in phosphate buffer pH 7.4. Shellac provides the enteric resistance, while inulin purports to retard the drug release until the formulation reaches the colon.	9
Shellac + sodium alginate	**Protect™ Enteric** coated tablets	Claimed to remain intact in 0.1M HCl for 2 h, while disintegrating at pH 6.8 (phosphate buffer). However, in a recent study[2], a slower release rate was observed after the acid stage when transferred to pH 6.8 phosphate buffer (< 50% release in 4 h) than in pH 7.4 phosphate buffer (80% release in 2 h).	2,10
4. **ZEIN**			
Zein + PEG-400 or glycerol	Coated tablets	While both organic and aqueous solutions resisted 2h at pH=1.2 for 2h, different lag times for drug release were observed when tested in pH 6.8 phosphate buffer. PEG-400 and glycerol were shown to influence the drug release, with PEG 400 formulation having a lower water uptake than glycerol, thus causing a more delayed onset of release.	11
Carboxymethyl zein	Tablet matrix	Authors claim that with carboxymethyl modification, zein becomes soluble at pH 4.5, thus, dissolving at the pH of the small intestine, yet being resistant to fasted gastric pH. However, due to chemical modification it potentially loses its GRAS status.	12

1: (Marzorati et al., 2015), 2:(Czarnocka and Alhnan, 2015); 3: (Ali-Merchant et al., 2009); 4: (Young et al., 2006); 5: (Evonik Industries AG, 2018); 6: (Kuntz, 2016); 7: (Dimantov et al., 2004); 8: (Limmatvapirat et al., 2008); 9: (Ravi et al., 2008); 10: (Young and Fraser, 2010); 11: (Li et al., 2010); 12: (Yin et al., 2015). **Note**: This table has already been publised in (Barbosa et al., 2017).

Cole et al., (2002) have coated HPMC based capsules with EUDRAGIT L 30 D-55. HPMC capsules were used instead of gelatine ones to tackle the embrittlement of the shell and of poor coating adhesion due to the gelatine smooth surface. These coated capsules resisted the acid challenge test and released their contents (>85% released) in pH 6.8 0.05M phosphate buffer within 1.5h of media change. These capsules were then tested *in-vivo* and their path was followed in 8 healthy individuals using gamma scintigraphy. Results showed that capsules completely disintegrated after 2.4 ± 0.9h, releasing their contents in the small intestine. Although many attempts are reported in the literature to coat hard capsules to enable gastroresistance (Cerea et al., 2008; Cole et al., 2002; Mahdi, 2015; Meghal et al., 2011; Reix et al., 2012) , this is yet not a common industrial practice (Cerea et al., 2008). This is because, the additional coating step poses as a time- and resource intense addition, hence increases the manufacturing costs. In addition, the quality costs also increase due to critical control on the coating parameters required to ensure consistency of the coating without compromising the integrity of the capsule shell. The smooth surface of gelatine capsules leads to poor adhesion of the polymeric coat, moreover the coating process often leads to increased brittleness of the capsules shells (Cole et al., 2002; Meghal et al., 2011). A more common approach is to fill enteric-coated (gastroresistant) granules or pellets into conventional hard gelatine capsule (Murachanian, 2010). The additional step of formulating polymeric coated granules or pellets is popular due to its advantages in gastric emptying over monolithic dosage forms and ability to tailor the drug release by using a combination of granules/pellets with varying coating thickness. Despite its advantages, this approach does not offer a flexible and cost-effective alternative to enteric coating. Therefore, if capsule shells can be formulated with built-in gastroresistance, they can be produced in bulk in a similar way to the standard capsules. These can then be supplied to pharmaceutical industries to be filled on standard high-speed capsule filing lines.

Cerea et al., (2008) have reported a dry-coating method for gelatine capsules to overcome the problems of classic wet coating technique to protect the capsule. Dry coating briefly consists on the spraying of the polymer in powder form simultaneously with a plasticiser, instead of the conventional spraying of a solution or dispersion containing the polymer and other excipients. The HPMC-AS dry-coated gelatine capsules exhibited no drug release until 2h in 0.1M HCl, followed

by complete release in 30 min on transfer to pH 6.8 phosphate buffer. The main drawback of this technique was the need of extremely high coating levels (22mg/cm^2) to prevent premature release in acid. The authors claim that the higher coating level was needed due to the less efficient curing process of the polymer under the dry-coating approach. A higher coating thickness was also reported by Mahdi (2015), who used EUD L100 to coat gelatine capsules. However, this involved a dip-coating method, which consists of repeated dipping and drying cycles. Although a different methodology was used to coat the capsules, a weight gain of 25% was still needed to completely warrant gastroresistance. Numerous other works employing both dip coating and spray coating methods reported the need for increased coating thicknesses when gelatine capsules were used (Meghal et al., 2011; Oliveira et al., 2013; Reix et al., 2012), which makes this approach more time and resource intensive.

In addition to the issues concerning overcoating capsule shells being an additional step, the approach also requires capsule to be prefilled with product before coating can take place. This poses another limitation in the use of these capsules and would require all companies to have the coating capabilities. If ready-made enteric capsules can be supplied to the industry, this would significantly reduce the costs of producing enteric hard capsules. Moreover, the capsules with built-in gastroresistance will have wider applications in controlling drug release and gastrointestinal targeting (both in human as well as in veterinary applications) as it would allow encapsulation of almost any drug or nutraceutical substance into empty shells, and allow their immediate use for R&D purposes, preclinical or clinical evaluations without extensive formulation development with potential reductions on the research and development cost.

1.1.2. Truly enteric hard capsules: the "pièce de résistance" for enteric formulations

Previous attempts to produce enteric hard capsules have been reported, however these either rely on an additional coating step, as referred above, or in the incorporation of a gum which would provide protection to acid-sensitive ingredients by a delayed-release mechanism, such as DRCaps™ (Marzorati et al., 2015; Smith et al., 2010). DRCaps™ do not exhibit a pH triggered release and instead rely on a time-delay in anticipation of timely emptying from stomach. Here the first problem lays regarding these formulations: the variability in gastric emptying times. Studies

have shown a very high intra- and inter-individual variability in gastric emptying times (Brophy et al., 1986; Davis et al., 1984; McConnell et al., 2008; Varum et al., 2010; Ziessman et al., 2009). Brophy et al., (1986) has shown that gastric emptying time of solid substances greatly varies not only between individuals, but also within the same individual (Figure 1.2A). Additionally, McConnel et al., (2008) demonstrated how gastric emptying times may be influenced by the ingestion of food increasing it to up to 5h (Figure 1.2B). Abrahamsson and colleagues also have shown that the gastric emptying greatly differs when there is a constant intake of food throughout the day, with gastric emptying times increasing up to more than 15h (Abrahamsson et al., 1996). This high variability creates an uncertainty in gastric emptying, which directly affects the efficacy of these products.

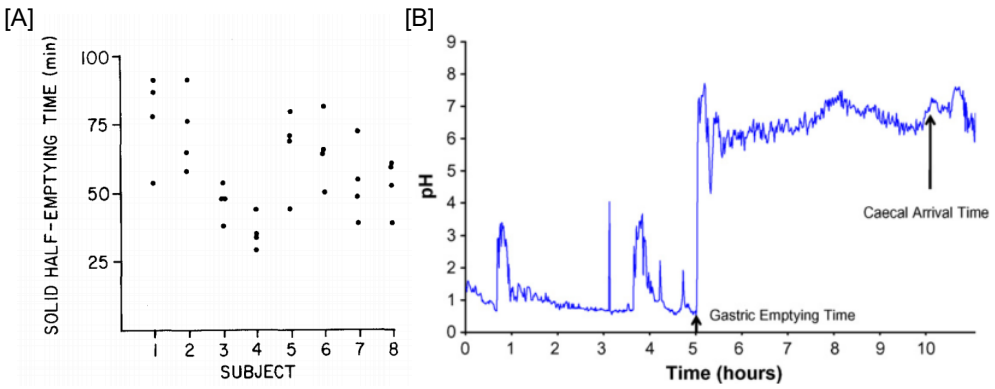

Figure 1.2: Variability of gastric emptying time. A: Gastric emptying time from 8 different subjects measured at different times (from (Brophy et al., 1986)*. B: pH profile from one subject using the Bravo® pH capsule given 30min before food and a standard lunch was administered at 4h. From McConnell et al. (2008).*

EnteriCaps® is a recent example of commercially available HPMC based gastroresistant capsules (Fagron, 2019). Although limited information is available regarding their constitution and the type of HPMC used, it is mentioned that capsule shells contain a gelling agent in addition to the HPMC, which may swell in acidic environment and can cause premature drug release. Despite the strong gastroresistance claims, the capsule exhibited nearly 15% drug release in gastric stage indicating poor gastroprotection.

The development of an enteric capsule should then be based on the intrinsic gastroresistance of its material, and not based on a delayed release. A more successful and realistic attempt to produce enteric capsules without the need for a coating was reported by Mehuys et al., (2005) using hot-melt extrusion. The authors produced HPMC AS-LG and PVAP capsules by extruding

the polymer mixed with a plasticiser into hollow cylinders, with metal inserts in the cylindrical die regulating the capsule thickness (Figure 1.3).

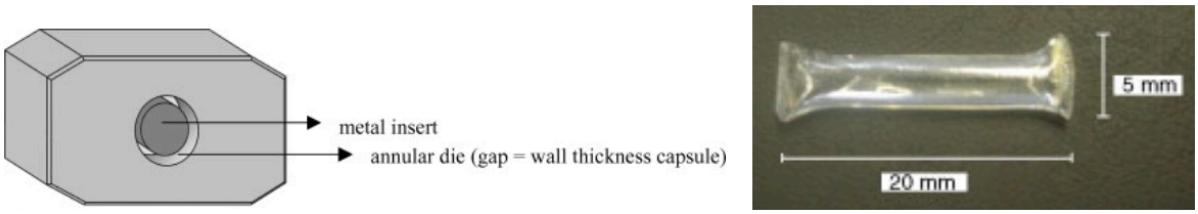

Figure 1.3: Schematic drawing of the die used for the extrusion of the capsules (left) and the resulting hot-melt extruded capsule. Reproduced with permission from Mehuys et al., (2005).

The extruded cylinders were then cut into 20mm pieces, which were filled with a model drug. Hot pincers were used to heat-seal the tubes, producing the capsules (Figure 1.3). These vehicles have proved to withstand the compendial acid test (2h, 0.1M HCl), showing a quick release when transferred to pH 6.8 phosphate buffer. It was noticed that the test was performed using a USP-III apparatus using 0.2M phosphate buffer which is much stronger than usual recommended 0.05 M phosphate buffer by the USP and this may explain the quick disintegration of the capsules in the buffer. The coating thickness was shown to influence the drug release, with increasing thickness causing longer lag times. This effect was more distinct with HPMC AS-LG capsules, with PVAP capsules showing similar lag times for 0.15-0.8 mm thick capsules, with only highly thick capsules showing significantly longer lag times (Figure 1.4). Again, the phosphate buffer used was much stronger than the compendial 0.05M which may cause inaccurate drug release profiles due to the excessive buffer capacity of this media, leading to drug releases occurring at earlier stages.

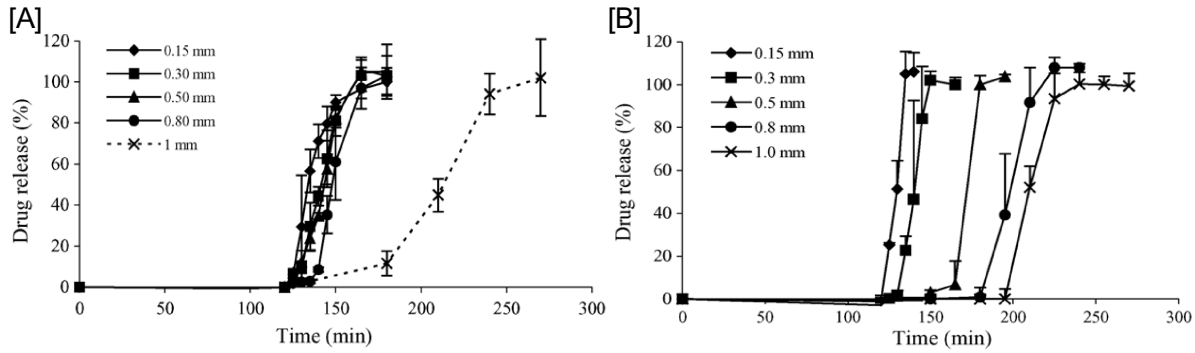

Figure 1.4: Drug release profiles of PVAP [A] and HPMC AS-LG [B] capsules with varying wall thickness after 2 h in 0.1M HCl and further transferred to 0.2M phosphate buffer pH 6.8. Adapted with permission from Mehuys et al., (2005)

Although this technology produced capsules with suitable gastroresistance, its industrial scale production is fairly limited. The production of these capsules would require very specialised equipment and hence will be costly. Moreover, the shape and appearance of these capsules renders them unsuitable for oral administration; the sharp edges due to heat seal will significantly affect the oesophageal safety and ability to swallow these dosage forms.

Very recently a new patent was made public with a new technique for dry coating of capsules (Zhu et al., 2019). Very briefly, this technique consists in the pre-heating of a capsule shell, spraying of the plasticiser immediately followed by the spraying of the coating powder, and then allow a curing time for film formation (Figure 1.5). This publication describes the successful use of EUDRAGIT L100-55 to form enterically coated capsules (with a coating level of 8.5%), indicating the possible application of this technique to produce enteric hard capsules. However, although an innovative technique, these coatings would have to be applied after capsule filling, creating the need of an added coating step and added industrial investment in equipment and method development. Nonetheless, this method also described the use of polymers used in extended release formulations, with release times up to 30h, showing its merit in tackling the issue of coating capsules.

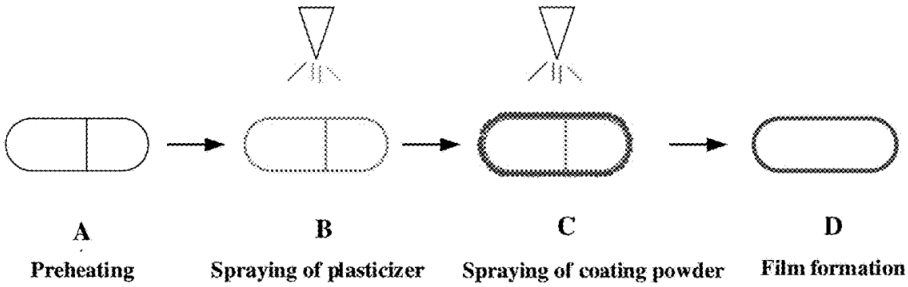

Figure 1.5: Schematic diagram of dry coating method. From Zhu et al., (2019).

Capsugel® and BioCaps have developed enTRinsic™ and Bio-VXR capsules respectively, both claiming to provide full enteric protection without the need for functional coatings (Benameur, 2015; BioCaps, 2019; Capsugel, 2019b). Capsugel® mentions the use of “pharmaceutical grades of cellulosic enteric derivatives (100%)”, however full composition is not disclosed. Evidence of clinical efficacy was shown using enTRinsic™ when compared to Nexium, an Esomeprazole commercial dosage form which uses gelatine capsules containing enterically coated pellets

(Benameur, 2015). In this study, the *in-vivo* performance of enTRinsic™ was validated, showing that the pharmacokinetic profiles of both formulations showed similar rates of drug absorption, peak time, elimination constant and half-life. BioCaps® also does not fully disclose the composition of their capsules, however the associated patent (Chang et al., 2015) mentions the use of a water-soluble polymer (pectin, propylene glycol alginate or xanthan gum), a water-soluble film forming polymer (gelatine, pullulan, polyvinyl alcohol, modified starch and/or cellulose ester), a gelling agent (gellan gum or carrageenan) and a coagulant (KCl, NaCl, $CaCl_2$, $MgCl_2$). These capsules are now commercially available, yet their clinical efficacy is not fully known.

In this thesis, an attempt has been made to design novel formulations of enteric hard capsules using various commercially available enteric polymers. Enteric hard capsules with built-in gastroresistance were successfully produced from EUDRAGIT (L100 and S100), HPMC AS-LF and HP-55 meeting the compendial tests for gastroresistant dosage forms. These are described in detail in Chapter 2.

1.2. Dissolution of enteric polymers: understanding the mechanics

Gastroresistant polymers rely on a pH-trigger to initiate their dissolution, instigated by the presence acidic functional groups, namely carboxylic acids. These groups, as any weak acid, possess an associated acidity constant (K_a) and a pK_a, which provides information regarding their pH-dependant ionisation. When in solution or suspension, the pH of the surrounding media will thus dictate the degree of ionisation of the polymer's acidic groups (HA). The Henderson-Hasselbalch equation (Equation 1.1) predicts that when $[A^-] = [HA]$, then $pH=pK_a$. At this stage, 50% of the acidic groups (A^-) will be deprotonated, and near complete ionisation will occur ~2 pH units above the pK_a (Figure 1.6). The pH dependant ionisation is also responsible for the pH dependant dissolution of these polymers (Figure 1.6).

$$pH = pK_a + \log\frac{[A^-]}{[HA]} \qquad \text{(Equation 1.1)}$$

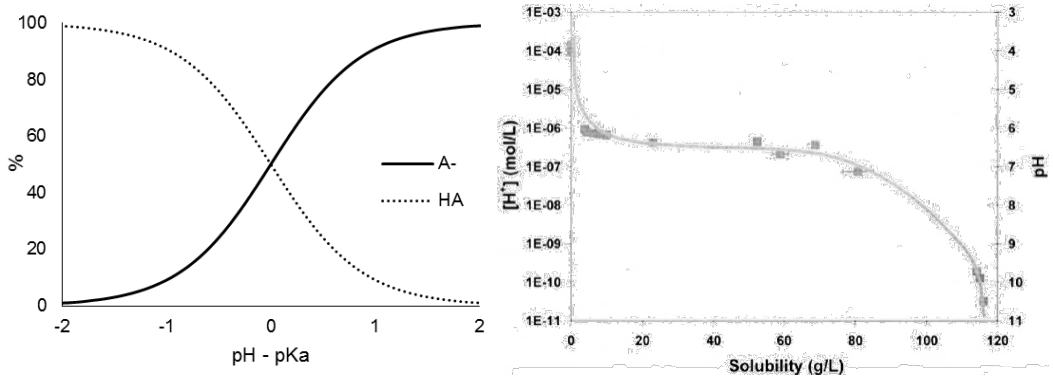

Figure 1.6: pH-dependant ionisation of a weak acid [HA] and its conjugated base [A-] based on the Henderson-Hasselbalch equation (left) and its correspondent effect on the solubility of the compound (right). Adapted from Nguyen and Fogler (2005).

This is explained by the intricate mechanics of the dissolution of the polymeric chains. Unlike non-polymeric materials, polymer dissolution is a multistep process where two different transport processes occur: solvent diffusion and chain disentanglement (Miller-Chou and Koenig, 2003). When a compatible solvent comes in contact with a polymer, it starts diffusing into the solid glassy surface of the polymeric material. This causes plasticization of the polymer, leading to the formation of a gel-like swollen layer, interfacing with the remaining polymer and with the solvent (Miller-Chou and Koenig, 2003). In the case of gastroresistant polymers bearing acidic functional groups, when in a medium with appropriate conditions leading to ionisation, a similar mechanism occurs, as shown by Nguyen and Fogler (2005). When the medium starts diffusing into the polymer, a gel layer is formed where acidic groups deprotonate and negative charges begin to accumulate (Figure 1.7). The resulting charges increase the repulsion between polymeric chains, which in addition to the plasticization by the solvent contributes to their disentanglement out of the gel layer and further dissolution into bulk solution. However, the deprotonation of the acidic groups causes an accumulation of the released H^+ ions at the boundary layer (Figure 1.7). At this stage, the accumulation of negative ions at the gel layer of the dissolving polymer (i.e. ionised acidic groups), leads to a potentially measurable charge on the surface of the dissolving polymer.

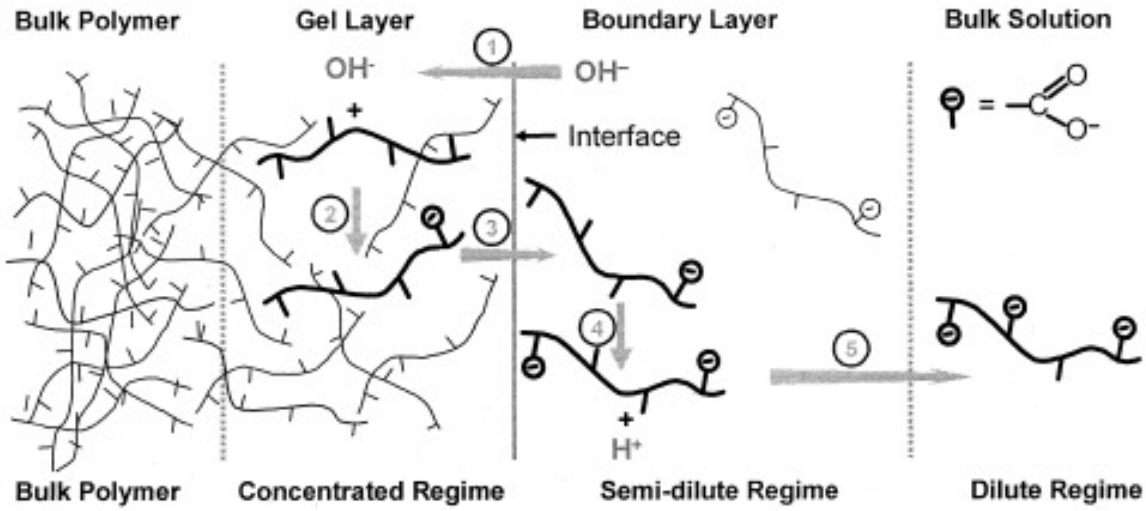

Figure 1.7: Representation of the dissolution of a polymer containing acidic functional groups. The encircled numbers represent (1) diffusion of water and hydroxyl ions into the polymer matrix to form a gel layer, (2) ionization of polymer chains in the gel layer, (3) disentanglement of polymer chains out of the gel layer to the polymer-solution interface, (4) further ionization of polymer chains at the polymer interface, (5) diffusion of disentangled polymer chains away from the interface toward the bulk solution (reproduced from Nguyen and Fogler (2005)).

During the dissolution of weakly acidic polymers the ionisation of the functional groups thus leads to the creation of negative charges on the surface of the polymer. Arising from the ionisation of their functional groups, these acquired charges may vary depending on the type and amount of group present in each polymer. Table 1.1 highlights some of the most commonly used enteric polymers, and also contains the differences between the functional groups present in each polymer. It is clear from the specifications of each polymer that the number and type of functional groups directly affects the dissolution pH threshold (DpHT) of the polymer, suggesting that these variables directly affect the dissolution of these polymers, and therefore of the carried active ingredient.

It is generally implied that polymers used in gastroresistant dosage forms targeted to the same area of the GI tract are interchangeable, provided that the drug release from these products in conventional buffers is similar. Enteric polymers may target different parts of the gut; however, several options exist for each area of actuation (Figure 1.8). Furthermore, each type of polymer possesses different functional groups, which may exhibit differences in their dissolution profiles. The pH dependent dissolution of these polymers generally relies on their ionisation behaviour in the luminal environment of the GI tract, and in-depth understanding can thus provide invaluable insights to understand how these polymeric materials behave in the different media.

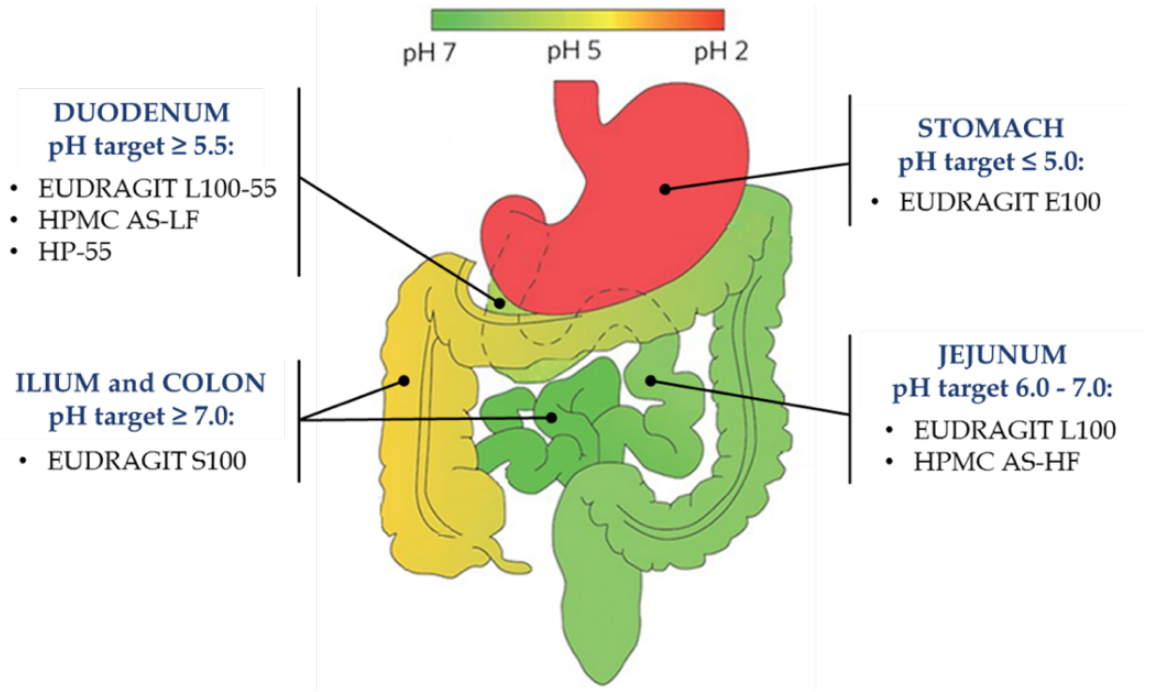

Figure 1.8: Schematic showing different polymers used for enteric and reverse enteric purposes, and their targets in the human gastrointestinal tract; Adapted from Khutoryanskiy (2015).

By studying the ionisation behaviour of these polymers over a range of pH, possible hints regarding their dissolution may be unveiled. In Chapter 3 a selection of enteric polymers was studied regarding their ionisation behaviour using a technique based on zeta potential, allowing further estimation of their pK_a values and comparison with published literature. Additionally, several natural polymers with pharmaceutical applications were investigated using the same technique.

1.3. *In-vivo* underperformance of enteric formulations: knowing the "why?"

Despite the promising results in *in-vitro* compendial dissolution tests, it is common for gastroresistant formulations to underperform *in-vivo* (Al-Gousous et al., 2019; Cole et al., 2002; Liu and Basit, 2010). This is due to unrealistic (non-physiological) conditions of dissolution media used in compendial methods (USP or EP), which are mainly for quality control testing in the industry and do not realistically mimic gastrointestinal fluids *in-vivo*.

For a substance to be absorbed and exert its effect, firstly it needs to become soluble in the medium where it is contained. Therefore, when administering a drug, it is of utmost importance to understand how and where it will dissolve in the GI tract with the composition and volume of GI fluids playing an essential role in the dissolution of active ingredients (McConnell et al., 2008). Particularly when referring to gastroresistant dosage forms, the polymeric coating is the first layer

between the drug and the dissolution medium. Therefore, its dissolution (or lack of) will directly influence the drug release. As explained in the previous section, the dissolution of enteric polymers is directly linked to the pH of the media, with acidic pH hindering the dissolution of the polymer. Nevertheless, polymer dissolution cannot simply be explained by the ionisation behaviour of these materials in media of different pH and the pH of the media is not solely responsible for the dissolution of the polymer. Spitael and Kinget (1977) have demonstrated this effect by reporting that the dissolution rate of EUD L100 in a pH 7.0 isotonic solution of sodium chloride was virtually zero, with the tested film not dissolving after 8h in this media. However, dissolution quickly occurred when phosphate buffer (66 mM) was used as the dissolution media. More recently, Nguyen and Fogler (2005) have shown that when in a medium without proton-carriers, the dissolution rate of both EUDRAGIT L100 and S100 was extremely low, even when tested at pH 9, which is well above the polymers DpHT. In the reported experiment, the presence of ammonia in the media (still at pH 9) greatly increased the dissolution rate of these polymers. Therefore, additionally to pH, proton-carriers also play an important role in polymer dissolution. Translating this to *in-vitro* release media, the buffering species present in solution would act as the proton-carriers, capable of accepting protons being generated from the ionisation of the polymeric chains, and carrying them away from the boundary layer, towards the bulk solution.

Thus, when testing the dissolution of a gastroresistant dosage form, the composition of the dissolving media should also be of great concern, not only its pH. It is clearly demonstrated that the dissolution rates of ionisable drugs and of enteric coated dosage forms (based on ionisation processes) are strongly influenced by the buffer capacity of the fluid and its composing species (Aunins et al., 1985; Nguyen and Fogler, 2005; Ozturk et al., 1988b; Ramtoola and Corrigan, 1989). Thus, it is imperative that the media used to simulate GI fluids are as similar as possible to the physiological ones, with the use of compendial phosphate buffers as mimicking media of the gut being a dramatic oversimplification as the ionic composition and the buffer capacity of this buffer is not remotely close to the one found in biological fluids in the intestine.

In addition to the effect of the buffer constitution and buffer capacity in the dissolution of ionisable drugs and enteric coatings, the surface tension also plays an important part due to its influence on

the wettability. This role is majorly played by pepsin in the stomach and by bile salts and phospholipids in the intestine (McConnell et al., 2008). In an attempt to consider these elements, more complex gastric and intestinal fluids were developed taking in consideration the differences of the fasted and fed state.

Initial attempts were made by Dressman (1998) and Galia (1998) to modify the pharmacopoeial fasted state simulated gastric fluids (SGF), by the addition of sodium lauryl sulphate (SLS) and Triton-X100 to decrease surface tension of the dissolution media. However both these modifications were later shown by Vertzoni et al.(2005) to overestimate gastric dissolution, who proposed a fasted state simulated gastric fluid (FaSSGF) containing pepsin and low amounts of bile salt (Sodium taurocholate) and lecithin (Table 1.3). This fluid is more similar to the constitution of fluids obtained from *in-vivo* samples than the SGF suggested by USP and the versions with synthetic surfactants (SLS and Triton) and shows better correlations to the physiological medium (Vertzoni et al., 2005).

Table 1.3: Composition and physicochemical properties of simulated gastric fluid (SGF_{SLS} and SGF_{Triton}) suggested by USP, the fasted state simulated gastric fluid (FaSSGF) and the in-vivo data of gastric contents in the fasted state. Adapted from (Vertzoni et al., 2005).

Composition	**SGF_{SLS}**	**SGF_{Triton}**	**FaSSGF**	***In-vivo*** **(fasted state)**
Sodium lauryl sulphate (%, w/v)	0.25	–	–	–
Triton-X100 (%, w/v)	–	0.1	–	–
Pepsin (mg/mL)	–	–	0.1	~ 0.8
Sodium taurocholate (µM)	–	–	80	~ 80
Lecithin (µM)	–	–	20	–
Sodium chloride (mM)	34.2	34.2	34.2	68 ± 29
Surface tension (mN/m)	33.7	32.0	42.6	41.0 ± 6.0
Osmolality (mOsmol/kg)	180.5 ± 3.6	157.7 ± 2.9	120.7 ± 2.5	191.0 ± 36
pH (adjusted with HCl)	1.2	1.2	1.6	1.4 ± 2.1

Regarding the fed state stomach, the ideal media should have similar physicochemical and nutritional proprieties of a meal and allow manipulations to simulate different stages of digestion and stomach secretions. Traditionally whole cow's milk (3.5% fat) has been used to formulate postprandial gastric media, due to its similarity in terms ratio of carbohydrate/fat/protein, pH (6.5–

6.6) and physicochemical properties to homogenized and undigested standard breakfasts (Klein et al., 2004).

Three media were developed by Jantratid and colleagues (Jantratid et al., 2008) to mimic different stages of food digestion in the stomach (Table 1.4). These media have the particularity of containing different proportions of UHT milk in their composition, mimicking the differences in the amount of protein and fat at different dissolution stages. The middle stage media was considered the default fed state simulated gastric fluid (FeSSGF), being suggested as the best option to globally simulate the fed state of the stomach. Although it cannot represent all meal types at all times of the postprandial phase, this is a broad representative of fed conditions in the stomach (Jantratid et al., 2008). An alternative to the use of UHT milk has been exploited, using a modified artificial liquid meal (Ensure® Plus with addition of 0.45% pectin), which has demonstrated to be more similar to the standard FDA breakfast (Klein, 2010).

Table 1.4: Composition and physicochemical properties of simulated gastric fluids considering different stages of the fed state, including the Fed State Simulated Gastric Fluid (FeSSGF). Adapted from (Jantratid et al., 2008).

Composition	**Early**	**Middle (FeSSGF)**	**Late**
Sodium chloride (mM)	148	237.02	122.6
Acetic acid (mM)	–	17.12	–
Sodium acetate (mM)	–	29.75	–
Ortho-phosphoric acid (mM)	–	–	5.5
Sodium dihydrogen phosphate (mM)	–	–	32
UHT-Milk/ Acetate Buffer	1:0	1:1	1:3
Osmolality (mOsmol/kg)	559	400	300
pH	6.4	5	3
Buffer capacity (mmol/L/ΔpH)	21.33	25	25

Concerning the intestinal phase, also fasted and fed simulated intestinal fluids were developed and improved (Dressman et al., 1998; Galia et al., 1998; Jantratid et al., 2008; Khoshakhlagh et al., 2015; Vertzoni et al., 2004).

Early in 1998, Dressman and co-workers firstly proposed a simulated intestinal fluid for both fasted (FaSSIF) and fed (FeSSIF) states (Dressman et al., 1998). Jantratid *et al.* (2008) later adjusted this medium due to the unrealistic quantities of bile salts and lecithin, and also replaced the

phosphate for maleate to obtain better correlation to the physiological fluid (FaSSIF-V2, vide Table 1.5). Bearing a pKa_2 of 6.27, maleate buffer is suitable for the required pH range of 5.4 to 6.5, allowing the inclusion in both fasted and fed state media (vide Table 1.5 and Table 1.6), yet maintaining the osmolality within physiological values (Jantratid et al., 2008). These changes were further validated by Söderlind and colleagues, who performed solubility studies in several neutral drugs including atovaquone, carbamazepine, cyclosporine, danazol, among others using the FaSSIF, FaSSIF-V2, pH 6.5 phosphate buffer and real human intestinal fluid (Söderlind et al., 2010).

Table 1.5: Composition and physicochemical properties of the first proposed fasted state simulated intestinal fluid (FaSSIF) and it's updated and more biosimilar version (FaSSIF–V2). Adapted from Jantratid et al. (2008) and Klein (2010).

Composition	**FaSSIF** (Dressman et al., 1998)	**FaSSIF–V2** (Jantratid et al., 2008)
Sodium taurocholate (mM)	3	3
Lecithin (mM)	0.75	0.2
Sodium dihydrogen phosphate (mM)	28.65	–
Maleic acid (mM)	–	19.12
Sodium Hydroxide (mM)	*q.s. ad* pH 6.5	34.8
Sodium Chloride (mM)	105.85	68.62
pH	6.5	6.5
Osmolality (mOsmol/kg)	~270	180 ± 10
Buffer capacity (mmol/L/ΔpH)	~12	10

Recently, a study by Khoshakhlagh and colleagues aimed to improve the FaSSIF medium by adding cholesterol in order to increase the similarities to the human intestinal fluid (Khoshakhlagh et al., 2015). The group prepared several media with different amounts of cholesterol aiming to mimic the differences in the bile fluids of male and female and also in cases of disease. The study showed improved solubility for the tested hydrophobic drugs, thus recommending the use of this media for *in-vitro* studies regarding these type of drugs in order to improve the IVIVC. For the development of fed state intestinal fluids, resembling the rationale for FeSSGF, the same group (Jantratid et al., 2008) developed three different fed state simulated intestinal fluids (FeSSIF), representing early, middle and late stages of the digestion process (Table 1.6).

However, such as for the gastric media, it is occasionally more practical to select a medium that is an overall representation of the intestine in postprandial situations. Unlike for the gastric media, a different "global" FeSSIF was developed (FeSSIF–V2), combining the postprandial changes in pH, buffer capacity, osmolality, bile components concentration and using physiologically relevant concentration of lipolysis products (Jantratid et al., 2008).

Table 1.6: Composition and physicochemical properties of simulated intestinal fluids considering different stages of the fed state and a "global" representation of the intestinal fed state (FeSSIF–V2). Adapted from Jantratid et al. (2008).

Composition/medium	**Early FeSSIF**	**Middle FeSSIF**	**Late FeSSIF**	**FeSSIF–V2**
Sodium taurocholate (mM)	10	7.5	4.5	10
Lecithin (mM)	3	2	0.5	2
Glyceryl monooleate (mM)	6.5	5	1	5
Sodium oleate (mM)	40	30	0.8	0.8
Maleic acid (mM)	28.6	44	58.09	55.02
Sodium Hydroxide (mM)	52.5	65.3	72	81.65
Sodium Chloride (mM)	145.2	122.8	51	125.5
pH	6.5	5.8	5.4	5.8
Osmolality (mOsmol/kg)	400 ± 10	390 ± 10	240 ± 10	390 ± 10
Buffer capacity (mmol/L/ΔpH)	25	25	15	25

Despite the development of all these media, and the improvement of the buffers by replacing phosphate by maleate, the intestinal fluids do not contain this buffer species, with the main buffering specie being bicarbonate (Liu et al., 2011). As an attempt to create a more biorelevant buffer, Liu and colleagues have developed a variation of the commonly used Hanks Buffer (*m*Hanks buffer), which almost perfectly mimics the jejunal fluid, in terms of composition and concentration, and also in terms of buffer capacity (Table 1.7). However, bicarbonate buffers are highly unstable, with the evaporation of CO_2 leading to the continuous increase in the pH. Therefore, an apparatus was designed to control and maintain the pH of bicarbonate buffers during dissolution tests (Merchant et al., 2013). Figure 1.9 shows the apparatus developed to automatically monitor and control the pH of bicarbonate buffers by actively sparging CO_2 into the dissolution media, allowing the stability of the buffer throughout dissolution tests.

Table 1.7: Comparison of the ionic composition (mM) and buffer capacity of jejunal fluid and phosphate and mHanks media. Reproduced with permissions from Liu et al., (2011).

Composition	Human jejunal fluid	Phosphate buffer (0.05M, pH 6.8)	*m*Hanks buffer (pH 6.8)
Bicarbonate	7.1	Not present	4.17
Phosphate	0.8	50	0.8
Potassium	5.1	50	5.8
Sodium	142	29	142
Chloride	131	Not present	143
Calcium	0.5	Not present	1.3
Magnesium	Not present	Not present	0.8
Buffer capacity (mmol/L/ΔpH)	3.2	23.1 ± 0.3	3.1 ± 0.2

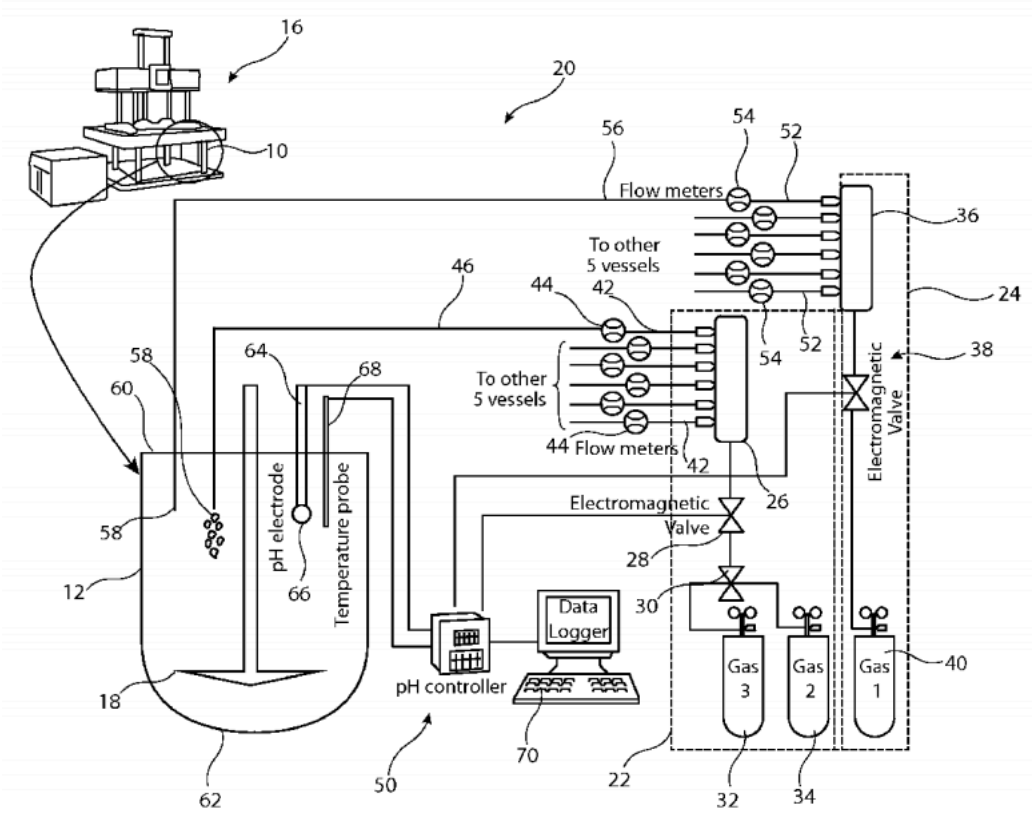

Figure 1.9: Auto pH™ system, an apparatus for dissolution testing of solid dosage forms, includes a chamber (12) for holding a solvent medium (18), in the preferred embodiment a bicarbonate based buffer system. The apparatus also includes a pH probe (66) which is connectable to a supply of carbon dioxide (32, 34), as well as to a supply of helium (40), the supplies being controlled by a control unit (50). The control unit (50) monitors changes in pH of the solvent medium (18) and feeds pH increasing or pH reducing gas from the supplies (32, 34, 40) into the chamber (12). The control unit (50) is able to maintain a uniform pH during testing or to provide a dynamically adjustable pH during testing, Adapted from Merchant et al., (2013).

To show the importance of the use of a proper dissolution medium to assess the dissolution of enteric coated products, Liu and colleagues performed dissolution studies on prednisolone coated tablets (Liu et al., 2011). These tablets were coated with different well-known enteric polymers and were tested using both phosphate and *m*Hanks buffers. Figure 1.10 noticeably shows the difference in using phosphate or bicarbonate buffer systems during the dissolution assay. When using phosphate buffer (Figure 1.10A), all coatings seem to start disintegrating shortly after being exposed to the medium, with a full release of the drug occurring before 90 min of exposure (210 min of dissolution test). However, the *m*Hanks buffer (Figure 1.10B) provides very distinct results. Using this buffer, the release onset occurs at least after 30 min of exposure (up to 60 min) with all coatings. Furthermore, significant differences in the release patterns can be observed with lower slopes observed for bicarbonate, representing a slower release of the drug, which indicates that the different buffers affect not only the onset of drug release, but also its release rate.

In Chapter 2 clear differences are shown in drug release from the produced enteric capsules in phosphate and bicarbonate buffers and Chapter 4 highlights the differences these two buffers exert in the dissolution rate of the tested enteric polymers.

The realization that the dissolution media explains why formulations perform poorly *in-vivo* despite successful *in-vitro* results answers only part of the enigma. More biorelevant dissolution media as the ones described may indeed help better predict the behaviour *in-vivo,* however it is necessary to comprehend what rules the dissolution of enteric polymers, how their pH dependent solubility is affected and what impacts their dissolution rate both *in-vitro* and *in-vivo.*

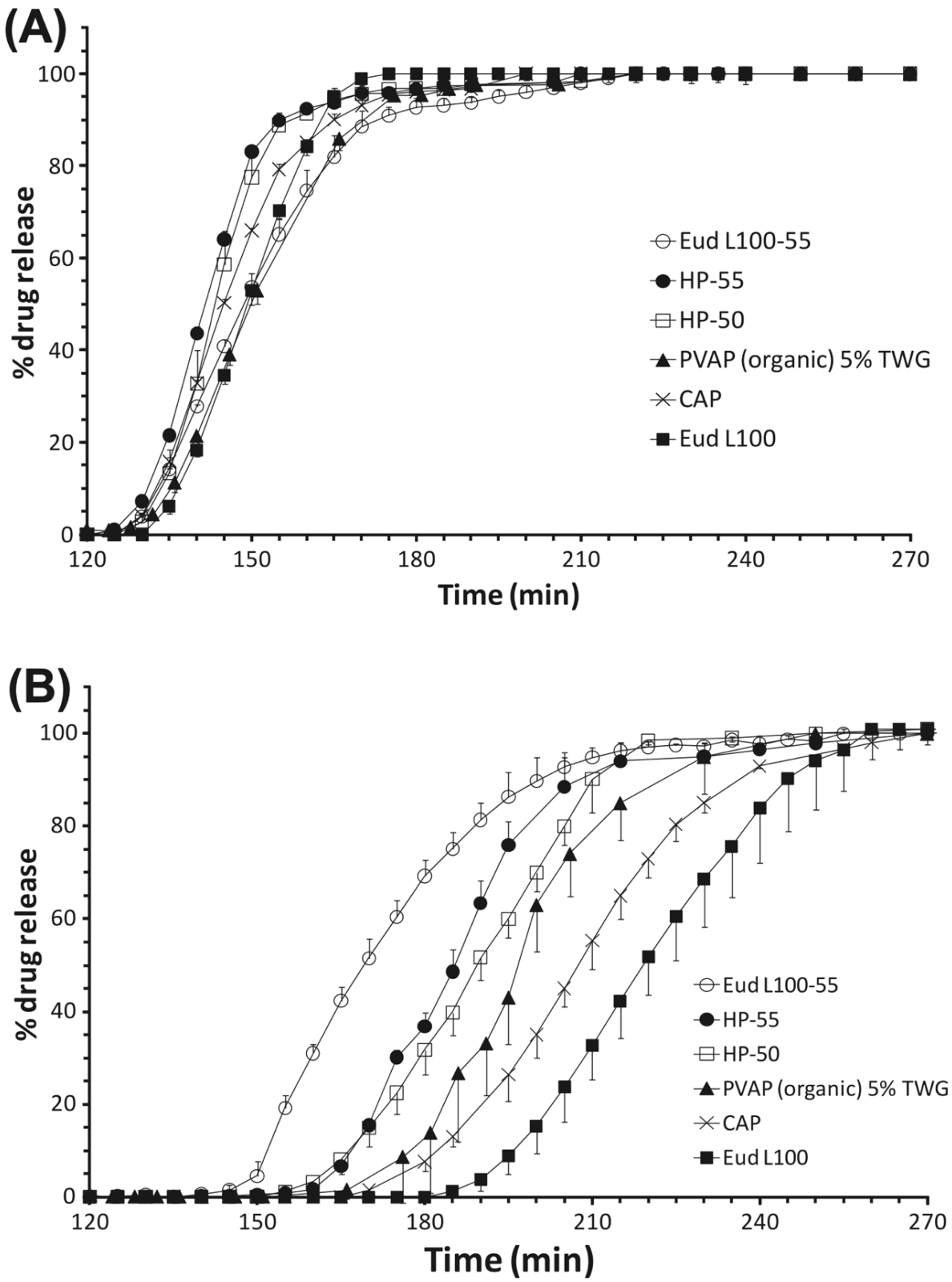

Figure 1.10: Drug release coated prednisolone tablets in 0.1M HCl for 2 h (data not shown) followed by pH 6.8 phosphate buffer (A) and mHanks bicarbonate buffer (B). Adapted from Liu et al., (2011).

1.3.1. Controlling the pH_m at the boundary layer: the ultimate regulator of dissolution

The microenvironmental pH (pH_m) is key for the dissolution of substances with pH-dependant solubility. The formation and manipulation of the microenvironment of different pH surrounding a dissolving substance has been exploited by different authors, aiming to improve or modulate drug dissolution in solid oral dosage forms (Doherty and York, 1989; Farag Badawy and Hussain, 2007; Siepe et al., 2006; Taniguchi et al., 2014; Tran et al., 2008).

Taniguchi and co-workers (2014) modulated the dissolution behaviour of various drugs by controlling the pH_m. Krieg and colleagues also refer the importance of this microenvironment, measuring the surface pH of dissolving drugs in media at different pH and buffer concentrations (Krieg et al., 2014). Later, Al-Gousous and co-workers (2019) deepened this understanding by showing that the buffer concentration greatly influences the pH_m, indicating that the pH and the concentration of the buffering species ultimately regulate the dissolution rates.

When referring to enteric polymers, which mainly rely on pH to initiate their dissolution, it is necessary to consider also the importance of both buffer type and buffer capacity in regulating dissolution. When in a medium with a pH higher than the polymer's dissolution pH threshold, ionisation of the acidic groups takes place, leading to the disentanglement of the polymer chains, and polymer dissolution. As previously mentioned, during early stages of dissolution, there is an influx of medium (containing water, hydroxyl ions and constituent salts) towards the polymeric matrix, which causes a gel layer to form due to ionisation of the polymer (Miller-Chou and Koenig, 2003). As the polymer ionises, protons are released and diffuse from the gel layer to the bulk solution. The layer between the gel layer and the bulk solution through which the generated protons diffuse is thus denominated "boundary layer". The continuous generation of H^+ ions caused by the ionisation of the polymer will eventually lead to their accumulation in this layer (Nguyen and Fogler, 2005), causing the lowering of the pH in this area. If the accumulation is extensive and the pH decreases enough to halt the ionisation (e.g. lowering near two pH units below pK_a), the dissolution of the polymer is dampened.

The accumulation of H^+ ions creates a microenvironment in this layer, where the pH is lower than the bulk pH. These H^+ are neutralised by the buffer species in solution, however the rate of this

neutralisation will depend on the buffer capacity of the medium. Therefore, the accumulation of H^+ ions in the diffusion layer, and consequently the pH_m will be highly dependent of the buffer capacity of the medium in which the polymer is dissolving (Figure 1.11). Therefore, the removal of the produced H^+ ions from this layer is key to the continuation of the dissolution process. This elimination occurs through buffering species present in the surrounding dissolution media. *In-vivo* this is occurring through naturally present buffering species in the intestinal fluid (bicarbonate and phosphate ions). When referring to *in-vitro* testing, the buffering species will vary according to the medium used (e.g. phosphate buffer, *m*Hanks buffer, Krebs buffer, FaSSIF, FeSSIF, etc.). Nevertheless, and more importantly, the rate at which the protons are removed from the boundary layer is directly related to the buffer capacity of the medium. The control of the pH_m should be discussed not in terms of the buffer concentration, as was done by Al-Gousous et al.,(2019), but the buffer capacity of the medium, which by providing sufficient buffering species in solution neutralises the H^+ ions being generated during polymer dissolution (Figure 1.11). Although buffer capacity is indeed proportional to the concentration of the buffer and most times is more convenient to mention buffer concentration values, it is the chemistry of each buffer species and its capacity to neutralise changes in pH that influences the dissolution of different materials, particularly ionisable substances (Sheng et al., 2009). Different buffering species with the same molarity may generate different buffer capacities, and consequently may exert distinctive control over the pH_m. Hence, buffer capacity should be addressed as the regulator of polymer dissolution.

The pH_m of dissolving enteric polymers has been mathematically modelled by Ozturk et al.,(1988a). Ozturk and colleagues proposed a mathematical model to describe the dissolution of enteric polymers and the release kinetics of weakly-acidic drugs from gastroresistant oral solid dosage forms. Later, the pH_m was not just modelled, but indeed detected and measured in enteric polymers by Harianawala et al.,(2002). Their method was based on a previously described idea for the detection of a microviscous layer formed during the dissolution of polyethylene glycol (Bogner et al., 1997), and was hypothesised that a similar region of higher viscosity could be detected on a dissolving enteric polymer (the gel layer), where protons would accumulate, leading to the possible measurement of the pH in this region (Harianawala et al., 2002).

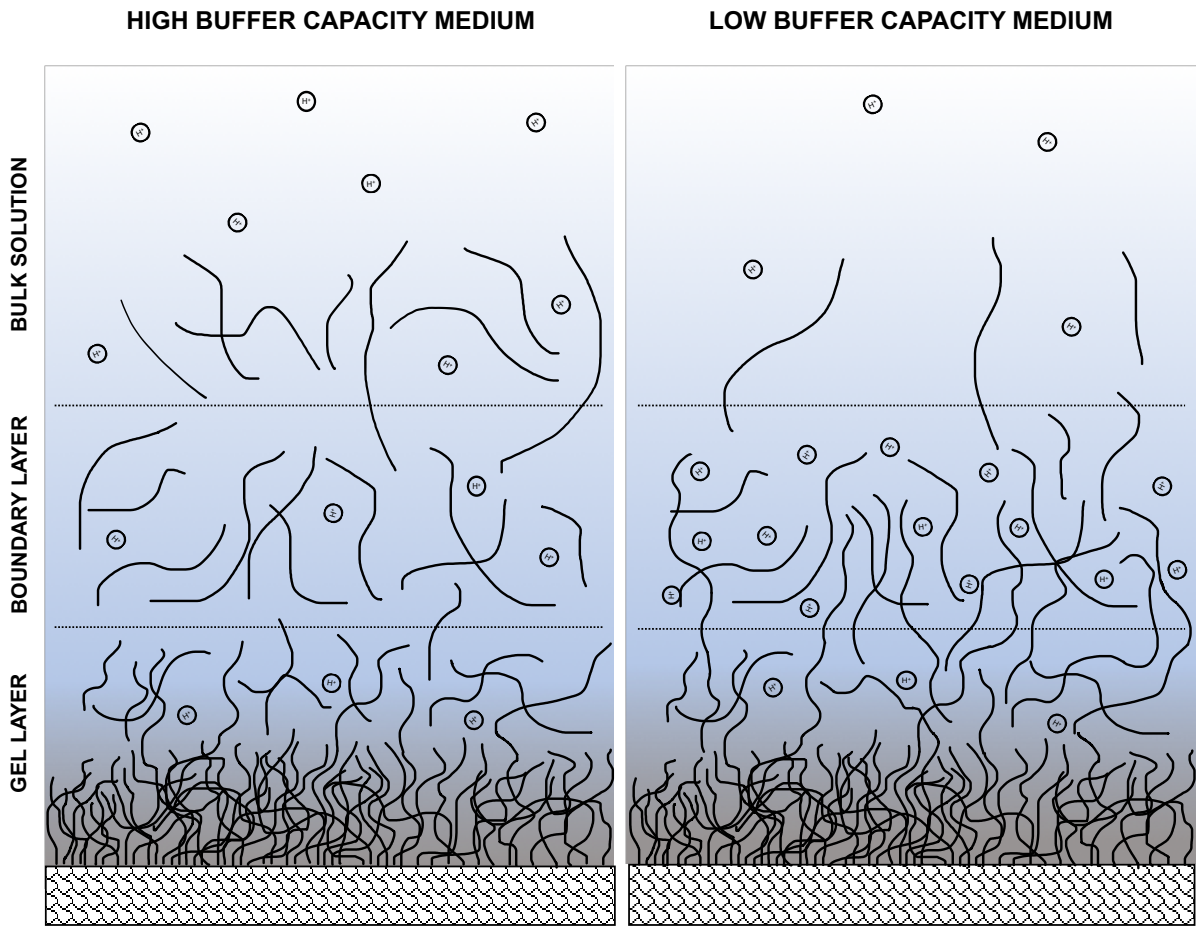

Figure 1.11: Schematic representation of the dissolution process of enteric polymers in high and low buffer capacity media, highlighting the difference in the accumulation of protons at the boundary layer.

The investigation performed by Al-Gousous et al.,(2019) regarding the effect of buffer concentration on the dissolution of enteric dosage forms has revealed that the effect of buffer concentration was considerably stronger than the bulk pH of the buffer (tested between pH 6.0 and 6.8). The authors have compared between the compendial 50 mM pH6.8 phosphate buffer and other bicarbonate buffers at different molarities. However, a direct comparison between phosphate and bicarbonate buffers at similar buffer capacities is still lacking, highlighting how the buffer chemistry and the buffer capacity indeed affect the dissolution of enteric coatings. Chapter 4 of this thesis delves into the effect of the buffer type and capacity on the dissolution rate of enteric polymers. The dissolution rate and the pH_m of different enteric polymers was determined using media at various buffer capacities and with different buffer species.

1.4. Thesis overview

This thesis commences (Chapter 1) by critically appraising the current state of the art in achieving gastroresistance, reviewing various polymers employed and the current understanding on how these formulations dissolve under *in-vitro* and *in-vivo* settings. Chapter 2 presents the development of enteric hard capsules which do not require any additional coating. The capsules were produced using acrylic- and cellulose-based enteric polymers commonly used in the industry for overcoating solid dosage forms. The novel capsules with built-in gastroresistance were filled with a model drug and successfully passed the compendial test for gastroresistant dosage forms. Additionally, these formulations were also tested using physiological bicarbonate-based buffers and the chapter also discusses the differences in drug release in compendial and physiological buffers.

Acknowledging the differences in drug release from different buffers and the underperformance of compendial release media in predicting *in-vivo* behaviour of enteric dosage forms, a multitude of experiments were designed in an attempt to better understand the polymer ionisation and dissolution.

The dissolution of enteric polymers involves (and is truly influenced by) the ionisation of the acidic functional groups on the polymer chains. Chapter 3, therefore, explores the ionisation behaviour of commonly used enteric polymers using a novel technique based on zeta potential measurements over a range of pH. The chapter includes the basis for method development and necessary validations performed. The pK_a of various enteric polymers was then measured using this technique. Additionally, the method was also applied to various natural polymers of pharmaceutical interest to study their ionisation behaviour and, where applicable, a pK_a value was also determined.

Following the ionisation studies, enteric polymer dissolution was explored further in Chapter 4 to look into mechanistic insights. The influence of buffer type and buffer capacity was studied on the dissolution rate of these polymers, the microenvironmental pH ($pH_{m)}$ and contact angle kinetics were also studied. During this work a new method was developed for the quantification of cellulose-based enteric polymers to measure the dissolution rate of these polymers. The technique may be used to simultaneously study polymer and drug dissolution from gastroresistant solid dosage

forms. The obtained results highlight the effect of both buffer capacity and polymer type on dissolution of these materials. The type of buffer used, and the buffer capacity actively influenced the experienced pH_m for these polymers, ultimately influencing their dissolution rate. The studies in this chapter explain the drug release profiles from the capsules produced in Chapter 2 and revealed how polymer dissolution rate directly affected the drug release.

1.5. Aims and Objectives

The main aims of this thesis include:

- **To develop a novel formulation for enteric hard capsules**

  This included the design and validation of novel hard capsules with built-in gastroresistance, which do not require a further coating step (Chapter 2).

- **To study the ionisation dependant solubility of enteric polymers**

  The objectives included the development of a method for the estimation of the pK_a of enteric polymers based on zeta potential. This method was developed and validated in Chapter 3 using various synthetic polymers commonly used in the industry to formulate gastroresistant dosage forms and was then applied to study the ionisation behaviour of various natural polymers.

- **To understand the factors governing the polymer dissolution and drug release from gastroresistant dosage forms**

  Chapter 4 involved the development of a methodology which would allow the quantification of enteric polymers to study the polymers dissolution rates. Secondly, the microenvironmental pH (pHm) of dissolving polymers was measured under different dissolution media and the contact angles kinetics of the same polymers were investigated. Finally, various factors governing dissolution of enteric polymers was analysed and discussed in detail in Chapter 4.

Chapter 2

ENTERIC CAPSULES:
ACHIEVING GASTRORESISTANCE WITHOUT COATING

The majority of this chapter is published in:

Barbosa, J. A. C., Al-Kauraishi, M. M., Smith, A. M., Conway, B. R., & Merchant, H. A. (2019). Achieving gastroresistance without coating: Formulation of capsule shells from enteric polymers. *European Journal of Pharmaceutics and Biopharmaceutics*, *144*, 174–179. https://doi.org/10.1016/j.ejpb.2019.09.015

2.1. Introduction

As mentioned in Chapter 1, the production of gastroresistant formulations using hard capsules has been attempted either by coating granules with enteric polymers and loading them in standard gelatine capsules, or by directly attempting to coat the capsules with said polymers. As stated in Section 1.1.1, although extensively reported, coating hard gelatine capsules is not a standard industrial practice. Therefore different companies have recently reported the development of truly enteric hard capsules, which do not require an additional coating step (BioCaps, 2019; Capsugel, 2019b). The constitution of these capsules is expectedly not disclosed and therefore these are not easily available for small scale clinical studies or for different types of studies involving polymer dissolution.

Hard capsules are typically industrially produced in large scale, through the use of specific equipment. Firstly, a solution of the capsule forming material is prepared, e.g. a formulation comprised of gelatine and other additives (colouring agents, plasticisers, preservatives, etc.). In the typical industrial process for the production of capsules, capsule pins are used as moulds for both capsule bodies and caps. These pins are dipped in the warm gelatine formulation and are then moved by a conveyor belt through a drying chamber, allowing the capsule shells to dry and harden at specific temperature and humidity. The hardened shells are then removed from the pins, cut to adequate sizes and assembled to form a final hard capsule. This is a process that demands specific equipment (such as the capsule moulds), and therefore is not easily reproduced in small scale research laboratories at a much smaller scale.

However, the ease of access to enteric hard capsules would be beneficial not only to study new pharmaceutical entities in small scale trials, but also in the study of the dissolution of enteric polymers, and how it is affected by a multitude of factors, such as pH, buffer type, buffer capacity, among others. The possibility of producing capsules in small scale using known and new materials would allow the testing of new enteric formulations and also help to increase the understanding of polymer dissolution and how this affects drug release from gastroresistant dosage forms.

Thus, in this work, gastroresistant capsule shells were developed using three of the most commonly used polymers in pharmaceutical industry for formulating gastroresistant dosage forms:

hydroxypropyl methyl cellulose acetate-succinate (HPMC-AS) and hydroxypropyl methyl cellulose phthalate (HPMC-P) and Methacrylic Acid - Methyl Methacrylate (EUDRAGIT®). Additionally, capsules based on acrylic polymers such as EUDRAGIT are not yet reported in the literature and as such, the production of EUDRAGIT enteric capsules was a novelty.

2.2. Materials and Methods

2.2.1. Materials

The acrylic (EUDRAGIT® L100 and S100) and cellulose based (HPMC AS-LF and HP-55) enteric polymers were provided in-kind as samples from Evonik Industries AG (Darmstadt, Germany) and Shin-Etsu (Chiyoda, Japan), respectively and their properties are summarised in Table 1. Sodium hydroxide, hydrochloric acid (37%) and ethanol were purchased from Fisher Scientific (Loughborough, United Kingdom). Gelatine (~300g Bloom, Type-A, porcine skin), Glycerol, lactose monohydrate, triethyl citrate and trisodium phosphate dodecahydrate ≥98% were purchased from Sigma-Aldrich (Dorset, United Kingdom). Ac-Di-Sol® SD-711 (croscarmellose sodium) and Kollidon® 30 (povidone) were provided in kind by FMC Health and Nutrition (Ireland). Prednisolone was purchased from Severn Biotech, Ltd (Kidderminster, United Kingdom).

Table 2.1: Enteric polymers used in this study and their characteristics.

Polymer	Brand name	Grade	Dissolution pH threshold	Manufacturer/ supplier
Methacrylic acid copolymer	EUDRAGIT®	L100	≥6.0	Evonik Gmbh, Darmstadt, Germany
		S100	≥7.0	
Hypromellose acetate succinate	Aqoat®	AS-LF	≥5.5	Shin-Etsu Chemical Co., Ltd., Japan
Hypromellose phthalate	-	HP-55	≥5.5	

2.2.2. Design and manufacture of capsule pin bars

For the production of capsules, two sets of pins (capsule moulds) were fabricated from pharmaceutical grade stainless steel (316SS) rods with different dimensions: one for the body of the capsule, and a second for the cap. Capsule pin bars were designed and manufactured in-house for a standardized capsule size “00” (Figure 2.1), according to the reported dimensions for this size (Podczeck and Jones, 2004).

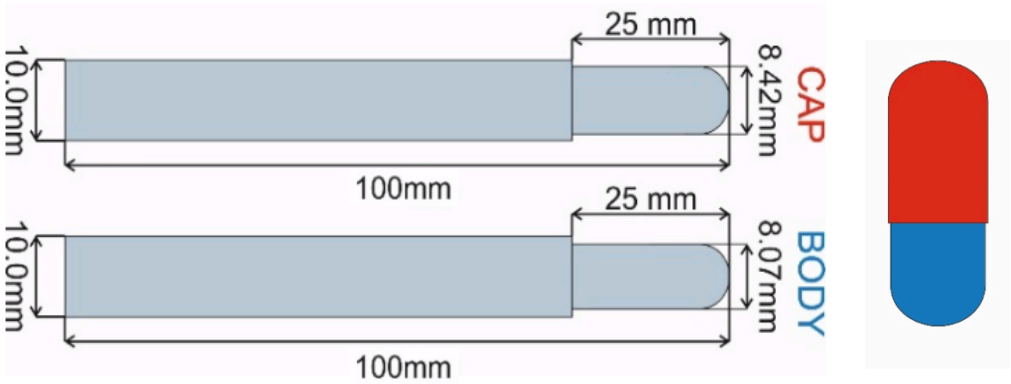

Figure 2.1: Schematic representation of capsule pin bars with the designed dimensions and of the formed capsule.

2.2.3. Production of hard capsules

To firstly develop the capsule manufacturing procedure, gelatine was used as a pilot material due to its well-known gelling proprieties and its ease of use. Using gelatine as a model material, the manufacturing procedure was developed and tested, until a hard capsule was obtained. A solution of 60% (w/w) gelatine in water was used with the gelatine solution being magnetically stirred and kept at 65ºC throughout the capsule production process. To produce the capsule shells, the pins from Figure 2.1 were immersed into the warm gelatine formulation, then withdrawn and inverted. The gelatine solution was then allowed to dry until the shells hardened, forming the cap and body of the capsule. The caps and bodies were then removed from the pins, cut to the desired length and assembled to form a finished capsule. The same manufacturing method was applied when experimenting on the enteric polymeric formulations.

2.2.3.1. Optimisation of enteric capsules

Capsules were formulated using different concentrations of polymer (20-30%) plasticised either with triethyl citrate (TEC) or glycerol at different concentrations (20-40%). The tested formulations are summarised in Table 2.2. These formulations were achieved based on background screening using capsules containing gelatine only, and a mixture of gelatine and enteric polymer. These results are not shown, as they were part of an MSc student's project, supervised during this PhD project. These formulations allowed both to improve the manufacturing technique and also to understand the differences in the hardening process of gelatine and polymeric capsules. Following

this, formulations containing only polymeric material only were pursued further and are discussed in this thesis.

The polymer concentration was key in obtaining a capsule with appropriate thickness that could be easily removed from the pins. The polymer concentration also governs the viscosity of the prepared solution. An optimum viscosity is essential for the polymer to adhere to the pins during the drying process and produce a uniform capsule of an appropriate shape. The type and concentration of plasticiser impacts upon the capsule shell elasticity and prevents brittleness.

Table 2.2: Composition of the tested formulations to produce gastroresistant capsule shells.

Formulation ID	Polymer	%a	Plasticiser	%b	Solvent
1.1	HP-55	20.0	Glycerol	20.0	Ethanol : Water (80:20[c])
1.2		20.0	TEC	20.0	
1.3		22.5	Glycerol	20.0	
1.4		22.5	Glycerol	30.0	
2.1	AS-LF	20.0	Glycerol	20.0	Ethanol : Water (80:20[c])
2.2		20.0	TEC	20.0	
2.3		22.5	Glycerol	20.0	
2.4		25.0	Glycerol	20.0	
2.5		25.0	Glycerol	30.0	
3.1	EUD L100	20.0	Glycerol	20.0	Ethanol : Water (97:3[c])
3.2		20.0	TEC	20.0	
3.2		25.0	TEC	20.0	
3.4		25.0	TEC	30.0	
3.5		27.5	TEC	20.0	
3.6		27.5	TEC	30.0	
3.7		27.5	TEC	40.0	
4.1	EUD S100	25.0	TEC	40.0	Ethanol : Water (97:3[c])
4.2		27.5	TEC	40.0	

HP-55 = Hypromellose phthalate-55; **AS-LF** = Hypromellose acetate succinate – LF;
EUD L100 = EUDRAGIT L100; **EUD S100** = EUDRAGIT S100; **TEC** = Triethyl citrate.
a: based on total weight, **b**: based on polymer weight, **c**: based on solvent weight

2.2.4. Tensile studies of produced capsules

The mechanical properties of the polymeric materials used in the production of the capsules were studied using a TA.XT2 Texture analyser (Stable Micro Systems Ltd, Surrey, UK) equipped with

tensile grips (tensile mode) and a cylinder probe (P/0.5''R; compressive mode). The films of each polymer were produced with the same formulation used for the capsules, casted on a flat surface and allowed to dry in the same conditions as the capsules would be. The thickness of the films was controlled by calculating the area of the surface where the film was casted, and systematically using a similar ratio of mass of polymer/area as it would be when using each formulation to produce the capsules. The films were then cut in dog-bone shaped pieces according to DIN EN ISO 527-2 for the determination of tensile properties, consisting of a rectangular testing area of 40x8mm. For each sample an average thickness was acquired, and the stress area was calculated. The tests were performed at a speed of 0.5 mm/sec, at 20 °C, with 10 replicates per sample. The slope of the linear range of the obtained stress vs. strain curves (tensile mode) corresponds to the Young's modulus for the respective polymeric films.

2.2.5. Prednisolone filled gastroresistant capsules

All prepared capsules were filled with prednisolone granules prepared by wet granulation. Briefly, the formulation contained prednisolone (5%), lactose monohydrate (88%), Kollidon® 30 (5%), Ac-Di-Sol® SD-711 (2%). The ingredients were mixed using a Caleva Multi Lab (Caleva Process Solutions Ltd, England). The wet mass was then extruded and the extrudate was spheronized using the corresponding module from the Caleva Multi Lab, followed by drying at 60 °C. The granules were then filled manually into capsule shells to an equivalent of 10 mg prednisolone per capsule.

2.2.6. Drug release from prednisolone-filled gastroresistant capsules

The drug release from prednisolone-filled capsules was tested using USP-II dissolution apparatus (PT-DT70 Dissolution Apparatus, Pharma Test Apparatebau AG, Germany). Six capsules were tested for each successfully prepared formulation following the USP <711> Dissolution monograph for delayed-release dosage forms. Briefly, AS-LF, HP-55 and EUD L100 capsules were firstly tested in 0.1M HCl (pH 1.2) for 120 min at 37°C, followed by pH 6.8 phosphate buffer (0.05M Na_3PO_4, pH adjusted with 1M HCl / 1M NaOH) or pH 6.8 *m*Hanks buffer (Liu et al., 2011) (136.9 mM NaCl, 5.37 mM KCl, 0.812 mM $MgSO_4 \cdot 7H_2O$, 1.26 mM $CaCl_2$, 0.337 mM $Na_2HPO_4 \cdot 2H_2O$, 0.441 mM KH_2PO_4, 4.17 mM $NaHCO_3$, pH adjusted to 6.8 using CO_2 (g)). Capsules of EUD S100

were also produced and tested, however, since this polymer was designed to target the distal gut, the dissolution testing included two media changes to reflect the aboral changes in pH down the intestine. The capsules were firstly tested in 0.1M HCl (pH1.2 for 2 hours) to represent gastric conditions followed by a change to pH 6.8 (for 4 hours) to simulate the pH of the proximal small intestine. Finally, the pH was adjusted to 7.4 for the rest of the experiment simulating the distal small intestine. Like other capsules, the test was conducted in both phosphate and *m*Hanks buffers, as described above in this section. For *m*Hanks buffer, the pH change from pH 6.8 to 7.4 was performed *in-situ* by sparging helium and the pH was then maintained during the dissolution studies by sparging CO_2, as described by Liu et al. (2011).

The release of prednisolone from HPMC AS-LF and EUDRAGIT capsules was quantified using an in-line UV spectrophotometer (Unicam UV/Vis UV2-200 spectrophotometer) at a wavelength of 246 nm. For the capsules containing HP-55, the release of the drug was quantified by HPLC-UV due to interference between the UV absorbance of the polymer and drug. The HPLC-UV system used was a Shimatzu LC-20AT with SIL-20A autosampler and an SPD-20AV UV detector. The samples were filtered through 0.2 µm syringe filters (Sartorius™ Minisart™ High Flow) and injected into a reverse phase C8 (5 µm particle size, 4.6x150 mm) column (Waters, Massachusetts, USA). The column was heated to 40°C and the mobile phase consisted of a mixture of water:tetrahydrofuran:methanol (68.8:25:6.2 v/v) flowing at 1.5 mL/min. Prednisolone was detected at 254 nm, at retention time of 2.7 min (Liu et al., 2011).

2.3. Results and discussion

2.3.1. Production of hard capsules

The use of gelatine allowed for a quick testing and development of a capsule manufacturing technique. Gelatine's gelling characteristics ensures that capsules are easily produced without the need for extended *know-how* and experience. Hence, the first gelatine capsules were produced as described in section 2.2.3 using the *in-house* designed capsule pins (Figure 2.2).

The challenge was then to transfer the methodology from using gelatine to an enteric polymer. The hardening of gelatine is based on its gelling proprieties, i.e. its rheological characteristics. Gelatine softens with increasing temperatures and hardens when the temperature decreases. This

behaviour is exploited when producing hard gelatine capsules, by manipulating the storage modulus (G') and the loss modulus (G'') of gelatine, hence the gelatine solution being warm when the pins are dipped. In very simple terms, the G' represents the elastic portion of the viscoelastic behaviour of a sample, and its related to its solid-state (e.g. when gelatine is hardened). On the other hand, G'' represents the viscous portion of the viscoelastic behaviour and is related to the liquid-state of the sample (i.e. when gelatine is softened).

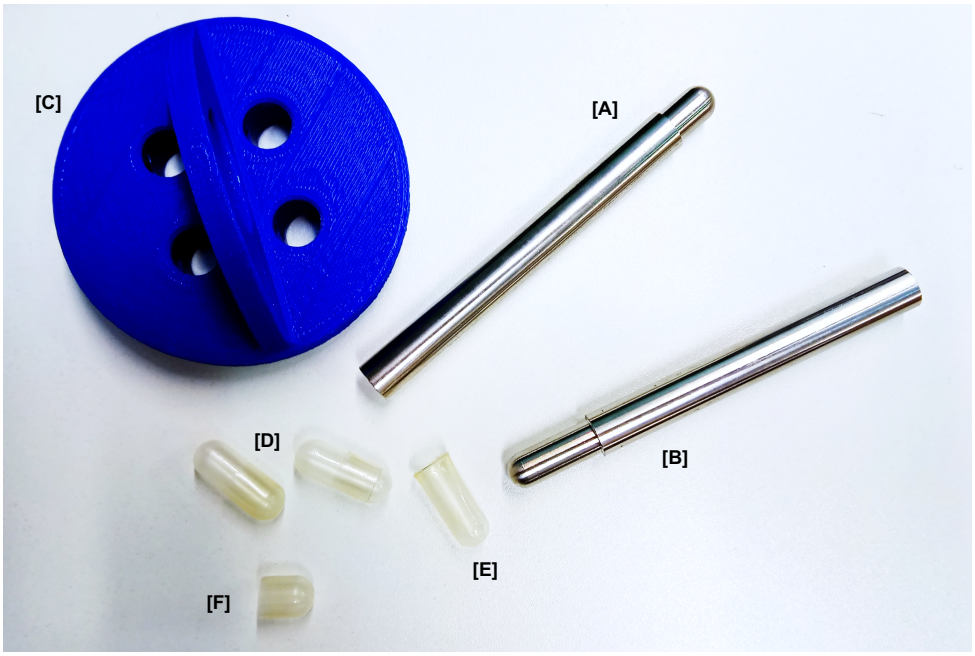

Figure 2.2: In-house produced capsule cap [A] and body [B] pins and support [C] used for the production of the depicted gelatine capsules (60%(w/w) gelatine solution in water) [D]. Example of an uncut body [E] and a cut cap [F] is shown.

Rheological measurements of G' and G'' vs temperature indicate the temperature at which a sample becomes more solid-like (G'>G'') or more liquid-like (G''>G') (Anton Paar GmbH, 2020). Thus, during capsule manufacturing, gelatine solutions are warmed to a predetermined temperature where G''>G', and the gelatine is "liquid" to allow the dipping of the capsule pins. The cooling of the solution then causes the inversion of the moduli (G'>G''), and the gelatine hardens forming the capsule shell.

A very different process occurs when forming polymeric capsule shells. In this process, the polymer is dissolved in a solvent, which slowly evaporates to allowing the formation of a film. In this case, an adjustment needs to occur in the manufacturing process, with G' and G'' no longer playing an important role in the hardening process of the shells. The sample solution needs to be fluid enough to allow the dipping of the pins, but viscous enough to adhere to the pin without dripping when

inverted to dry. Additionally, the thickness of the formed capsules has to be considered as well, as this characteristic greatly influences the dissolution of the polymer, and therefore its enteric proprieties. The thickness of the final capsule depends on the concentration of the prepared solution, with more concentrated polymeric solutions yielding thicker capsules. An interplay between polymer concentration and plasticiser type and concentration if thus extremely important. In the end, the development of a formulation for the production of enteric capsules has to a provide a final solution with appropriate viscosity to allow the dipping of the pins, ensure its adherence without dripping and form a capsule with appropriate thickness. Consequently, several formulations were prepared and tested (Table 2.2), aiming to achieve optimum conditions.

2.3.1.1. Optimisation of capsule formulation

Various polymeric formulations were tested to achieve optimum gastro-resistant capsules from each enteric polymer. Table 2.3 summarises the final optimised formulation for each polymer that yielded a capsule with appropriate thickness, smoothness and gastroresistance. Lower concentrations of polymer and plasticiser yield thinner capsules, which would brake during their removal from the pins or during handling. Lower concentrations of plasticiser also caused striations to appear along the capsule body during the drying process. Examples of failed capsules are shown in Figure 2.3, showing capsule which were too brittle due to low amounts of plasticiser (Figure 2.3 A and B) and the effect of the wrong plasticiser on an AS-LF capsule (Figure 2.3 C), producing excessive striations, deformations and yellowed capsules.

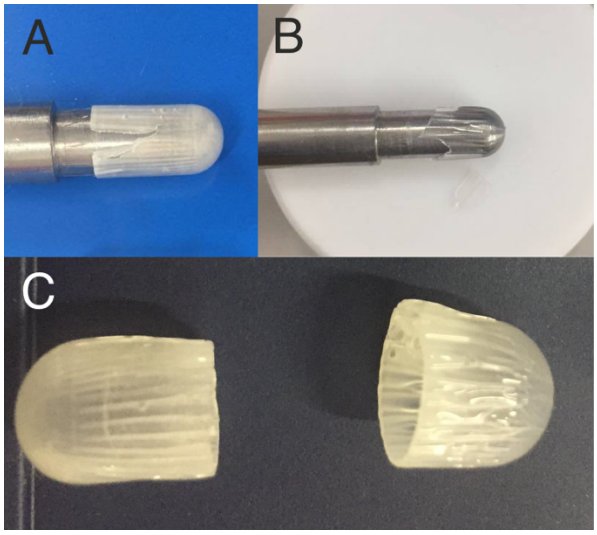

Figure 2.3: Examples of failed capsules. A – HP-55 capsule (formulation 1.3); B – EUD L100 capsules (formulation 3.2); C – AS-LF capsule (formulation 2.2),

Table 2.3: Composition of optimised capsule formulations for each enteric polymer

	HP-55	HPMC AS-LF	EUDRAGIT® L100	EUDRAGIT® S100
Polymer weight	22.5%[a]	25%[a]	27.5%[a]	27.5%[a]
Glycerol	30%[b]	30%[b]	-	-
Triethyl citrate	-	-	40%[b]	40%[b]
Ethanol	80%[c]	80%[c]	97%[c]	97%[c]
Water	20%[c]	20%[c]	3%	3%

a: based on total weight, b: based on polymer weight, c: based on solvent weight

The caps and bodies were cut to appropriate length for "00" size (Podczeck and Jones, 2004), their dimensions was measured with a digital micrometre (Table 2.4) and were finally assembled into finalised, ready to fill capsules (Figure 2.4). The dimensions of optimised capsule formulations were in accordance with the size and tolerances used by commercial suppliers of hard capsules (Capsugel, 2013).

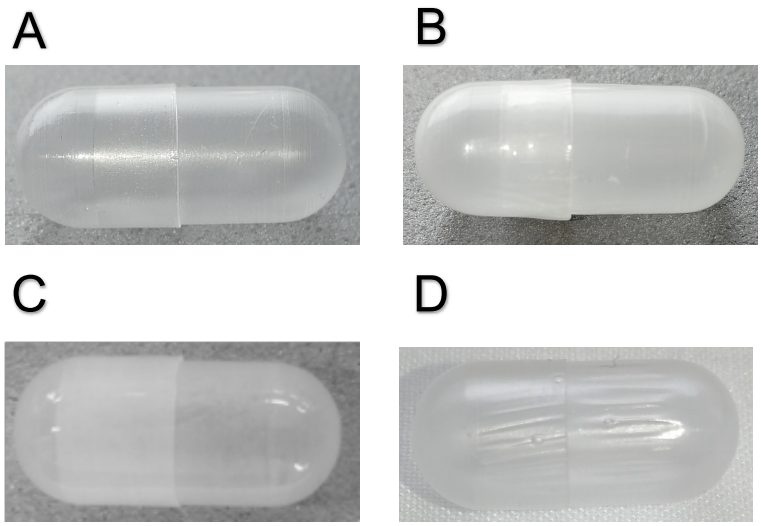

Figure 2.4: Capsules obtained from optimised formulations of EUD L100 (A), AS-LF (B), HP-55 (C) and EUD S100 (D).

Table 2.4: Dimensions (mean ± STD, n=6) for the size "00" size produced from optimised formulations.

	HP-55		HPMC AS-LF		L100		S100	
	Body	Cap	Body	Cap	Body	Cap	Body	Cap
Outer Diameter (mm)	8.51 ± 0.04	8.18 ± 0.04	8.52 ± 0.03	8.17 ± 0.03	8.53 ± 0.04	8.16 ± 0.02	8.52 ± 0.05	8.17 ± 0.02
Thickness (mm)	0.104 ± 0.02	0.097 ± 0.01	0.119 ± 0.01	0.104 ± 0.02	0.108 ± 0.02	0.114 ± 0.02	0.115 ± 0.02	0.109 ± 0.01

2.3.2. Tensile strength

From the stress vs. strain plots obtained from the tensile tests on the polymeric films (Figure 2.5), the elastic moduli were calculated from the obtained slope and are summarised in Table 2.5. The measured Young's moduli of the polymers used in this work are comparable to reported values of gelatine used to formulate capsules (De Carvalho and Grosso, 2006; Park, 2009), exhibiting resistance to elastic deformation similar to that of standard gelatine hard capsules. It is worth noticing a lower yield point for the EUD S100 profile, which is in line with brittleness of the S100 formulated capsules. Although the yield point was comparatively lower for these capsules (~5 MPa), it may not adversely affect the mechanical stability of the capsule during packaging, storage or transportation. The Young's modulus for these films also suggests the resistance to elastic deformation was comparable to other polymers. Moreover, S100 capsules also met the acid challenge test and subsequent drug release in buffer was satisfactory (vide s.3.3.3 for further details).

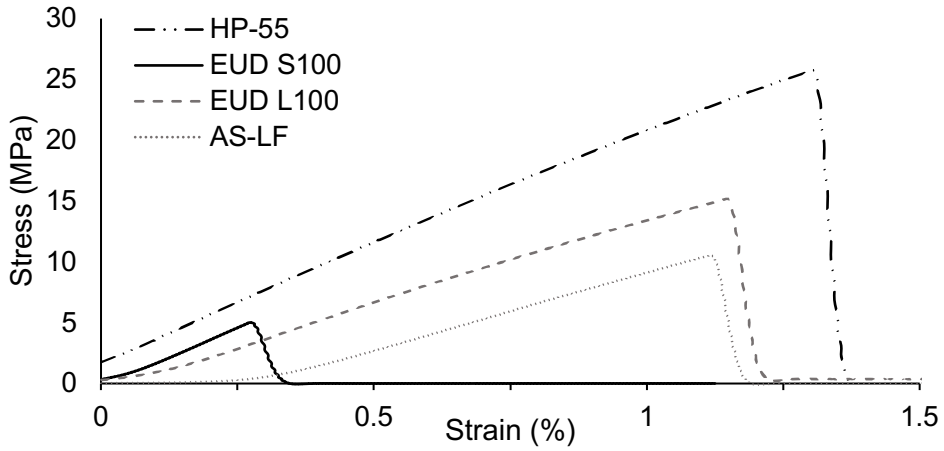

Figure 2.5: Stress vs strain plots of HP-55, EUD L100, AS-LF and EUD S100 polymeric films. The slope of the linear region in profiles relates to the Young's modulus.

Table 2.5: Young's modulus of polymeric films used to formulate capsules shells. The values represent average ± STD (n=9)

Polymer	Young's modulus (MPa)
HPMC AS-LF	15.61 ± 2.10
HP-55	17.38 ± 0.83
EUD L100	13.84 ± 2.98
EUD S100	16.66 ± 2.90
Gelatine	19.5 ± 1.6[a]; 15.12 ± 0.05 [b]

a: (Park et al., 2007); b: (de Carvalho and Grosso, 2006)

2.3.3. Drug release from produced capsules

Prednisolone release from optimised formulations (Table 2.3) for HPMC AS-LF, HP-55 and EUDRAGIT L100 capsules is shown in Figure 2.6A. There was no drug released during the first 2 hours in acid, confirming the acid resistance of the dosage forms as per pharmacopoeial requirements. All capsules rapidly ruptured, exhibiting a drug release within ~5 min on transfer to 50 mM compendial phosphate buffer pH 6.8. The drug release from enteric capsules was therefore comparable to equivalent polymer-coated conventional gastroresistant tablets reported by Liu et al., (2011).

As expected, drug release in physiological bicarbonate buffer was delayed significantly and profiles between different polymers were not superimposable. Despite HPMC AS-LF and HP-55 being marketed for a dissolution pH threshold above pH 5.5, their release profiles in bicarbonate buffer were discriminatory, despite being similar in phosphate buffer. Interestingly, prednisolone release from HPMC AS-LF capsules was similar in compendial phosphate and bicarbonate buffers, with a lag-time (time until at least 1% of drug is released) in the bicarbonate buffer of around 15 min compared with around 5 min in phosphate buffer. However, for HP-55 this lag time was much longer in bicarbonate buffer with no drug released until an hour in buffer. EUDRAGIT L100 exhibited highest lag-time when tested in bicarbonate buffer, with the drug release delayed for 2 hours after transferring to the buffer phase. The much-delayed release of the drug from enteric capsules in physiological bicarbonate buffer was not surprising and also complies with previous reports of drug release behaviour from conventional enteric polymer-coated tablets in bicarbonate buffer (Liu et al., 2011). This suggests that the behaviour of the enteric polymers is similar when used as coatings on conventional tablets or to produce capsule shells. Although longer lag-times are observed for enteric capsules (Table 2.6) as compared with coated tablets in Liu et al. (2011), these can be attributed to the differences in the thickness of the capsule shells compared with the thickness of an enteric coating film applied to a tablet. The thickness of a typical coating on gastroresistant tablet is about 50 to 75 microns, with tablet edges usually more thinly coated than the faces (Merchant, 2012). Hence, the coating layer around the edges mainly controls the lag-time in drug release. On the other hand, the produced enteric capsule shells exhibited a uniform

thickness ~100 microns (Table 2.4) which is twice more than the classic film coating, contributing to the increased lag times.

Table 2.6: Lag time for the drug release (until 1% release) from polymeric capsules and from conventional polymer-coated tablets at pH 6.8 (EUD L100, HP-55 and AS-LF) or pH 7.4 (EUD S100), pre-exposed to 0.1M HCl pH 1.2 for 2h. Data from polymer-coated tablets from Liu et al. (2011) and Ibekwe et al. (2006).

	Lag times (min) in phosphate buffer				Lag times (min) in bicarbonate buffer			
	HP-55	**AS-LF**	**EUD L100**	**EUD S100**	**HP-55**	**AS-LF**	**EUD L100**	**EUD S100**
Gastroresistant Capsules	3.2 ±1.6	2.2 ±0.4	15.0 ±1.4	16.0 ±4.0	67.5 ±2.9	18.2 ±2.7	130.4 ±18.3	237.3 ±8.1
Coated Tablets	5[1]	15[1]	11[1]	65[2]	35[1]	32[1]	77[1]	130[2]

HP-55: Hypromellose phthalate-55; **AS-LF**: Hypromellose acetate succinate – LF;
EUD L100: EUDRAGIT L100; **EUD S100** = EUDRAGIT S100.
1: Liu et al. (2011); 2: Ibekwe et al. (2006)

Nevertheless, the order in which the polymers start dissolving and the capsules start releasing the drug is the same as previously reported for coated tablets (Liu et al., 2011), exhibiting a rank order of time until drug release of HPMC AS-LF< HP-55< EUD L100. ASLF and HP-55 capsules are therefore suitable for gastroresistant applications to target the drug in proximal gastrointestinal tract, analogously to already existing capsule-based formulations (e.g. Deltacortil®, Nexium®, Voltarol®, Pariet®, etc.).

The drug release profile from EUD S100 capsules is shown in Figure 2.6B. These capsules were subjected to two media changes, the first to pH 6.8 and the second to pH 7.4. As expected, no drug release occurred during the acid phase (confirming gastroresistance) and in pH 6.8 (both in phosphate and bicarbonate buffers) however the drug was released at pH 7.4 within 15 min in phosphate buffer and a much-delayed release in bicarbonate buffer (~4 hours).

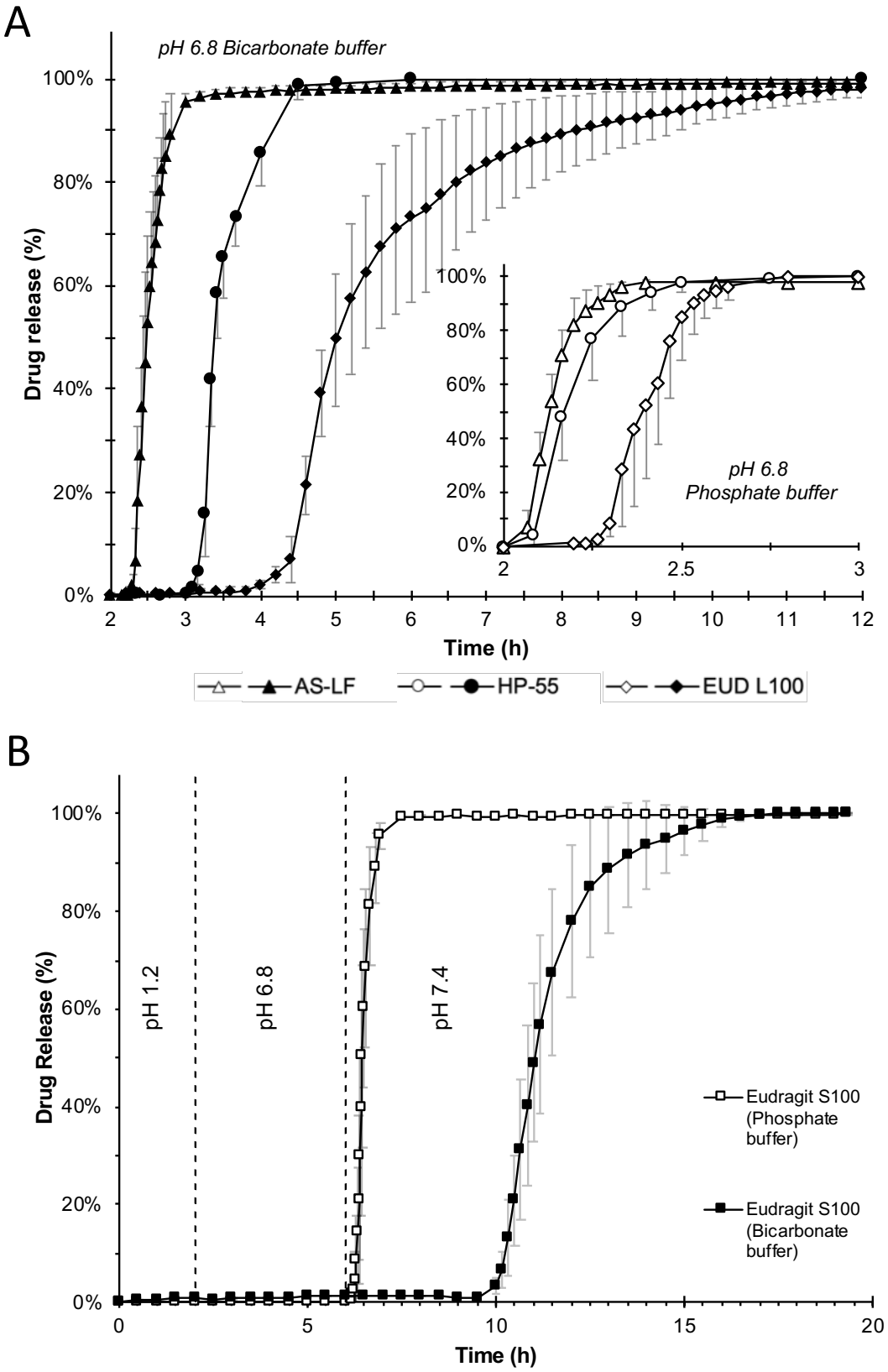

Figure 2.6: Prednisolone release from enteric capsules in 50 mM compendial phosphate buffer (empty symbols) and physiological bicarbonate buffer, mHanks (filled symbols). [A]: HP-55, EUD L100 and AS-LF capsules at pH 6.8, after 2 h-exposure to 0.1M HCl (not shown); [B]: EUD S100 capsules at pH 7.4 following 2 h in 0.1M HCl and 4 h in pH 6.8 buffer.

This slower release in bicarbonate buffer is not unexpected and longer lag times in this buffer were already reported by Goyanes et al. (2015). Therefore, L100/S100 based capsules are promising candidates to target pharmaceutical/nutraceutical agents to the distal gastrointestinal tract, such as Asacol®, Octasa®, Salofalk®, pre/probiotics etc. The drug release from these capsules can however be improved by further optimising the capsule shell, for instance by using pH responsive polymer blends, such as: S100/L100. A dual trigger system (pH and bacteria) comprising two independent but complementary release mechanisms can be embedded in capsule shells. This fail-safe system has recently shown promising results in the clinic in delivering high dose oral mesalazine to inflammatory bowel disease patients (D'Haens et al., 2017).

Intra- and inter-tablet coating variability in solid dosage forms is a significant factor responsible for the huge exhibited pharmacokinetics variability (e.g. Deltacortil ® (Merchant, 2012)), which is further aggravated by other variables such as gastric emptying time (McConnell et al., 2008). The capsules produced in this work do not need an additional coating step, and once translated to industrial production, the controllable and low variability of capsule wall thickness may reduce in-vivo variability associated with coating inconsistency in conventional products. Moreover, gastrointestinal targeting may be easily achieved by bespoke capsules shells produced at large scale where drug release can be tailored by the polymer blend and capsule wall thickness.

2.4. Conclusion

Gastroresistant capsule shells were successfully produced, ensuring gastroresistance without the need of additional coating. A range of enteric polymers (HPMC derivatives and acrylate-based polymers) were used to produce enteric capsule shells to target various regions within the GI tract: duodenum – HPMC AS-LF and HP-55 (pH 5.5); jejunum – EUD L100 (pH 6.0); ileocolonic – EUD S100 (pH 7.0). The produced capsules were very similar to classic immediate release hard gelatine capsules in appearance and resistance to elastic deformation. The technology, if warranted at industrial scale, can allow production of capsule shells in bulk, similar to conventional capsules, and will enable the industry to produce gastroresistant dosage forms without coating on a conventional capsule filling line. This will also be beneficial in early discovery and development in

formulating gastroresistant dosage forms for preclinical and clinical trials. This work has already been published in a peer-reviewed scientific journal (Barbosa et al., 2019).

Results showing the differences in drug release in phosphate and bicarbonate buffers have led to further exploration of the effect different buffer may exert in polymer dissolution and thus drug release. Therefore, the following chapters will focus on the search of a better understanding of how drug release from enteric dosage forms is influenced by the surrounding media. This will be studied with particular emphasis on the influence of the release media in polymer dissolution and polymer ionisation.

Chapter 3

ZETA POTENTIAL:
THE FIRST CUES TO UNDERSTAND POLYMER IONISATION

The majority of this chapter is published in:

Barbosa, J. A. C., Abdelsadig, M. S. E., Conway, B. R., & Merchant, H. A. (2019). Using zeta potential to study the ionisation behaviour of polymers employed in modified-release dosage forms and estimating their pKa. *International Journal of Pharmaceutics: X*, *1*, 100024. https://doi.org/10.1016/j.ijpx.2019.100024

3.1. Introduction

In-vivo dissolution of polymeric coatings is a complex interplay between the ionisation constant of the polymer and the characteristics of gastrointestinal fluid, such as fluid volume, ionic concentration, buffer pK_a and capacity. According to the Henderson-Hasselbalch equation, the pK_a of a weak acid corresponds to the environmental pH at which the concentration of the protonated (HA) and unprotonated (A^+) forms are equal (vide Figure 1.6). At this pH, the weak acid will be partially ionised; whereas almost a full ionisation is expected when the environmental pH is 2 units above its pK_a (Figure 1.6).

The enteric polymers employed as gastro-resistant coatings behave as weak acids in solution and exhibit a pH-dependant ionisation. At a pH above the polymer's pK_a value, the carboxylic acid groups tend to ionise, increasing [A^-] and proportionally decreasing [HA] which will increase polymer's solubility, leading to complete dissolution (Figure 1.6). This ionisation produces a proportional increase in negatively charged groups on the surface of the dissolving polymer yielding a net negatively charged surface. The charged surface acts thus as a solid particle, with a surface potential, affecting the ions in the surrounding media. This behaviour at this solid-liquid interface can be compared to a zeta potential as it represents the electrical potential at the shear plane, which separates a stationary layer and a mobile layer of charges (Figure 3.1).

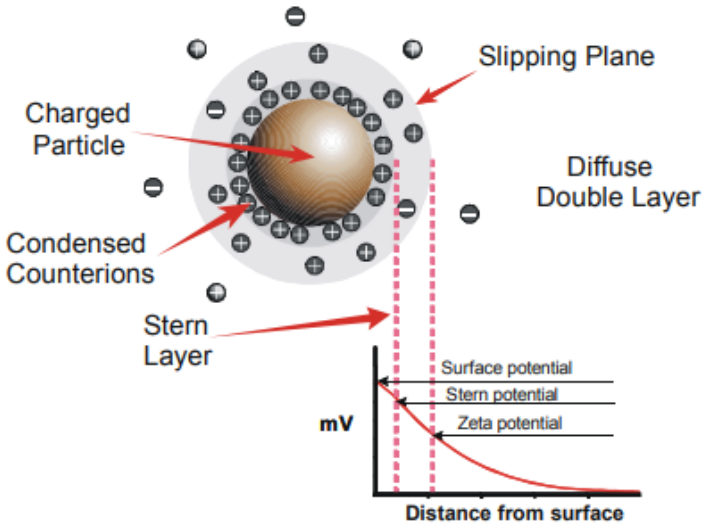

Figure 3.1: A schematic showing the potential difference as a function of distance from the charged surface of a particle in a medium (Malvern Instruments Ltd, 2005).

Zeta potential is an indirect measurement of the charge present at the slipping plane (Figure 3.1), obtained by electrophoretic light scattering (ELS). This technique measures the electrophoretic

mobility of a particle or molecule in a solution or dispersion, i.e. when an electric field is applied, particles will move in accordance with its charge, towards the positive or negative electrode. This mobility is tracked by monitoring the light scattered by the particles and is then converted to a correspondent zeta potential value. Mobility of charged particles will depend not only on the particle zeta potential value, but also on its size, on the ionic strength of the media and the chemistry and molecular weight of the specie being measured.

In the case of gastroresistant polymers, the increase of the pH of the medium will result in an augmented ionisation of the acidic groups, which leads to a proportional accumulation of protons and an increase in the charge at the polymer's surface. This in turn should be measurable as an increment in the zeta potential. The maximum absolute value of the zeta potential ($Zeta_{max}$) therefore corresponds to the maximum ionisation of the polymer, i.e. when $[A^-]$ is maximal. Hence, an equal concentration of the weak acid to the concentration of its conjugated base ($[A^-] = [HA]$) can be attributed to the median between the $Zeta_{min}$ and the $Zeta_{max}$, and the corresponding pH of the medium will correspond to the pK_a value of the polymer.

An early work by Burke and Barrett (2003), described the use of zeta potential to determine the apparent pKa value of multi-layered thin films assembled in colloidal silica. Later, a new method was developed to calculate the pKa of multi-layered thin films based on the surface tension measurements on the surface-to-air interface (Dickhaus and Priefer, 2016). As the authors describe a number of techniques have been reported to determine the pKa of acids (e.g. potentiometric, UV-Vis spectrometry, HPLC, conductometry, polarimetry, computational, among others), yet mentioning they will not all be suitable to all kinds of acids, such as long chain acidic polymers.

The hypothesis in this work was to show that zeta potential measurements may be used as a simple and economical technique to study the ionisation behaviour of gastroresistant polymers and determine their pK_a value. The technique would be performed under different conditions, mimicking the pH changes across the GI tract, allowing the study of the ionisation behaviour of different polymers for a range of pharmaceutical applications, aiding in a more rational formulation development for gastroresistant dosage forms.

3.2. Materials and methods

3.2.1. Materials

Hydrochloric acid NIST 1M and sodium hydroxide NIST 1M solutions were purchased from Fisher Scientific (Leicestershire, UK). EUDRAGIT® and HPMC AS/P polymers used in this work were kindly provided as samples from Evonik Industries AG, Germany and from Shin-Etsu, Japan, respectively. Their proprieties are summarized in (Table 3.1).

Table 3.1: Synthetic polymers used in this study, respective characteristics and structures.

Polymer	Brand name	Grade	Dissolution pH threshold	% ionisable groups	M.W. (g/mol)	Manufacturer/ supplier
				Dimethyl aminoethyl [1]		
Methacrylic acid copolymer	EUDRAGIT®	E100 [A]	≤5.0	20.8 - 25.5	47.000	Evonik GmbH, Darmstadt, Germany
				Methacrylic acid [2]		
		L100 [B]	≥6.0	46.0 - 50.6	125.000	
		S100 [B]	≥7.0	27.6 - 30.7	125.000	
				Succinoyl [3]		
HPMC acetate succinate (AS)	Aqoat®	LF [C]	≥5.5	14.0 – 18.0	18.000	Shin-Etsu Chemical Co., Ltd., Japan
		HF [C]	≥6.8	4.0 – 8.0	18.000	
				Phthalyl [4]		
HPMC phthalate (HP)	-	HP-50 [D]	≥5.0	21.0 – 27.0	78.000	
		HP-55 [D]	≥5.5	27.0 – 35.0	84.000	

[A]

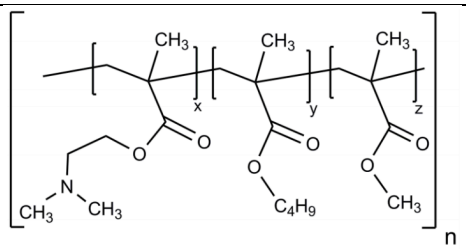

[B]

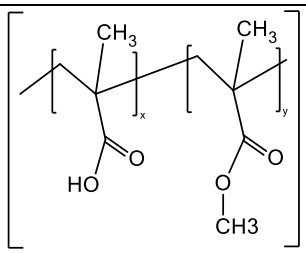

[C]

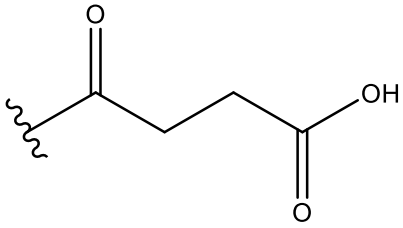

[D]

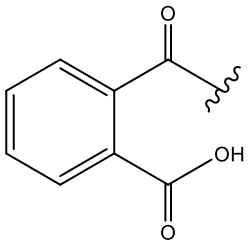

A: *x – dimethylaminoethyl methacrylate, y – butylmethacrylate, z – methyl methacrylate (ratio x : y : z - 2:1:1);*
B: *x – Methacrylic acid, y – Methyl Methacrylate (ratio x:y : L100 - 1:1 / S100 – 1:2);*
C: *Succinoyl groups;* ***D:*** *Phthalyl group.*
1: Evonik Industries AG, (2015)*; 2: Evonik Industries AG,* (2012)*; 3: Shin-Etsu Chemical Co.,* (2018)*; 4: Shin-Etsu Chemical Co.,* (2002)

Tara and Konjac gums were acquired from Ingredients UK Limited (Hampshire, UK). Sodium alginate (180947), gum arabic (G9752), κ-carrageenan (22048), chitosan (75-85% deacetylation, 448877), guar gum (G4129), and high-methoxyl citrus peel pectin (P9135) were purchased from Sigma-Aldrich (Dorset, UK). Locust bean gum (GC1233) was purchased from Glentham Life Sciences (Wiltshire, UK). Psyllium husk powder was acquired from Bulk Powders® (Sports Supplements Ltd, Colchester, UK). Supplier product codes for the natural gums are given in brackets.

Arabinoxylan was provided by a colleague from the research group. Arabinoxylan was obtained from psyllium husk powder via an alkaline hydrolysis followed by ultrafiltration (Campbell et al., 2019).

3.2.2. Method validation for pK_a determinations

To determine the pK_a value of different polymers, the zeta potential of polymeric dispersions at different pH was measured and their ionisation behaviour was assessed. For this, the preparation of the dispersions had to be tested and optimised, such as the measurement parameters and the method for the calculation of the pK_a. The work was divided in two stages, with the first being the validation of the method. In this phase, the tested polymers were commercially available polymers used as coatings in gastro-resistant dosage forms (Table 3.1). The use of these well-known polymers with their detailed characteristics (dissolution pH threshold, type of ionisable groups and their quantity) allowed for a more robust and controlled validation of the technique.

3.2.2.1. Optimisation of polymeric dispersions

The first stage of the method development was the optimisation of the polymeric dispersions to be measured by ELS to determine the zeta potential of the tested polymers. It is essential with ELS to have a properly prepared dispersion, not only due to large agglomerates interfering with the light scattering, but more importantly due to the need to have enough dispersed particles that may be detected by the laser during the ELS measurements. Agglomerated particles will interfere with the measurement, however if the number of well-dispersed particles greatly overcomes the agglomerates, the quality and reproducibility of the measurement is assured. Hence, the main goal

of this stage was to achieve maximum efficiency in producing a good dispersion with low size particles.

Since the zeta potential measurements were performed at a range of pH from 2-12, the starting media could be a solution at pH 2 or at pH 12, which would be titrated in the appropriate direction. When a gastro-resistant dosage form is administered, the pH it withstands will be acidic in the stomach and will gradually increase as the stomach empties its content to the intestine and travels further down the GI tract. Therefore, the acidic pH was chosen as a starting point in order to resemble the pH variations in the GI tract.

Three sets of dispersions for each polymer were prepared at 0.5% (w/v) in 0.1M HCl, with the first being stirred on a magnetic stirring plate for 10 min at 1.000 rpm, the second homogenised for 10 min in a high-shear mixer (Silverson L5M mixer) at 5.000 rpm and the third on a magnetic stirring plate for 5 min at 1.000 rpm, followed by 5 min in the high-shear mixer at 5.000 rpm. The polymers used and their characteristics are summarised in Table 3.1. Next, the particle size of these mixtures was measured by dynamic light scattering (DLS), using a Malvern Zetasizer Nano ZS (Malvern Panalytical Ltd., Royston, UK).

After the optimisation, dispersions were prepared at different concentrations (0.1-0.5% (w/v)) to test possible concentration effects in the zeta potential.

3.2.2.2. Optimization of zeta potential measurements

The second stage involved zeta potential measurements, which were performed using a Malvern Zetasizer Nano ZS (Malvern Panalytical Ltd., Royston, UK) coupled to an MPT2 automatic titration unit. This experimental setup allows the auto-titration and recirculation of sample in an enclosed system with robust and reproducible measurements. The software allows for multiple choices to be made, especially regarding the type of titrant used (acid or base), the concentration of the titrant, the intervals of pH to be titrated and the tolerance of obtained pH for each titration step. The type of titrant used was NaOH, however the concentration, the pH increments and the pH tolerance had to be optimised. Concentrations of titrants of 0.05, 0.1 and 1M NaOH were tested. The increments tested were 0.1, 0.2, 0.3 and 0.5 units of pH with tolerances of 0.02, 0.05, 0.1 and 0.15. Sample

runs acquired data in triplicate for each pH value and each polymer concentration was tested in triplicate.

After the measurement conditions were optimised, the titrations were also performed in the inverse direction (i.e. from pH 12 to 2) with 1M HCl. The reverse titration would show any potential effect of dissolved and dispersed states of the polymer on zeta potential measurements and in pK_a values estimations. The MPT-2 contains a pH probe which was accurately calibrated daily at controlled room temperatures and the calibration data compared to previous measurements to assure reproducibility of the obtained data.

3.2.2.3. Optimization of calculations

The pK_a value of the tested polymers was estimated based on the obtained zeta potential vs pH curves. The methodology for calculating the pK_a value evolved over the course of the work and as more data was being generated. For each sample, data in triplicate was averaged and a zeta potential vs pH curve was obtained, from which a minimum ($Zeta_{min}$) and maximum ($Zeta_{max}$) zeta potential plateaus were defined. The early method of calculation involved extrapolating the pH value corresponding to half of the $Zeta_{max}$. As this method proven to not be accurate, a new approach followed which considered both $Zeta_{min}$ and $Zeta_{max}$ into calculations. This approach considered the median value between $Zeta_{min}$ and $Zeta_{max}$ and from there the pH value which would correspond to the pK_a was found. Ultimately, the final method for calculation involved the determination of the median zeta value. This value was then be used to find the corresponding pH value using a linear regression of the zeta potential vs pH curve, fitted between the $Zeta_{min}$ and $Zeta_{max}$ plateaus (Figure 3.2).

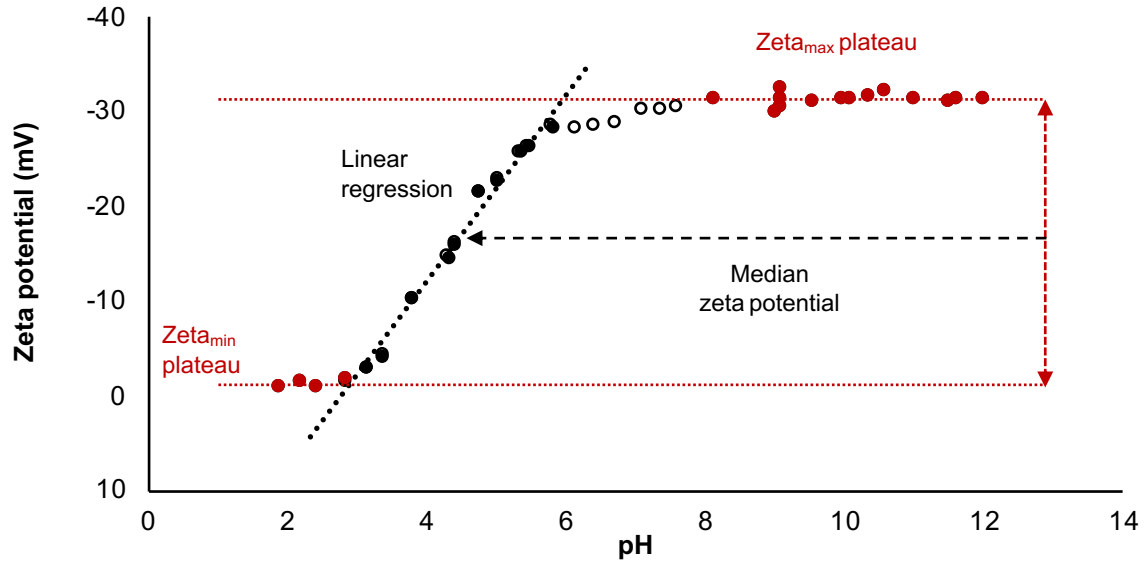

Figure 3.2: Example of analysis applied to each zeta potential vs. pH curve, with the determination of the Zeta$_{min}$, Zeta$_{max}$ and median zeta potential, applied to the linear regression to determine the corresponding pH, i.e. pK$_a$.

3.2.2.4. Zeta potential measurements and pK$_a$ determination at different concentrations

Considering the methodology used for the zeta potential determination (DLS), the effect of the concentration of the polymeric dispersions needed to be assessed to validate the robustness of the technique over a range of concentrations. Therefore, suspensions with different polymer concentrations (from 0.1-0.5% w/v) were prepared as optimised in section 3.2.2.1 and the zeta potential was measured. To assess the possible significance of polymer concentration influence, a statistical analysis was performed on the determined pK$_a$ values using One-way ANOVA tests, with a significance level of 0.05. Differences were considered non-significant when $p>0.05$.

3.2.3. Ionization studies and pK$_a$ determination of natural materials

Following the optimisation and validation of the methodology using commercially available synthetic polymers, diverse natural materials with well-known uses in food and pharmaceutical applications were tested. The ionisation behaviour of these polymers was investigated and, where applicable, their pK$_a$ value was estimated. Considering the nature of these materials and previous experience handling natural polymers, these samples were titrated only over a pH range of 2 to 10 to not cause hydrolysis and degradation at extreme alkaline conditions.

Table 3.2: Natural materials used in this study and their food and pharmaceutical applications.

Gum	Structure	Common uses and applications
1. Gums containing acidic moieties		
Gum Arabic	Main chain consisting of β-(1,3) linked galactose units with branches of β-(1,6) linked galactose and arabinose with terminal rhamnose and glucuronic acid. Contains 2% of protein within the structure [1].	Suspending agent, emulsifying agent, binder in tablets, demulcent and emollient in cosmetics [2,3], osmotic drug delivery [4].
Citrus peel pectin	Linear chain of α-(1,4) linked galacturonic acid units, with up to 80% of these occurring as methyl esters. Contains up to 4% of rhamnose units, which are then linked to arabinose, galactose and xylose side chains [1].	Thickening agent, suspending agent, stabilizer [2, 5], floating beads [6], controlled drug delivery (ocular [7], transdermal [8], colonic [9, 10])
Alginate	Linear structure consisting of (1,4) linked β-mannuronic and α-guluronic acids, with proportions depending on the source [1].	Thickening agent, stabilizer [2, 5], sustained release agent [11, 12], film coatings [13], mucoadhesive systems [14].
Arabinoxylan	Main chain consisting of β-(1,4) xylose, substituted with arabinose on the C-2 and/or C-3 positions [15] and phenolic acids (e.g. ferulic acid) linked to C-5 position of arabinose [16].	Wound dressing [17], gelling agent [18], controlled drug delivery systems [19]
2. Gums containing basic moieties		
Chitosan	Deacetylated derivative of chitin composed of randomly distributed β-(1-4)-linked glucosamine (deacetylated unit) and N-acetyl-glucosamine (acetylated unit) [14].	Tissue engineering [20, 21, 22, 23, 24, 25, 26], wound dressing [27, 28], antibacterial [29], drug delivery [30].

Table 3.2: Natural materials used in this study and their food and pharmaceutical applications.

Gum	Structure	Common uses and applications
3. Sulphated gums		
κ-carrageenan	Disaccharide repeat unit of β-(1,3) linked galactose-4-sulfate and α-(1,4) linked 3,6-anhydrogalactose residues [1].	Thickening agent, gelling agent, stabilizer [2], laxative [5], tablet matrix [31], controlled release agent [32, 33, 34].
4. Gluco and galactomannans		
Guar gum	Main chain consisting of β-(1,4) mannose units with galactose with α-(1,6) linked branches. Mannose to galactose ratio is 2:1 [1].	Binder, disintegrant, thickening agent, emulsifier, laxative [2,5], sustained release agent [35], colon targeted drug delivery [36].
Tara gum	Main chain consisting of β-(1,4) mannose units with galactose with α-(1,6) linked branches. Mannose to galactose ratio is 3:1 [1].	Thickener, stabilizer [2,5], controlled release agent [37, 38, 39].
Locust bean gum	Main chain consisting of β-(1,4) mannose units with galactose with α-(1,6) linked branches. Mannose to galactose ratio is 4-4.5:1 [1].	Thickener, stabilizer [2,5] and controlled release agent (oral, buccal, colonic, ocular and topical) [40].
Konjac	Main chain consisting of β-(1,4) mannose and glucose units with α-(1,3) linked branches. Mannose to glucose ratio is 1.6:1 [1].	Gelling agent, thickener, emulsifier, stabilizer[5] Controlled release formulation [41, 42, 43, 44].

1: (Williams and Phillips, 2003a), 2: (Williams and Phillips, 2003b), 3: (Beneke et al., 2009), 4: (Lu et al., 2003), 5: (Prajapati et al., 2013) 6: (Sriamornsak et al., 2007), 7: (Giunchedi et al., 1999), 8: (Musabayane et al., 2003), 9: (Vandamme et al., 2002), 10: (Wong et al., 2011), 11: (Hodsdon et al., 1995), 12: (Maiti et al., 2009), 13: (Rajsharad et al., 2005), 14: (Kesavan et al., 2010), 15: (Dornez et al., 2009), 16: (Mendis and Simsek, 2014) 17: (Aduba et al., 2019), 18: (Niño-Medina et al., 2010) 19: (Tulain et al., 2018), 20: (Kawakami et al., 1992), 21: (Mattioli-Belmonte et al., 1999), 22: (Tze Wen Chung et al., 2002), 23: (Taek Woong Chung et al., 2002), 24: (Hu et al., 2004), 25: (Wang et al., 2005), 26: (Shalumon et al., 2009), 27: (Kumar et al., 2010), 28: (Madhumathi et al., 2010), 29: (Rahman Bhuiyan et al., 2017), 30: (Ali and Ahmed, 2018), 31: (Picker, 1999), 32: (Leong et al., 2011), 33: (Li et al., 2014)*, 34: (Mahdavinia et al., 2015), 35: (Al-Saidan et al., 2005), 36: (Chourasia and Jain, 2004), 37: (Zeng et al., 2005), 38: (Rutz et al., 2013), 39: (Ma et al., 2017), 40: (Dionísio and Grenha, 2012), 41: (Du et al., 2006), 42: (Alvarez-Manceñido et al., 2008), 43: (Fan et al., 2008), 44: (Wang et al., 2014) .*

3.3. Results

3.3.1. Method validation for pK_a determination

For the validation of the proposed method, the acrylic and HPMC-based polymers were used. Their ionisation behaviour was obtained over a range of pH and their pK_a was calculated. The optimisation of the technique and of the calculation parameters are described in the following sections.

3.3.1.1. Optimization of polymeric dispersions

For the optimization of the polymeric dispersions used in the zeta potential measurements three methods were tested involving a magnetic stirring plate, a high shear mixer or a combination of both.

Results showed that using the magnetic stirring plate alone was not enough to break the agglomerates formed during the mixing at low pH, not forming a suitable dispersion to be measured by ELS. The use of the high-shear mixer alone was also not optimal, as without the wetting of the particles induced by the magnetic stirring, these would adsorb to the metallic end of the mixer, dampening the homogenisation.

From Figure 3.3 is possible to observe that with the addition of the homogenisation step, particle size in all dispersions decreased extensively. AS-LF and AS-HF showed a less pronounced reduction, however this is due to the already low particle size achieved by simple stirring. These polymers are supplied as much finer powders than the remaining polymers, thus showing much lower values of particle size. The combination of magnetic stirring followed by high-shear mixing was therefore chosen to continue the preparation of the following polymeric dispersion for zeta potential measurements.

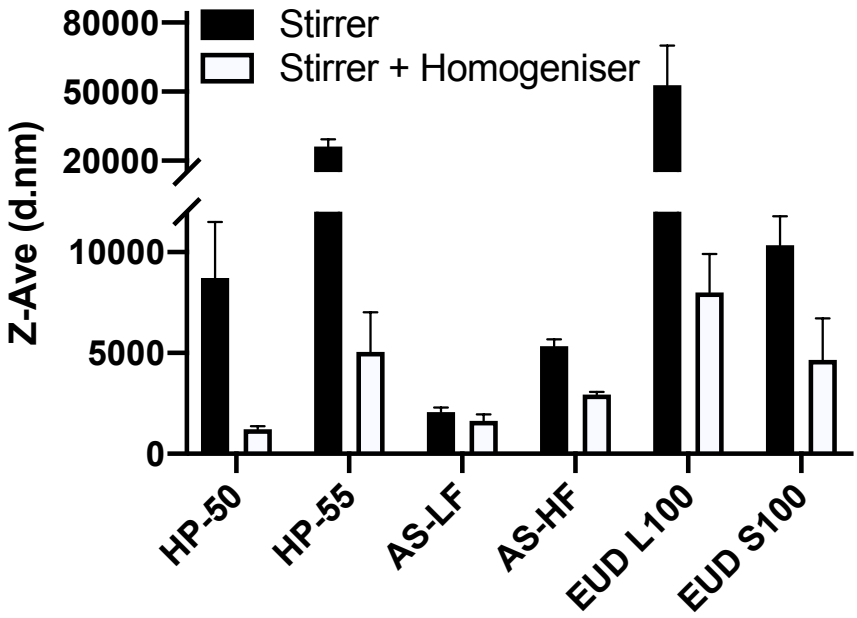

Figure 3.3: Particle size (dynamic light scattering) measurements of the prepared dispersions using the magnetic stirrer alone, or a combination of magnetic stirring + high-shear mixer.

3.3.1.2. Optimisation of measurement parameters

The choice of the pH increments and tolerance was based on the reproducibility of the results, time of run per sample and actual conclusion of the measurements.

Increments in pH of 0.1 or 0.2 units would lead to long run times per sample, reaching 7 h for 0.1 units and about 4 h for 0.2 units. Also, small increments in pH would require smaller tolerances, causing the algorithm of the software to not accept the obtained pH more often after titrations, and continuing to titrate for longer times until acceptance was achieved. This would lead to much longer run times, with runs sometimes not being concluded due to excessive time used in titrating the sample. On the other hand, increments of 0.5 units would lead to less data points in the titration curves, providing less accurate results for further calculation of the pK_a value.

As already mentioned, tolerances of 0.02 and 0.05 would cause severe delays to the titrations and increase the sample run time. However, the need for a higher tolerance arose not only from the long run times when using smaller tolerances, but also due to the reproducibility of the measurements. When the tolerance was low (0.02 or 0.05) and the software's algorithm would not accept the obtained pH after a titration, more volume of titrant was added until acceptance. However, near the pK_a, even small volumes of titrant will cause a great impact in the pH, so it was

common that the pH would increase too much at certain pH points when lower tolerances were used, due to over-addition of titrant. This would provide zeta potential vs. pH curves with missing values near the pK_a and non-matching replicates, decreasing the accuracy of the calculations, and providing over or underestimated pK_a values. In the end, the combination of titration parameters which provided the smoothest, less time-consuming titrations and less prone to errors consisted in increments of 0.3 units with a tolerance of 0.15 units.

3.3.1.3. Optimisation of pK_a determination

For the calculation of the pK_a value, different analyses were applied to the generated data. As stated before, the pK_a value corresponds to the pH at which an ionisable molecule contains 50% of its groups ionised. Following this, the first method to calculate the pK_a consisted in simply halving value of $Zeta_{max}$ which would correspond to 50% ionisation and use it to extrapolate the corresponding pH. However, this approach was very keen to errors as it did not account for the $Zeta_{min}$ values, causing over- or underestimations of the pK_a when the $Zeta_{min}$ was not zero.

Improving from the incomplete methodology, the second approach accounted for both $Zeta_{min}$ and $Zeta_{max}$, using both to determine the median Zeta potential, necessary to extrapolate the corresponding pH. This allowed for a more accurate determination of the true zeta potential variation caused by the shifting pH, leading to more reproducible results.

Aiming for a more automated method, slight alterations were made. Both $Zeta_{min}$ and $Zeta_{max}$ were calculated from the average of each plateau, with the median Zeta determined using these averages, and a linear regression was fitted to the linear portion of the zeta potential vs. pH curve to extrapolate the corresponding pK_a value (Figure 3.2).

This final approach allowed calculations with minimised errors and was applied for the optimisation of the previously described parameters of the measurement (pH interval and tolerance), allowing to exclude sub-optimal measurement parameters.

3.3.2. Zeta potential measurements of synthetic polymers

The zeta potential measurements of the tested synthetic polymers are summarised in Table 3.3, where a clear trend between zeta potential and environmental pH can be seen with all

measurements showing an increase in the zeta potential with an increase in the environmental pH. This is not surprising for weakly acidic polymers. The opposite trend was observed for EUDRAGIT E100 (a weak base), with zeta potential decreasing with increasing pH, showing that this polymer is more extensively ionised at lower pHs, i.e., $pH<pK_a$.

The weakly acidic polymers exhibited a near zero zeta potential at low acidic pH (pH ≈ 2), suggesting most of the polymeric species were at their unionised state (>99%) (Figure 1.6). As the pH increases, there is an increase in the ionised fraction (i.e., [HA] to [A^-]) which results in a net increase in negative charge on the polymer surface causing an increase in the zeta potential, which plateaus when most of the HA has been converted to A^-. Interestingly, the shape of the zeta-profiles was independent of polymer concentrations used (Figure 3.4), hence increasing the reliability of measured pK_a values using this technique.

The $Zeta_{max}$ was determined from zeta profiles and the pK_a value of each polymer was estimated accordingly. Table 3.3 summarises the estimated pK_a values using this technique in comparison with the reported literature values.

3.3.2.1. Effect of polymer concentration

It can be argued that a change in polymer concentration may influence the $Zeta_{max}$ and therefore can affect the pK_a value estimation. Therefore, the effect of polymer concentrations on pK_a value estimation was also studied to ascertain the reliability of the measurement. Interestingly, the concentration of the polymeric dispersion does not affect the pK_a value estimation (Figure 3.5), with statistical analysis exhibiting no significant differences ($p>0.05$) in the estimated pK_a values between different concentrations.. In the case of HP-50, however, the estimated pK_a value appeared to decrease with increasing polymer concentration from 0.1 to 0.5% w/v. To confirm this behaviour, a higher concentration of 1% w/v was tested, and no significant difference was found ($p >0.05$) in estimated pK_a values across concentrations.

Figure 1.6 indicates that at an environmental pH two units above the polymer's pK_a value extensive ionisation occurs, which leads to complete dissolution of polymeric chains. However, this may not be the case with every polymer, and whilst some may dissolve enough to enable drug release at earlier stages of ionisation, others may only allow the release of the drug at much later stages.

Table 3.3: Summary of estimated and reported pKa values for the commonly used synthetic polymers.

Polymer	Dissolution pH threshold	$Zeta_{max}$	Estimated pK_a	Reported pK_a *
Synthetic polymers				
EUDRAGIT E100	≤ 5.0 [1]	24.88 ± 1.66	8.45 ± 0.14	9.0 [4]
HP-50	≥ 5.0 [2]	-14.69 ± 0.89	3.99 ± 0.09	4.20 [5]
HP-55	≥ 5.5 [2]	-19.75 ± 0.95	3.54 ± 0.20	4.49 [5] 4.83 ± 0.04 [6]
HPMC AS-LF	≥ 5.5 [3]	-15.25 ± 1.14	4.80 ± 0.20	5.10 ± 0.07 [7] 5.09 ± 0.05 [6]
EUDRAGIT L100	≥ 6.0 [1]	-29.88 ± 1.80	4.45 ± 0.13	6.62 ± 0.04 [7] 6.45 ± 0.03 [6]
HPMC AS-HF	≥ 6.8 [3]	-8.76 ± 0.29	4.85 ± 0.16	4.82 ± 0.03 [7] 5.15 ± 0.05 [6]
EUDRAGIT S100	≥ 7.0 [1]	-27.61 ± 0.59	4.91 ± 0.13	6.76 ± 0,03 [7] 6.66 ± 0.05 [6]
Natural polymers				
Gum Arabic		-12.13 ± 0.13	3.20 ± 0.11	3.18 ± 0.02 [7, #]
Citrus pectin		-16.05 ± 0.57	3.37 ± 0.04	3.5 [8]
Alginate		-29.94 ± 1.45	3.45 ± 0.03	3.4 [9]; 4.4 [10]
Chitosan		28.79 ± 1.11	6.75 ± 0.22	6.32 ± 0.02 - 6.47 ± 0.03 [11]
Arabinoxylan		-19.26 ± 1.08	4.61 ± 0.19	-

**: potentiometric determinations from literature.*
[#]: based on glucuronic acid pK_a value in gum Arabic
1: Evonik Industries AG (2019), *2: Shin-Etsu Chemical Co.* (2002), *3: Shin-Etsu Chemical Co.* (2018), *4: Quinteros et al.,* (2011), *5: Davis et al.,* (1986), *6: Riedel and Leopold* (2005), *7: Schmidt-Mende* (2001).

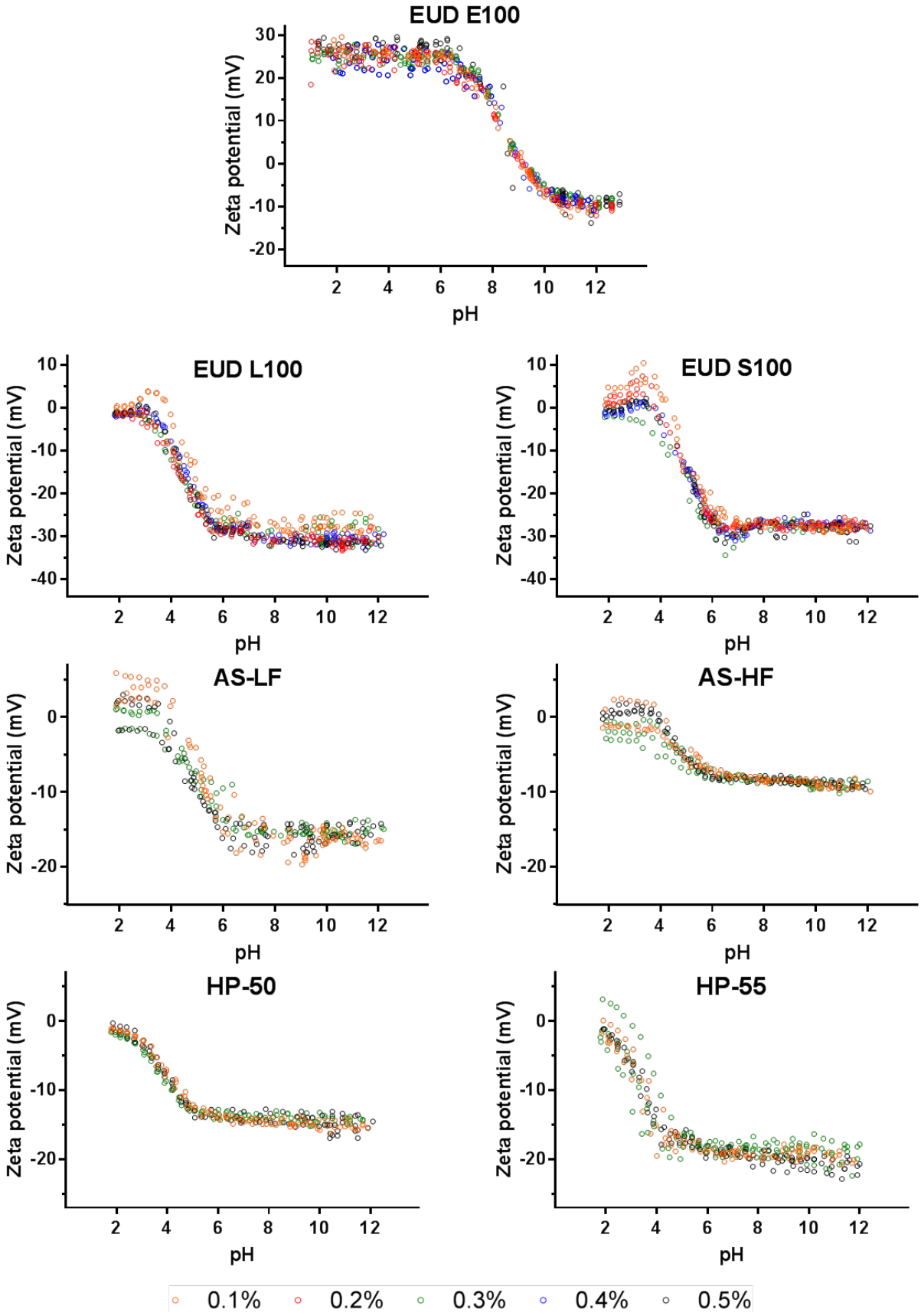

Figure 3.4: Zeta potential vs. pH profiles of various synthetic polymers at concentrations from 0.1 - 0.5 % (w/v) showing no significant effect of changes in concentration on zeta-profiles and pK_a value estimation.

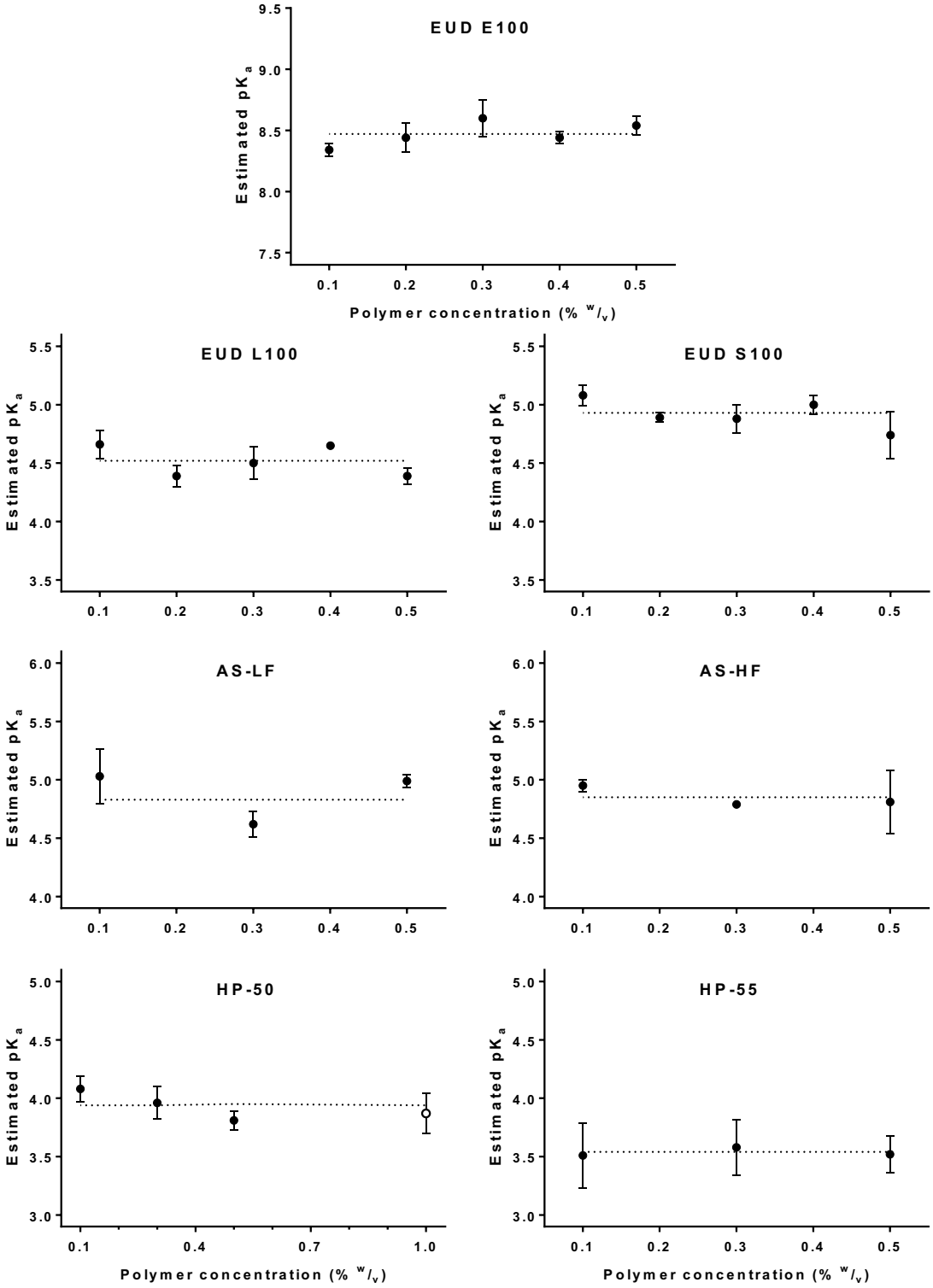

Figure 3.5: Effect of polymer concentration (0.1% - 0.5%w/v) on pK_a value estimation. Closed symbols (●) represent the estimated pK_a values corresponding to polymer concentation. The open symbol (○) on HP-50 graph represents an additional measurement at 1%w/v polymer concentration to confirm a possible trend. No significant difference was found between concentrations ($p>0.05$) for all tested polymers.

3.3.2.2. Hydrophobic effects on zeta potential measurements

Certain polymers (e.g. EUDRAGIT L100 and S100) demonstrate a slightly positive zeta potential at lower pHs (pH 2 to 4) (Figure 3.4), particularly at the lowest concentration studied (0.1% w/v). However, this effect disappears at polymer concentrations ≥ 0.3%w/v. This may be attributed to the non-ionised state of these polymers at low concentrations under acidic conditions. At low pH ($pH<<pK_a$), the acidic moieties of the polymeric chains are unionised and undissolved, which increases the polymer's hydrophobicity compared to when some charged species are present, causing the polymer structure to fold so to reduce the exposed surface area of the chains. Hydronium ions (H_3O^+) behave more hydrophobically than water molecules, accumulating at the interface between water and a hydrophobic media (Luxbacher, 2014; Vácha et al., 2008). Therefore, at acidic pH, the adsorption of H_3O^+ ions to the uncharged polymeric chains creates a slightly positive charged surface at very low polymer concentrations as seen in Figure 3.4. On increasing pH, the ionisation of the acidic groups produces a substantially more negatively charged surface and hence an overall negative zeta potential. This effect was absent at higher polymer concentrations (≥ 0.3%) possibly due to the increased polymer/hydronium ion ratio. The polymeric chains are therefore less densely covered by the positively charged H_3O^+ ions. This renders negligible movement of the particles during measurements when a charge was applied during electrophoretic light scattering and generated a signal near zero mV.

3.3.2.3. pH dissolution threshold vs. pK_a

Figure 3.6 compares the estimated pK_a value of polymers to their reported dissolution pH thresholds. For all enteric polymers, it was found that the reported dissolution pH thresholds were always above the estimated pK_a value. In contrast, EUDRAGIT E100, a reverse enteric polymer, contains ionisable amine groups. Therefore, complete ionisation (i.e., dissolution) of the polymer is expected below its measured pK_a value. As mentioned earlier, the manufacturers do not mention how the dissolution pH thresholds were calculated and there is no known standardisation of approach among different polymer manufacturers. It is likely, that some may report complete dissolution of a polymeric film at a given pH while others may rely upon the onset of drug release from the enteric coated a dosage form. In our study, the rank order of polymer dissolution pH-

thresholds did not follow the measured pK_a value for some polymers. For instance, the estimated pK_a value for HP-50 was higher than for HP-55 despite its lower dissolution pH threshold. This can be attributed to the polymer structure and the density of acidic (ionisable) moieties on polymer backbone (Table 3.4).

It can be seen from the zeta potential measurements (Figure 3.4) that EUDRAGIT L100, HPMC AS-LF and HP-55 have higher $Zeta_{max}$ values compared to their counterparts, EUDRAGIT S100, HPMC AS-HF and HP-50, respectively. This is in agreement with density of acidic ionisable groups on the polymer (Table 3.4).

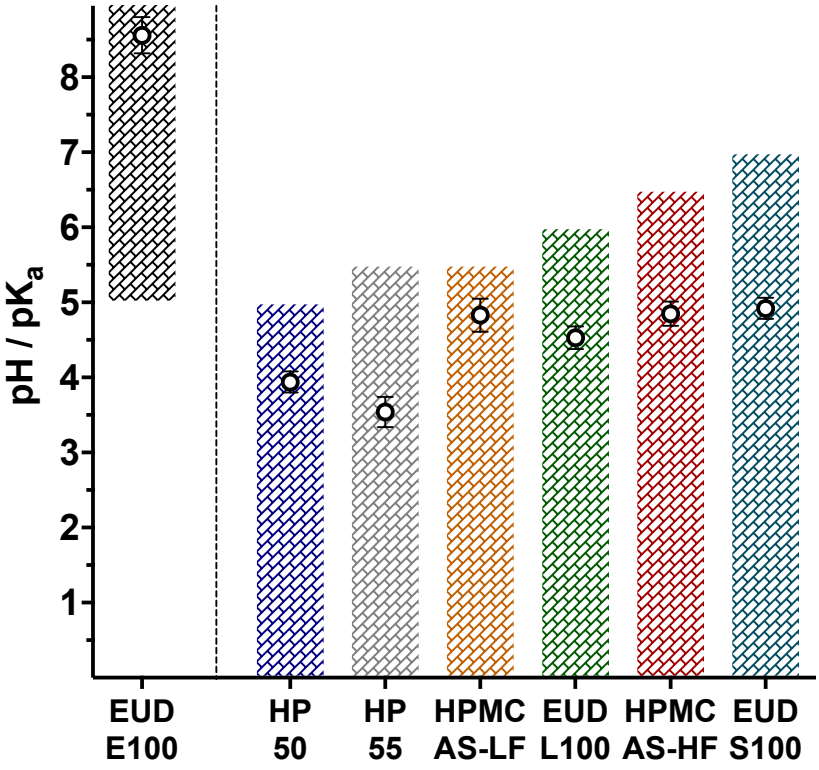

Figure 3.6: Dissolution behaviour of the tested polymers. The bars represent dissolution pH-thresholds (i.e., shaded areas represent the pH at which the polymers are undissolved). The open circles (○) represent the estimated pK_a value (mean ± STD, n=9), using the proposed technique.

Table 3.4: Composition of the respective free carboxyl groups of the studied polymers and respective structures.

Polymers	% ionsable groups	pH Dissolution Threshold	$Zeta_{max}$ (mV)
HP-50	21-27% (phthalyl) [1]	5.0	-14.69 ± 0.89
HP-55	27-35% (phthalyl) [1]	5.5	-19.75 ± 0.95
HPMC **AS-LF**	14-18% (succinoyl) [2]	5.5	-15.41 ± 1.22
HPMC **AS-HF**	4-8% (succinoyl) [2]	6.8	-8.76 ± 0.29
EUDRAGIT **L100**	46-50% (methacrylic) [3]	6.0	-29.88 ± 1.80
EUDRAGIT **S100**	23-30% (methacrylic) [3]	7.0	-27.73 ± 0.52

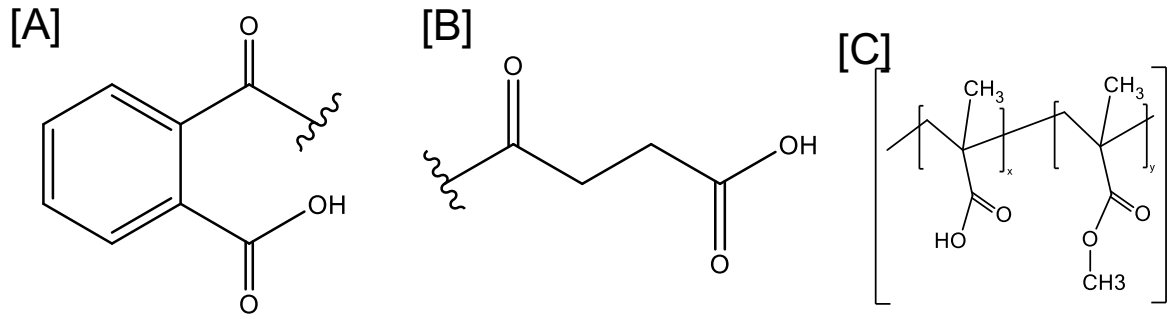

***A:** Phthalyl group; **B:** Succinoyl groups; **C:** x – Methacrylic acid, y – Methyl Methacrylate.*
1: (Shin-Etsu Chemical Co., 2002)*, 2:* (Shin-Etsu Chemical Co., 2018)*, 3:* (Evonik Industries, 2012)

A lower pH dissolution threshold is reported by the manufacturers for polymers containing succinoyl (HPMC AS) or methacrylic groups (EUDRAGIT S100/L100) if higher number of acidic moieties are present on the polymer backbone (Table 3.4). For these polymers, increased density of ionisable species achieves the degree of ionisation needed to show significant dissolution at a lower pH than a polymer with lower density of ionisable species. The latter would need a higher pH to attain the degree of ionisation needed for the dissolution of the polymeric strands. However, this is not true for the polymers containing a phthalyl group (HP 50/55). In this case, the polymer with higher number of acidic functional groups (HP-55) exhibited the highest dissolution pH threshold. This may be due to the presence of an aromatic acidic moiety that hinders the dissolution of the polymeric chains when compared to an aliphatic substituent group (such as HPMC AS) (Figure 3.7). The process of dissolution of a polymer involves water diffusion into the polymer matrix, which eventually leads to the disentanglement of the polymeric chains and consequent dissolution (Figure 3.1D). For these polymers, the presence of the aromatic group may influence its solubility by two factors.

Firstly, the aromatic ring creates a more planar spatial conformation (Figure 3.7E). Due to a higher number of sidechains on the HP-55 polymer backbone (and thus a higher number of aromatic rings), increased interaction between polymeric chains (π-π interactions and hydrophobic interactions within the aromatic rings) may occur. This may mean more complex entanglement of the polymeric chains, and possibly a slower dissolution. This would explain why the estimated pK_a value for HP-50 is higher than the one for HP-55 (3.94 vs. 3.54), even though its dissolution pH threshold is lower. Secondly, the phthalyl group has less conformational flexibility compared to the succinoyl group, as it only contains two rotatable bonds and both are on the same side of the aromatic ring (Figure 3.7F) whereas all the carbons in the succinoyl group can freely rotate (Figure 3.7C) .This causes an increased rigidity in phthalyl groups compared to the succinoyl group leading to less freedom of movement during the disentanglement of the polymeric chains (Figure 1.7). Ultimately, this effect hampers polymer dissolution, despite the ionisation of acidic moieties across polymer chains. Therefore, for these polymers, the presence of aromatic rings possibly plays a more important role in polymer dissolution than its ionisation.

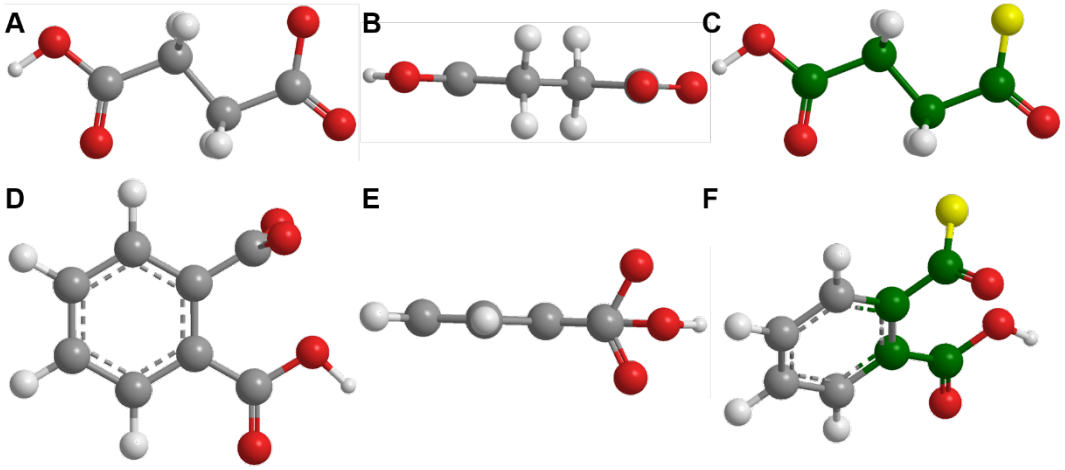

Figure 3.7: 3D structures of succinoyl (A, B and C) and phthalyl (D, E and F) groups. Atoms in green represent rotational bonds. Atoms in yellow represent the binding site to the remaining polymer structure. Figure drawn using information from Shin-Etsu Chemical Co. (2018, 2002).

3.3.2.4. pK_a estimation: Zeta potential vs potentiometric determinations

In this work, the pK_a value of various polymers was measured based on their ionisation behaviour obtained from the zeta potential profiles. The proposed method may present more accurate pK_a estimations than the traditional potentiometric determination, which are based on measuring bulk solution pH (the concentration of H^+). However, it is evidenced that the pH at the boundary layer

(the interface between the polymeric coatings and the media, Figure 1.7) may greatly differ from the bulk pH (Harianawala et al., 2002; Krieg et al., 2014) and therefore can significantly influence the ionisation and dissolution of these polymers. The boundary layer has an abundance of H^+ being released from the dissolving polymer which do not diffuse into the bulk solution readily, rendering it more acidic than the bulk solution. Potentiometric determinations therefore rely on bulk pH of the media and do not consider conditions within the boundary layer. This leads to an underestimation of the titrant needed to raise the bulk pH thus shifting the titration curve to slightly higher pH values leading to over estimation of pK_a values. Hence, the effective pK_a values of these polymers are expected to be lower than the apparent potentiometric determinations.

In contrast, studies involving zeta profiles rely on zeta potential (i.e., charge) determinations using dynamic light scattering. These measurements relate to the net charge acquired by the dissolving polymer at the boundary layer instead of relying merely on bulk pH determinations. This leads to lower pK_a values estimations than those reported by potentiometric methods (Table 3.3) and therefore a more accurate representation of ionisation behaviour of these polymeric materials at the boundary layer.

3.3.3. Ionisation and pK_a determination of natural polymers

After satisfactory method development and determinations using well-known synthetic polymers, the described method was employed to study the ionisation behaviour of some commonly used natural gums (polysaccharides) over a range of pH values. The studied polysaccharides differ significantly in their chemical structures and distinctive ionisation behaviour was found from their zeta profiles.

3.3.3.1. Gums containing acidic moieties

This group represented gums containing sugar acids. They comprise sugar monomers where terminal hydroxyl groups are oxidised to carboxylic acids forming uronic acids. The presence of these ionisable groups may therefore play an important role in the polysaccharide dissolution. From this group of polysaccharides, gum arabic, citrus pectin, sodium alginate and arabinoxylan were studied and their ionisation behaviour is shown in Figure 3.8 and estimated pK_a values are summarised in Table 3.3.

The shape of the zeta profiles corresponds to typical weak acid ionisation behaviour as found with gastro-resistant polymers, which can be attributed to the presence of uronic acids moieties in the polymeric structure or phenolic acid residues in the case of arabinoxylan. Alginate has a much higher $Zeta_{max}$ than gum Arabic and citrus pectin, arising from differences in their polymeric structure. Gum Arabic possesses a chain of galactose units containing acidic units only at the terminus of each branch (Table 3.2). Citrus pectin contains a long chain of galacturonic acid units; however, 80% of these are in the form of methyl esters, hence reducing the number of available ionisable groups. Alginate, on the other hand, has a linear structure comprising repeating units of mannuronic and guluronic acids. This explains a higher $Zeta_{max}$ found in alginate compared to pectin and gum arabic. Arabinoxylan, on the other hand, has its ionization behaviour dictated not by uronic acid residues, but by the phenolic acids in its structure, such as ferulic acid. Interestingly, arabinoxylan, HP-50 and HP-55, which bear similar functional groups (aromatic acids) have displayed similar $zeta_{max}$ (~20mV), which further demonstrated the influence of the present functional groups.

The ionisation behaviour of these polymers was similar to those employed in a typical gastro-resistant formulation. Therefore, these polymers have been extensively investigated to formulate modified release delivery systems (Albertini et al., 2010; Alvarez-Lorenzo et al., 2013; Arroyo-Maya and McClements, 2015; Bagheri et al., 2014; Chen and Subirade, 2009; Chuang et al., 2017; Czarnocka and Alhnan, 2015; De Barros et al., 2015; Kesavan et al., 2010; Lambert et al., 2008; Lu et al., 2003; Luo et al., 2015; Maiti et al., 2009; Reis et al., 2006; Sansone et al., 2011; Shi et al., 2016, 2013; Sriamornsak et al., 2007; Vandamme et al., 2002; Villena et al., 2015; Wang et al., 2014; Wong et al., 2011; Wu et al., 2016; Zhang et al., 2014).

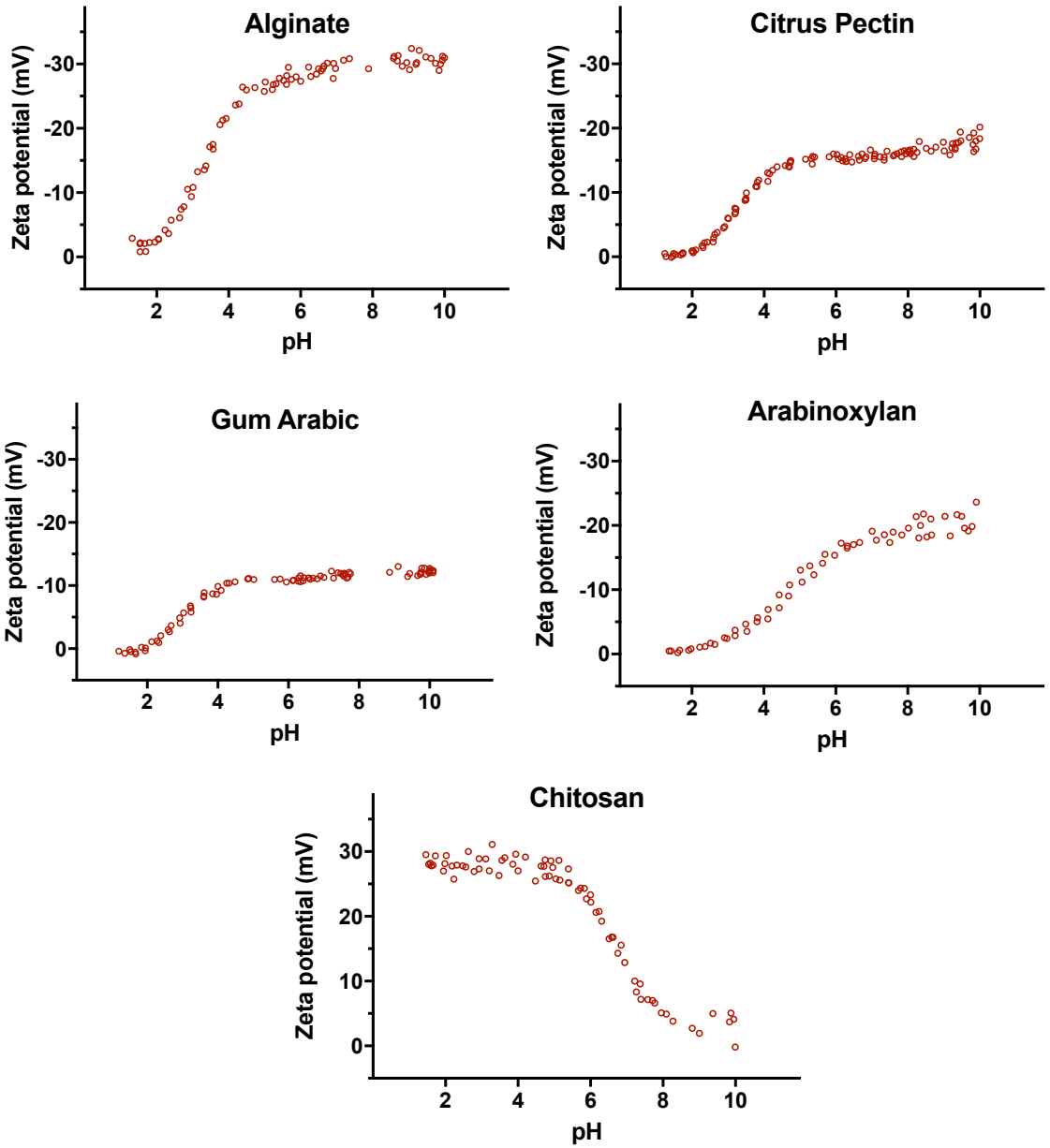

Figure 3.8: Zeta potential vs. pH profiles of polysaccharides containing acidic (alginate (0.05% (w/v)), Citrus pectin (0.3% (w/v)), Gum Arabic (0.3%(w/v)), and Arabinoxylane (0.3% (w/v))) and basic (Chitosan (0.1% (w/v)) moieties.

Probiotic Pearls™ is a commercially available example containing a blend of gelatine and pectin in the outer layer to provide gastric acid protection to encapsulated probiotics (Nature's Way Products, 2011a, 2011b). These systems are however more suitable for drug delivery to the colon. Nutrateric® is another commercially available coating formulation comprising a pH independent ethylcellulose film containing alginate (Colorcon®, 2019), which acts as pH dependent pore former. There are, however, some reports in literature of premature drug release in gastric conditions and much delayed drug release in small intestinal conditions post gastric emptying with alginate-based

formulations (Ali-Merchant et al., 2009; Czarnocka and Alhnan, 2015). Similar to synthetic polymers, the ionisation profile of the tested gums containing acidic moieties were not affected by different concentrations (data not shown).

3.3.3.2. Gums containing basic moieties

Chitosan was selected to represent gums containing basic moieties and the zeta potential profile of chitosan is shown in Figure 3.8. As expected, chitosan shows maximal ionisation at pH << pKa, similarly to EUDRAGIT E100, the commercially available reverse enteric polymer. At low pH (~2–4) the amine groups in chitosan are fully ionised producing a maximum zeta potential, which drops as the pH increases and polymer becomes less ionised. The versatility of chitosan has prompted extensive studies in designing immediate release (Imai et al., 2000; Rasool et al., 2012) and controlled release (Imai et al., 2000; Shi et al., 2008; Yuan et al., 2010) drug delivery systems.

3.3.3.3. Gluco and galactomannans

Gluco- and galactomannans are widely used natural gums comprising mannose backbone with glucose or galactose side chains, respectively. These polymers are mainly composed of the two sugars which do not contain any ionisable moieties, and therefore are referred to as neutral polysaccharides. From this group of polysaccharides, Guar, Tara, Locust bean and Konjac gums were studied and their zeta profiles are shown in Figure 3.9. As expected, all four gums show a zeta potential near zero mV throughout the tested pH range. The absence of acidic or basic (i.e. ionisable) groups causes the gum to maintain neutrality, and therefore a pK_a value estimation is not applicable.

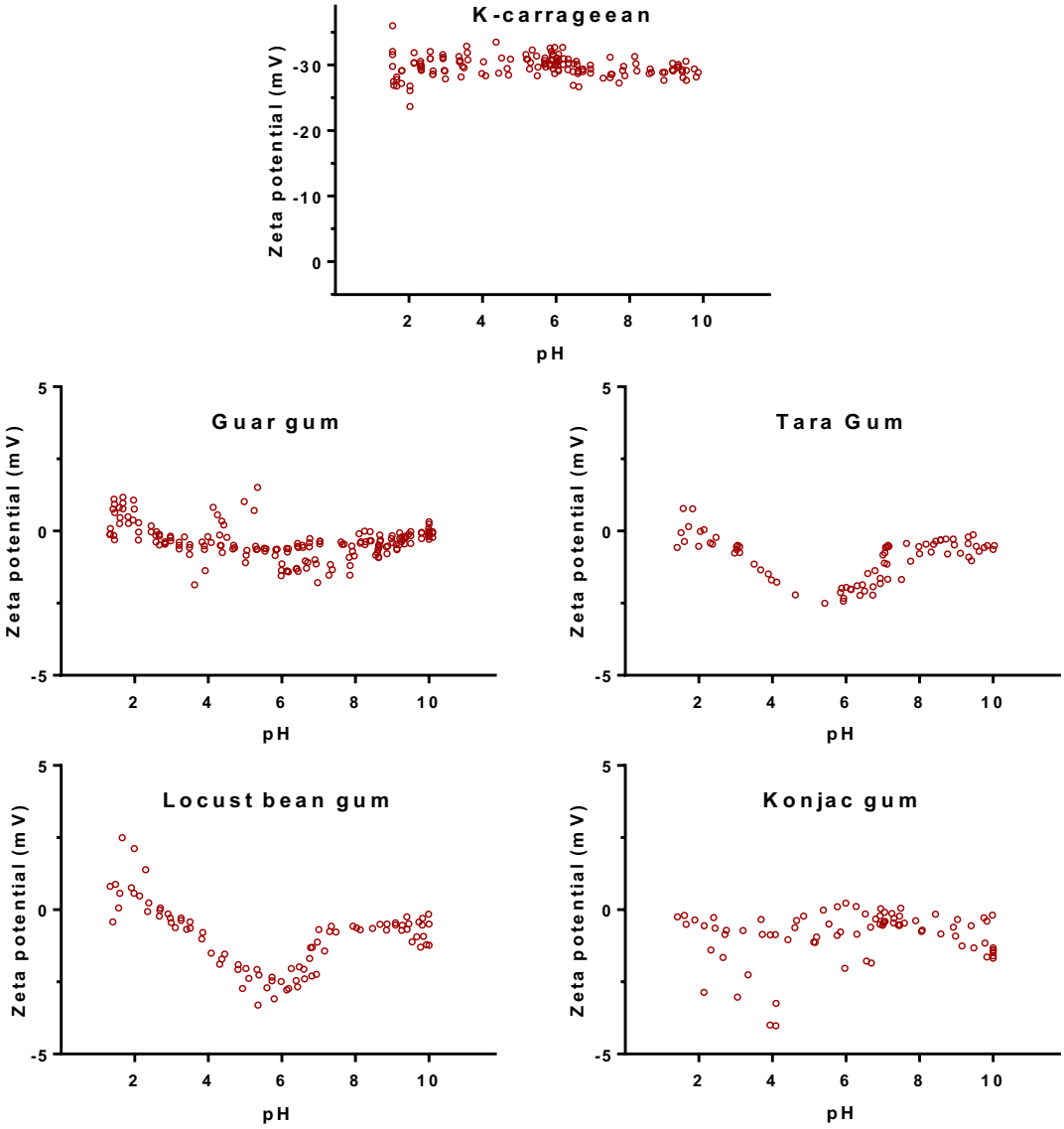

Figure 3.9: Zeta potential vs. pH profiles of the studied sulphated (K-carrageenan) and neutral polysaccharides (Guar, Tara, Locust bean and Konjac gums) at concentration 0.1% (w/v).

3.3.3.4. Sulphated polysaccharides

Marine algae produce sulphate-containing polysaccharides, such as fucans, ulvans and carrageenans (Patel, 2012). Carrageenans have been studied for drug delivery purposes, showing promising uses both in immediate release (Ghanam and Kleinebudde, 2011) and in delayed release formulations (Picker, 1999). Figure 3.9 shows the ionisation behaviour of κ-carrageenan, a sulphated polysaccharide, which attained a highly charged ionised state ($Zeta_{max}$= -30 mV) over the entire pH range used in this study (pH 2-10). Contrary to the weak acid groups (for instance carboxylic acids) found in other natural gums, these polysaccharides contain sulfonyl groups.

Sulfonic acids are strong acids and completely dissociate in water. This indicates that this group will have a very low pK_a, with ionisation occurring throughout the tested pH range

3.4. Final considerations

Obvious limitations can be argued from the use of this technique especially when applied to polymeric materials: a) the folding of the polymeric chains and consequent exposure of functional groups may influence the readings and thus the pK_a value determination; b) when the polymer is precipitated, the non-dissolved particles may interfere with the laser diffraction, providing false results; c) the stabilisation of the polymeric solutions is not achieved during the read times, possibly yielding unreal values. Despite the plausibility of these arguments, they may be countered by the highly reproducible results: although not all data is shown here, all polymers were measured numerous times, with data showing minimal deviation on the readings, as can be seen as an example in Figure 3.4; if the reproducibility between measurements is acceptable, either conformational changes of the polymeric chains and exposure of functional groups is unimportant, or it remains similar when conditions are identical. This would mean that when more biorelevant media are used, the obtained results will, as desired, more closely represent the polymer conformation *in-vivo*. Argument b) and c), regarding the phase when the polymer is precipitated and subsequent dissolution and stabilization of the solution can be simply argued by recalling that these are the condition the polymer encounters *in-vivo*: firstly in the stomach, where it is undissolved at a low pH, followed by a sharp increase of the surrounding pH at the duodenum bulb, leading to its quick ionisation. Additionally, regarding the possible interference of precipitated particles with the measurement, again the interpretation of the obtained results and their reproducibility provides a certain measure of assurance that acquired data is indeed reliable.

The molecular weight of the used polymers is also worthy of consideration. The polymers used in this work were significantly different in terms of molecular weight, ranging from 18.000 to 125.000 g/mol). The impact of these differences was not assessed, nor the influence of particle sizes. These two parameters would thus be considered in future development and work using this technique.

3.5. Conclusion

This chapter describes the work involved in the development of a new methodology for the estimation of the pK_a value of ionisable polymers based on zeta potential. The nature of the technique, in direct relation to the surface charge of the particle (in this case, a polymer) may provide more accurate information regarding the ionisation behaviour and pK_a value than more commonly used potentiometric methods.

This methodology allows for the ionisation study of both known and new polymeric materials, providing information regarding their potential use as gastroresistant materials. Addicionally, the use of more biorelevant media, mimicking the transitions in the GI tract (0.1M HCl and a biorelevant buffered system) will help understand the ionisation that possibly occurs *in-vivo* and obtaining this information for new polymers for enteric applications will lead to a better understanding of their dissolution behaviour, further aiding the rational design of drug delivery systems.

Chapter 4

MECHANISTIC INSIGHTS:
CAUSES, EFFECTS AND ULTIMATE REGULATION OF POLYMER DISSOLUTION

4.1. Introduction

For enteric polymer dissolution to occur, a pH threshold needs to be surpassed, so that the polymer has sufficient ionised groups to start this process. Nevertheless, when referring to gastroresistant polymers, pH is not the only factor for a successful dissolution. Indeed, the medium has to be at a suitable pH to ionise the polymer, yet there is also the need for a buffering species that will constantly neutralise the H^+ ions which would otherwise accumulate in the boundary layer. Information regarding specific dissolution mechanisms, and the true influence of the release media are scarce. Previous research has shown the limitations of using compendial phosphate-based release media (Liu et al., 2011), and indicated the importance of using a release medium with similar ionic composition and buffer capacity to biological fluids.

According to the United States Pharmacopoeia and the European Pharmacopoeia, the recommended tested medium for enteric coated dosage forms is 50 mM pH6.8 phosphate buffer. However, as seen in Table 1.7, the buffer capacity of this buffer and of the intestinal fluid (23.1 and 3.2 mmol/L/ΔpH, respectively) is remarkably different. During the dissolution of an enteric polymer, a higher capacity buffer would more effectively remove the ions accumulating at the boundary layer, and hypothetically increase its dissolution rate, ultimately affecting the dissolution of the drug. Without constant removal of the produced H^+ ions from the boundary layer by the buffer species, the accumulation of protons would lead to a decrease in pH in the vicinity of the polymer surface, halting its dissolution. Therefore, this discrepancy in buffer capacity of the recommended *in-vitro* dissolution media and the biological fluids will result in poor IVIVC as already reported by multiple studies (Al-Gousous et al., 2019, 2015; Garbacz et al., 2008; Karkossa and Klein, 2017; Merchant et al., 2014; Varum et al., 2014). This research thus aims to show the importance of buffer capacity in maintaining the appropriate pH_m during the dissolution of enteric polymers when testing gastroresistant dosage forms and also deepen the understanding regarding the effect of both the buffer species and the ionised functional groups in polymer dissolution rates.

To measure the dissolution rate, it is necessary to accurately measure polymer dissolution during a dissolution test, by quantifying the dissolved polymer over time. With this in mind, a methodology was developed based on the phenol-sulphuric acid (PSA) method. This method was firstly

described by Dubois et al.(1956), for the quantification of carbohydrates. The PSA method has since then been used and modified for the quantification of sugar in diverse samples (Chow and Landhäusser, 2004; Gerchakov and Hatcher, 1972; Jain et al., 2017; Kushwaha and Kates, 1981) and was more recently adapted by Ghori et al., (Ghori et al., 2014) for the quantification of HPMC released from the matrix of modified release tablets. Since this method was developed for the quantification of sugars, one of its limitations is the type of polymers it is able to detect. As previously described, the most commonly used enteric polymers are acrylic acid derivatives, cellulose derivatives and polyvinyl acetate phthalate (PVAP). This method allows for the quantification of cellulose derivatives, as these polymers can be broken down into simple sugars, therefore, different grades of HPMC-AS and HPMC-P were chosen to be used in this work.

The method used by Ghori et al., (2014b) was modified to decrease sample processing times and to increase reproducibility, allowing for the quantification of HPMC-based gastro resistant polymers. The dissolution rate of different enteric polymers was measured using the described method in a range of release media (phosphate and bicarbonate-based buffers) with different buffer capacities and was correlated with the determined pH_m values and with previously reported pK_a values (Chapter 3). Contact angle measurements were also performed for these polymers, using the same media as probes. Ultimately, the correlation between buffer capacity, buffer species, pH_m, pK_a, contact angle and dissolution rate of the polymers should allow for a better understanding of the mechanics of polymer dissolution.

4.2. Materials and Methods

4.2.1. Materials

Hydrochloric acid (37%w/w), Phenol (99+%w/w), sulfuric acid (95%w/w, Extra Pure), Ethanol (99%+w/w, Extra pure) and the salts used to prepare the buffer solutions were acquired from Fisher Scientific (Leicestershire, UK). Triethyl citrate (≥99%w/w) and talc (powder, 10 µm) were purchased from Sigma-Aldrich (Dorset, UK). Sodium hydroxide (98.5-100.5%w/w, pellets) was obtained from VWR International (Leicestershire, UK). The enteric polymers used in this study (hypromellose acetate succinate (HPMC AS) LF and HF, hypromellose phthalate (HP) 50 and 55 were kindly provided as samples from Shin-Etsu Chemical Co. (Chiyoda, Japan).

4.2.2. Preparation of polymeric disks

Throughout the work, the samples used consisted of polymeric disks prepared by adding appropriate amounts of each formulation shown in Table 4.1 into the wells of a 12-well plate (Thermo Scientific™ BioLite). The solutions were then allowed to evaporate at 40°C, forming the disk samples with ~22 mm diameter at the bottom of the wells, which were then retrieved, cut and used for later testing.

Table 4.1: Formulations used to prepare polymeric disks, based on Liu et al., (2011)

HPMCAS LF / HF		**HPMCP HP-50 / HP-55**	
Polymer weight	20 g	Polymer weight	20 g
Triethyl citrate	4 g (20%[a])	Triethyl citrate	2 g (10%[a])
SLS	0.6 g (3%[a])	Ethanol	230.4 g (80%[b])
Water	352 g	Water	57.6 g (20%[b])

SLS: Sodium lauryl sulphate; **a**: based on polymer weight; **b**: based on solvent weight

4.2.3. Polymer dissolution studies

4.2.3.1. Buffer capacity determination

Phosphate and *m*Hanks buffers with different buffer capacities (β) were used as dissolution media in this work. Buffer capacity is the ability of the buffer to resist changes in its pH and it can be measured by adding aliquots of acid/base to a buffer system and recording the corresponding pH. Buffer capacity (β) was calculated as reported previously by Liu and colleagues (2011) using equation 4.1.

$$\beta = \frac{\Delta AB}{\Delta pH} \qquad \text{(Equation 4.1)}$$

Where AB is the increment in mol/L of the amount of acid or base added to produce a pH change of ΔpH in the buffer. β in all media was measured at a pH change of 0.5 units (ΔpH) on addition of the hydrochloric acid. This pH direction was chosen as it is the one relevant to our system, as during polymer dissolution H^+ are produced and the pH will drop.

To determine β, all media were titrated from pH 6.8 to 6.3 with 0.1M HCl and the pH was recorded with each subsequent addition of titrant. The buffer capacity was modulated and determined by modifying the molarity of the main buffer specie of each medium. The composition of the prepared media is shown in Table 4.2.

Table 4.2: Composition of the phosphate and bicarbonate buffers used

	Concentration (mmol/L)					
Phosphate buffer						
KH_2PO_4	**5.0**	**10.0**	**20.0**	**30.0**	**50.0**	
NaOH	3.40	6.50	10.90	15.35	23.50	
Bicarbonate buffer						
$NaHCO_3$	**4.17***	**10.0**	**20.0**	**30.0**	**40**	**50.0**
KH_2PO_4	0.441	0.441	0.441	0.441	0.441	0.441
$Na_2HPO_4 \cdot 2H_2O$	0.337	0.337	0.337	0.337	0.337	0.337
NaCl	136.9	131.07	121.07	111.07	101.07	91.07
KCl	5.37	5.37	5.37	5.37	5.37	5.37
$MgSO_4 \cdot 7H_2O$	0.812	0.812	0.812	0.812	0.812	0.812
$CaCl_2.2H_2O$	1.26	1.26	1.26	1.26	1.26	1.26

*Liu et.al, 2011

4.2.3.2. Dissolution rate of enteric polymers

To assess the influence of buffer capacity on the dissolution rate of each polymer, dissolution of the produced sample disks was performed using phosphate (5mM, 25mM and 50mM) and bicarbonate (4.17mM, 20mM and 40mM) buffers. The samples were placed on a support, which allowed the dissolution to occur only from the exposed face of the disk. The support was then submerged in a beaker containing 1L of medium at 37°C, pH 6.8 and aliquots were collected at specific timepoints, with appropriate reposition of fresh medium (Figure 4.1A). The media was stirred using a magnetic stirrer, and across tests the conditions were kept consistent (magnetic stirrer, beaker, stirring plate, and stirring speed (30rpm)) to maintain a constant the flow of media across the surface of the disk. The collected aliquots were stored at 4°C for later analysis.

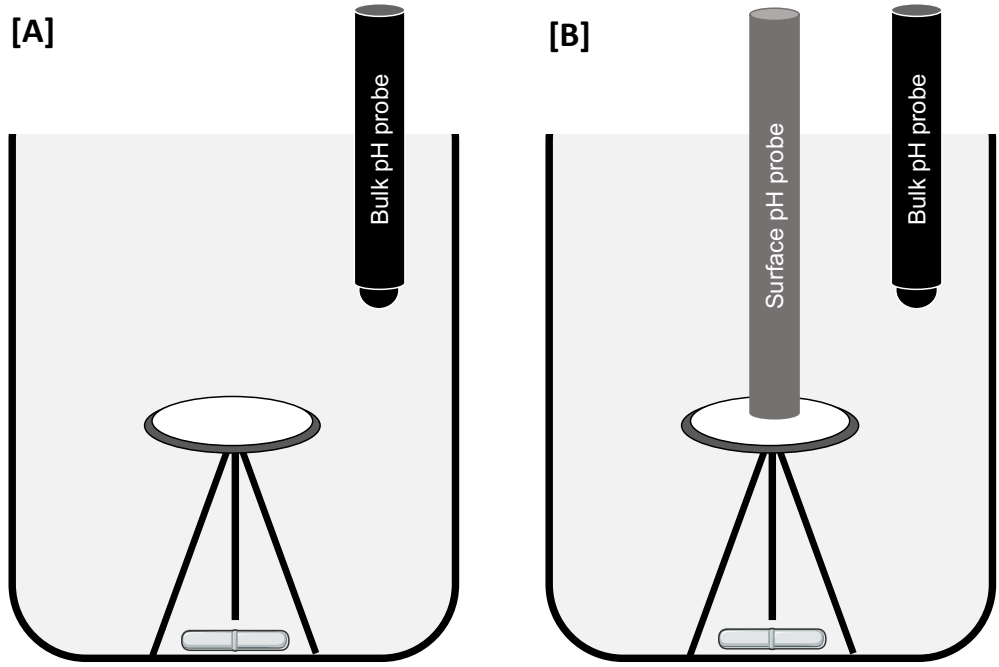

Figure 4.1: Schematic representation of the experimental layout used for the dissolution of polymeric disk (A) and for microenvironmental pH determination of polymeric disks (B).

4.2.3.3. Quantification of enteric polymers

The method used to quantify the dissolving polymer was adapted to improve the processing time and to minimise human and instrumental errors compared to previous studies (Dubois et al., 1956; Ghori et al., 2014). The first adaptation was to replace the test tube referred in previous studies with a 12-well microplate. The plate method had been previously adapted from Masuko et al., (2005), who used it for the quantification of sugars in samples.

In this method, samples collected at each timepoint during dissolution of the polymeric disks were processed in triplicate, and each replicate sample was then measured in triplicate. Briefly, 1100 µL of each sample was added in triplicate (A, B, C) to each column (1, 2, 3 and 4) of a Nunc™ Nunclon-Δ surface treated 12-well plate (Figure 4.2) followed by the addition of 3250 µL of concentrated sulfuric acid to each well. Next, 640 µL of 5% (w/w) phenol in 0.1M HCl was added and the mixture was homogenised using the pipette tip. The plate was then placed in a water bath at 30°C for 20 minutes. Subsequently, a sample from each well was transferred in triplicate to a Nunc™ 96-Well Microplate (as shown in Figure 4.2) and the absorbance was measured on a Tecan Infinite® F50 plate reader (Tecan Trading AG, Switzerland) at 490nm.

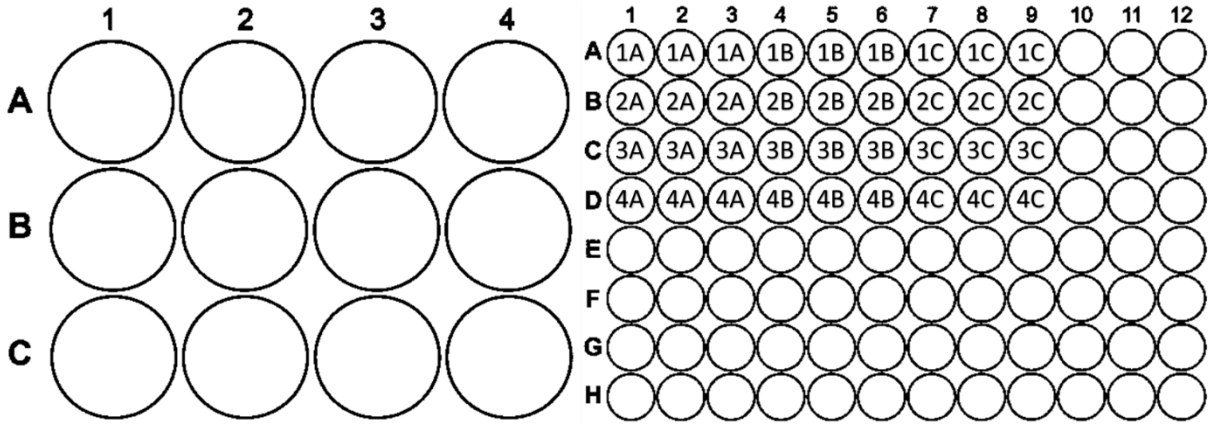

Figure 4.2: Layout of the distribution of the samples (1-4) in triplicate (A-C) on the 12-wel microplate (Left) and the correspondent transfer to the 96-well plate for absorbance reading. Each 96-well plate can contain up to 10 samples processed in triplicate and read in triplicate.

A calibration curve was performed for all tested polymers and a linearity was obtained for a range of concentrations from 0.1-20mg/L. The obtained calibration curves for all polymers showed a limit of quantification below 1mg/L (Table 4.3).

Table 4.3: Linear regressions obtained from the calibration curves of the tested polymers with the respective limits of detection (LOD) and quantification (LOQ).

AS-LF	AS-HF	HP-50	HP-55
y = 0.0071x +0.0016	y = 0.0060x +0.0018	y = 0.0044x +0.0018	y = 0.0061x + 0.0003
R^2 = 0.9997	R^2 = 1	R^2 = 0.9997	R^2 = 0.9998
LOD = 0.3288 mg/L	LOD = 0.2668 mg/L	LOD = 0.3212 mg/L	LOD = 0.2723 mg/L
LOQ = 0.9964 mg/L	LOQ = 0.8086 mg/L	LOQ = 0.9733 mg/L	LOQ = 0.8551 mg/L

4.2.4. Contact Angle measurement

Contact angle is influenced by the type of surface that is being tested, with higher angles occurring for more hydrophobic surfaces, and lower angles for more hydrophilic ones. Therefore, the sessile drop method was employed to determine the wettability of the polymers at different pH and in different buffers. An Ossila Goniometer (Ossila Ltd, Sheffield, UK) and specialised Ossila Software V2 were used to capture the contact angle variation and data analysis, respectively. Following the acquisition of the data, image analysis was performed to acquire information regarding the contact angle kinetics, where volume and basal area of the droplets were measured. For the measurement, 15 µL droplets of the liquid probe, 0.1M HCl or buffer were released from a micro-syringe from a constant height (3 cm) for consistency purposes (Figure 4.3). To assess the different wettability of

the polymers throughout a typical dissolution study, the media used in this study were 0.1M HCl pH 1.2, pH 6.8 phosphate buffer (5 mM, 25 mM and 50 mM) and pH 6.8 bicarbonate buffer (4.17 mM, 20 mM and 40 mM) (vide Table 4.2). The monitored contact angle variations were then plotted against time. All the experiments were conducted at room temperature.

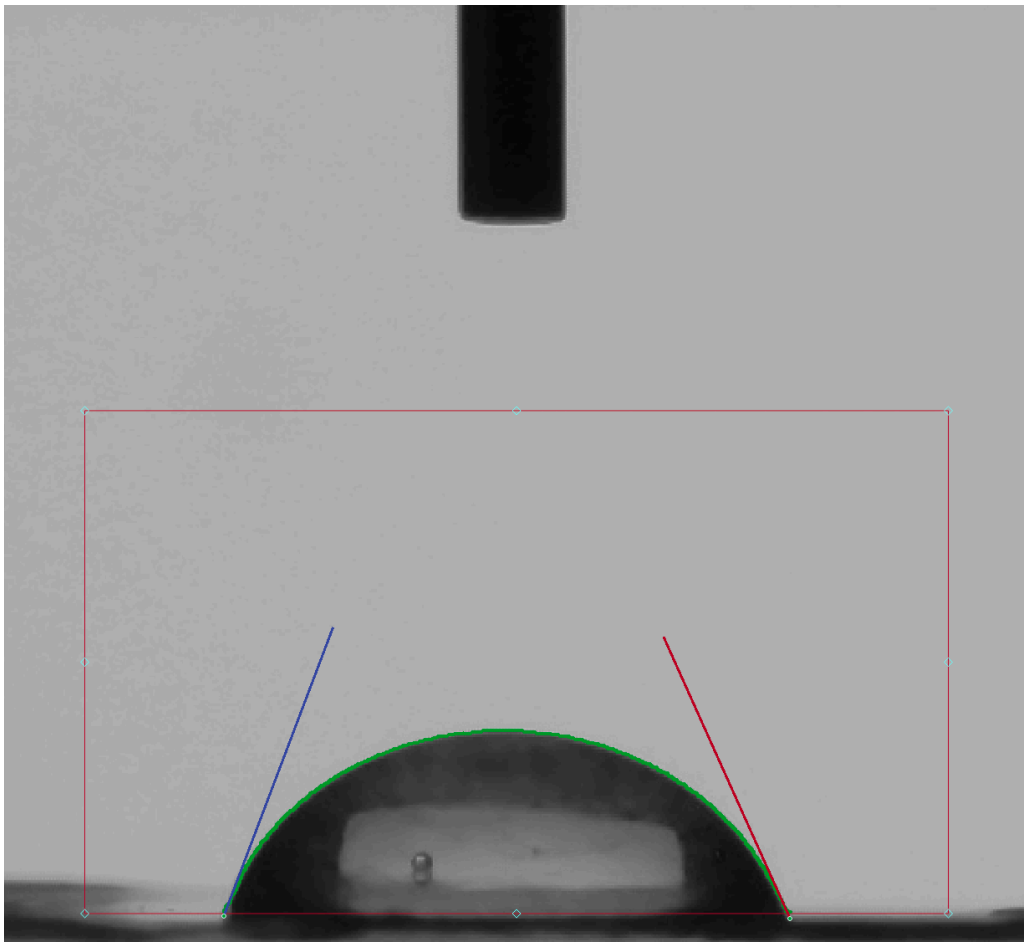

Figure 4.3: Example of contact angle measurement with a drop of media on polymeric disk sample, analysed using Ossila Contact Angle software.

4.2.5. Microenvironment pH measurements

Using a similar experimental layout as in section 4.2.3.2, polymeric disks were placed on the same support, and two pH electrodes were used: one to measure the bulk pH of the medium (HI-1090B/5, Hanna Instruments, Bedfordshire, UK) and a surface pH electrode (In-Lab Surface Pro-ISM, Mettler-Toledo, Leicester, UK) to measure the pH_m (Figure 4.1B).

The surface electrode was placed at 100 μm from the polymeric disk and the distance was kept constant throughout the various measurements. This was achieved by placing a spacer between the polymeric disk and the surface electrode which was then removed before each measurement.

To verify the influence of the buffer capacity of the medium on the pH_m, phosphate buffers (5 mM, 25 mM and 50 mM) and bicarbonate buffers (4.17 mM, 20 mM and 40 mM) at pH 6.8 were used.

4.3. Results and discussion

4.3.1. Buffer capacity determination

Buffer capacities were determined for each buffer as described above, and the results are summarised in Table 4.4. The determined β for phosphate buffer 50 mM and bicarbonate buffer 4.17 mM are in agreement with the ones determined by Liu et al., (2011). Figure 4.4 shows the relationship between buffer concentration and the determined buffer capacity. As expected, β increases with concentration, however this effect seems more pronounced for bicarbonate buffer, which increases at a higher rate than the phosphate buffer.

Table 4.4: Determined buffer capacities (β) for phosphate and bicarbonate buffers at different concentrations.

Phosphate buffer		**Bicarbonate buffer**	
Buffer concentration (mM)	Buffer capacity, β (mmol/L/ΔpH)	Buffer concentration (mM)	Buffer capacity, β (mmol/L/ΔpH)
5	2.32 ± 0.06	4.17	2.31 ± 0.03
10	4.58 ± 0.15	10	5.97 ± 0.13
20	9.97 ± 0.07	20	12.30 ± 0.42
30	14.67 ± 0.30	30	18.86 ± 0.21
50	26.08 ± 0.24	50	31.66 ± 0.99

Note: Measurements performed with 100 mL of sample, titrated from pH 6.8 until pH 6.3 with 0.1M HCl. Average ± STD (n=3).

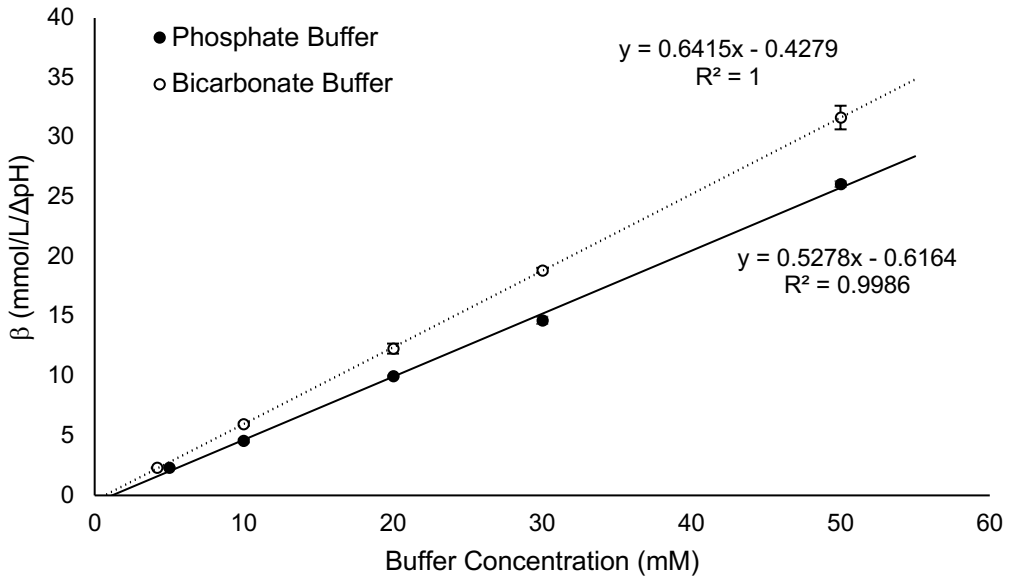

Figure 4.4: Relationship between buffer concentration and buffer capacity (β) for phosphate and bicarbonate buffers.

4.3.2. Quantification of enteric polymers

The used method was developed to increase efficiency in sample processing for the quantification of HPMC-based polymers compared to the original reported method (Dubois et al., 1956). In previous work, samples had to be processed individually, one in each test tube and reagents had to be added carefully to test tubes with "the stream of acid being directed against the liquid surface rather than against the side of the test tube" (Dubois et al., 1956). By adapting the method to be carried out in a microwell plate, time efficiency was gained by allowing samples to be processed in parallel, with the reagents being added using micropipettes. In the original method, after the addition of all the reagents, samples would stand for 10 min, were shaken and placed in a water bath for 10-20 min. Ghori et al., (2014) reports the use of a vortex stirrer to improve sample mixing, thus decreasing standing time. Nevertheless, this technique required an average of 2-3 min to process each sample (excluding incubation in the water bath). The optimisation of the microwell method allowed for a processing time of around 7-8 min per plate (i.e. 12 samples), reducing processing time to around one fifth of the original time. Additionally, the space occupied by the materials was also improved, as test tubes with the corresponding supports are much bulkier than a simple 12-well plate. Considering the reagents used (sulphuric acid and phenol) safety measures indicate that this kind of reaction should occur within a fume-hood, where space to work is even more important. Microplates being easily stacked warrant a safer environment to work than glass

test tubes. Finally, the reagent volumes were also reduced, leading to less liquid waste especially relevant in this reaction due to the presence of phenol in the waste, requiring specialist and separate waste treatment. Regarding the absorbance readings, a greater time efficiency was achieved, with 96-well plates being read within seconds, as compared to much more laborious readings using UV-Vis spectrophotometers. In less than 10 seconds, 96 samples can be read, compared to an average of 1 minute per sample using traditional UV-Vis spectrophotometers and cuvettes.

4.3.3. Dissolution rate of enteric polymers

The dissolution rate of the tested polymers was calculated and a linearity between polymer dissolution rate and buffer capacity was found (Figure 4.5, Table 4.6). As expected, the dissolution rate rises as the buffer capacity of the medium increases. The increased buffer capacity allows for more effective removal of accumulated H^+ ions at the boundary layer which arise from polymer ionisation (Figure 1.11). With the removal of these ions from the boundary layer, the microenvironmental pH is maintained above the polymer's dissolution pH threshold. However, with lower buffer capacities the less extensive removal of H^+ ions will lead to a lower pH at the boundary layer, hampering polymer dissolution (i.e. low dissolution rate).

Table 4.5: Dissolution rate (mg/min/cm^2) of tested polymers in different buffer media.

	Phosphate			**Bicarbonate**		
	5 mM	**25 mM**	**50 mM**	**4.17 mM**	**20 mM**	**40 mM**
HP-50	0.125 ±0.011	0.356 ±0.028	0.643 ±0.026	0.220 ±0.023	0.496 ±0.040	0.790 ±0.043
HP-55	0.121 ±0.011	0.283± 0.030	0.593 ±0.024	0.134 ±0.009	0.396 ±0.023	0.738 ±0.006
AS-LF	0.125 ±0.014	0.356 ±0.021	0.623 ±0.037	0.166 ±0.011	0.434 ±0.038	0.748 ±0.003
AS-HF	0.036 ±0.004	0.114 ±0.013	0.171 ±0.012	0.083 ±0.011	0.157 ±0.038	0.295 ±0.032

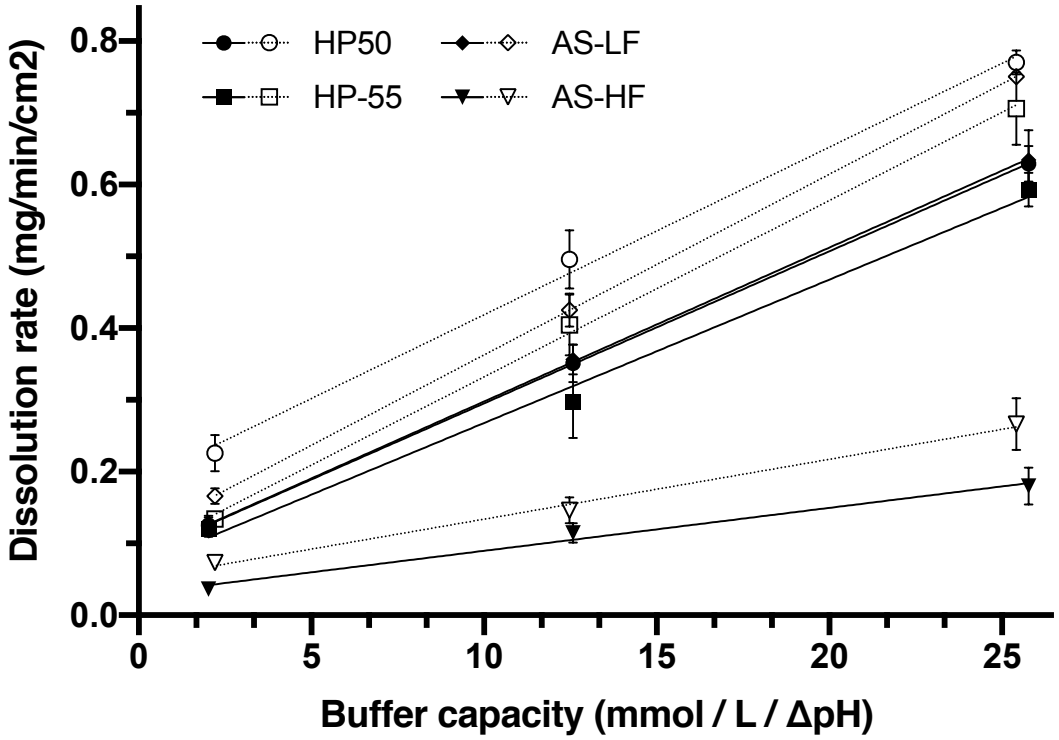

Figure 4.5: Correlation between dissolution rate and buffer capacity for each tested polymer in phosphate (filled symbols) and bicarbonate (empty symbols) buffers.

Table 4.6: Linear regression analysis of the effect of buffer capacity of bicarbonate and phosphate buffers on the dissolution rate of the studied polymers (in reference to Figure 4.5).

	Phosphate	**Bicarbonate**
HP-50	$y = 0.021\ (\pm 7.19 \times 10^{-5})\ x + 0.083\ (\pm\ 1.19 \times 10^{-3})$ $R^2 = 1.000$	$y = 0.023\ (\pm 1.44 \times 10^{-3})\ x + 0.184 (\pm\ 2.37 \times 10^{-2})$ $R^2 = 0.9962$
HP-55	$y = 0.020\ (\pm 1.62 \times 10^{-3})\ x + 0.068\ (\pm\ 2.70 \times 10^{-2})$ $R^2 = 0.9934$	$y = 0.025\ (\pm 8.59 \times 10^{-4})\ x + 0.086\ (\pm\ 1.41 \times 10^{-2})$ $R^2 = 0.9988$
AS-LH	$y = 0.021\ (\pm 2.38 \times 10^{-4})\ x + 0.083\ (\pm\ 3.95 \times 10^{-3})$ $R^2 = 0.9999$	$y = 0.025\ (\pm 3.10 \times 10^{-5})\ x + 0.111\ (\pm\ 5.09 \times 10^{-4})$ $R^2 = 1.000$
AS-HF	$y = 0.006\ (\pm 6.98 \times 10^{-4})\ x + 0.030\ (\pm\ 1.16 \times 10^{-2})$ $R^2 = 0.9866$	$y = 0.008\ (\pm 6.28 \times 10^{-4})\ x + 0.050\ (\pm\ 1.03 \times 10^{-2})$ $R^2 = 0.9944$

Interestingly, when comparing buffers with similar buffer capacities, dissolution rates are higher for bicarbonate buffer than phosphate buffer for all polymers studied. Also worthy of remark is the capacity of bicarbonate buffer to discriminate different dissolution rates between all polymers, whereas when using phosphate buffer only AS-HF is significantly different from the other three polymers. Additionally, statistical analysis (two-way ANOVA) indicated that in the studied dataset, the buffer concentration contributed 4x more to the variance than polymer type. This is even further

intensified when excluding AS-HF from the analysis, revealing that in this case, buffer concentration is accountable for 97% of variance. Even though polymers contribute to the variance (i.e. polymer type affects the obtained dissolution rate) the buffer concentration is thus the main cause contributing to the difference in dissolution rates. Therefore, and in accordance with the polymers' dissolution pH thresholds (see Table 3.1), the dissolution rate of the tested polymers in bicarbonate ranks as follows: HP-50 > AS-LF > HP-55 > AS-HF.

At all tested concentrations of phosphate and bicarbonate buffers, AS-HF has shown the lowest dissolution rate. This is not at all unexpected and may be explained by its reported dissolution pH threshold. This polymer is reported to dissolve above pH 6.8, which is exactly the pH at which the test was conducted. However, as this polymer ionises and protons are released and accumulating at the boundary layer between the polymer and the medium, a drop in pH occurs, as the capacity of the buffer to remove the generated H^+ ions is limited. Since the pH of the medium is so close to the polymer dissolution pH, small drops in the pH immediately affect the dissolution of the polymer, which in turn causes the low dissolution rate of AS-HF. This effect is not as pronounced for the other polymers, since their dissolution pH thresholds are lower, allowing for broader pH fluctuations to occur before impacting dissolution. There is further discussion on this polymer in section 4.3.4 exploring how the higher dissolution pH affects the microenvironmental pH surrounding the polymer surface.

Differences in dissolution rates of drugs using different media have been previously reported and explained by Sheng and colleagues (2009). The authors studied how the dissolution rate of two drugs was influenced by the use of different buffers, at different concentrations. Similar to results found in this study, Sheng and colleagues verified that increasing bicarbonate buffer concentrations from 5 mM to 15 mM increased the dissolution rate of the studied drugs. The authors also found that although tested at the same pH and buffer concentration, the dissolution of both drugs in phosphate and bicarbonate was inherently different. Unlike Sheng and co-workers who used buffer concentration as the comparable variable, in this work the emphasis was on buffer capacity. Results showed that when using phosphate and bicarbonate buffers at different concentrations yet with the same buffer capacity (e.g. 50 mM phosphate buffer and 40 mM

bicarbonate buffer), the dissolution rate was higher in bicarbonate. This observation further corroborates Sheng's results, i.e., although pH and either buffer concentration or buffer capacity may be kept constant, there can still be differences in the dissolution rates when using different buffers. The authors hypothesise that chemical and physical dissimilarities between phosphate and bicarbonate, especially the pK_a and the diffusion coefficient, give rise to the different performances of these buffers. The reported (Sheng et al., 2009) diffusion coefficient for the $H_2PO_4^-$ /HPO_4^{2-} ions is $11.5x10^6$ cm^2/s, whereas H_2CO_3 and HCO_3^- have higher diffusion coefficients ($19.25x10^6$ cm^2/s and $12.35x10^6$ cm^2/s, respectively). Furthermore, the authors attempted to design a surrogate phosphate buffer for bicarbonate by theoretical analysis, using the film model and the reaction plane model (Sheng et al., 2009). This allowed them to select a concentration of phosphate buffer which would perform similarly to a 15 mM bicarbonate buffer, yielding similar dissolution rates for the class II drugs. However, results have shown that not only the buffer chemistry is important, but also the entity being dissolved. For ketoprofen, 13.0 mM phosphate buffer was used as a surrogate buffer, which yielded a dissolution rate that was 86% of the one obtained using a 15 mM bicarbonate buffer. As for indomethacin, a 3.5 mM phosphate buffer was used, and the dissolution rate was 108% of that obtained using the 15 mM bicarbonate buffer. Both drugs performed quite differently using the studied buffers, with indomethacin being more sensitive to phosphate than ketoprofen. The authors further suggest that a surrogate phosphate buffer should therefore be modelled for each drug on a case-by-case basis using the suggested models.

The results obtained in this study can be explained using the same rationale, with the differences between phosphate and bicarbonate being due to the intrinsic characteristics of these buffers, such as the pK_a and the diffusion coefficient. As previously mentioned, polymers and small molecules greatly differ in terms of dissolution mechanics. The dissolution of solid polymeric materials involves an important first step, the diffusion of the solvent through the polymeric entangled chains. Higher diffusion coefficients may then indicate quicker diffusion of the medium through the polymeric chains, increasing the speed of the dissolution process, thus increasing the dissolution rate.

4.3.3.1. Case study: Translating polymer dissolution rate to effective drug release

The study of dissolution rate of enteric polymers is ultimately linked to the need to understand how this may affect drug release. In Chapter 2, enteric hard capsules were prepared, and prednisolone release was measured under different buffers. As mentioned before, clear differences in the drug release were found when using the compendial 50 mM pH 6.8 phosphate buffer and a more biorelevant 4.17 mM pH6.8 bicarbonate buffer (refer to Table 4.2 for more details regarding the buffer) (Figure 2.6). When tested in phosphate buffer, a quick drug release was observed from both AS-LF and HP-55 capsules, with these two polymers showing very similar lag times until 1% of drug release occurred (vide Table 2.6). Similarly, the reported dissolution rate for these two polymers was shown to be indistinguishable when tested in the same 50 mM pH6.8 phosphate buffer. However, when tested using the 4.17 mM pH6.8 bicarbonate buffer, there was a clear distinction in the drug release profile of the two polymers, with higher lag times for HP-55 than AS-LF (67.5 and 18.2 min, respectively, vide Table 2.6). This same distinction was observed when measuring the dissolution rates of these two polymers using the same buffer with AS-LF showing a higher dissolution rate than HP-55, consequently affecting the drug release from the capsules.

These results confirm how polymer dissolution rate may directly affect drug release from an enteric dosage form. Additionally, this also confirms the feasibility of using filled enteric hard capsules of different materials to study the effect of different media on the drug release.

4.3.4. Microenvironmental pH measurements

Considering how the buffer capacity influences the dissolution rate of the polymers by removing accumulated H^+ ions from the diffusion layer, the measurement of the pH_m over time and under different media should provide a good indication of how the medium affects the mechanics behind polymer dissolution. The performed study aimed to measure the pH at the diffusion layer investigating the influence of the buffer capacity on the pH_m using phosphate (5 mM and 50 mM) and bicarbonate (4.17 mM and 50 mM) buffers at pH 6.8 (Figure 4.6).

The difference between 5mM and 50mM phosphate buffer was immediately noticeable. The higher buffer capacity of the 50mM phosphate buffer was enough to hold the pH of the medium in the vicinity of the dissolving polymer close to the original pH, never dropping below ~6.5. Throughout

the tests with both buffers and at both concentrations, the bulk pH probe registered a pH value of 6.8 ± 0.05. However, when using 5 mM phosphate buffer, distinctions between polymers were immediately more noticeable, as the pH dropped sharply. As shown in Table 4.7, AS-HF had the highest pH_m after 30 min, followed by AS-LF, HP-55 and HP-50.

Table 4.7: Determined pH_m for the tested polymers in phosphate and bicarbonate media, after 30 min of exposure.

	Phosphate		**Bicarbonate**	
	5mM	**50mM**	**4.17mM**	**40mM**
HP-50	5.48 ±0.01	6.54 ±0.04	5.35 ±0.04	6.42 ±0.04
HP-55	5.61 ±0.03	6.61 ±0.02	5.53 ±0.05	6.49 ±0.01
AS-LF	5.98 ±0.01	6.66 ±0.03	5.86 ±0.04	6.55 ±0.02
AS-HF	6.09 ±0.04	6.73 ±0.01	6.02 ±0.02	6.65 ±0.01

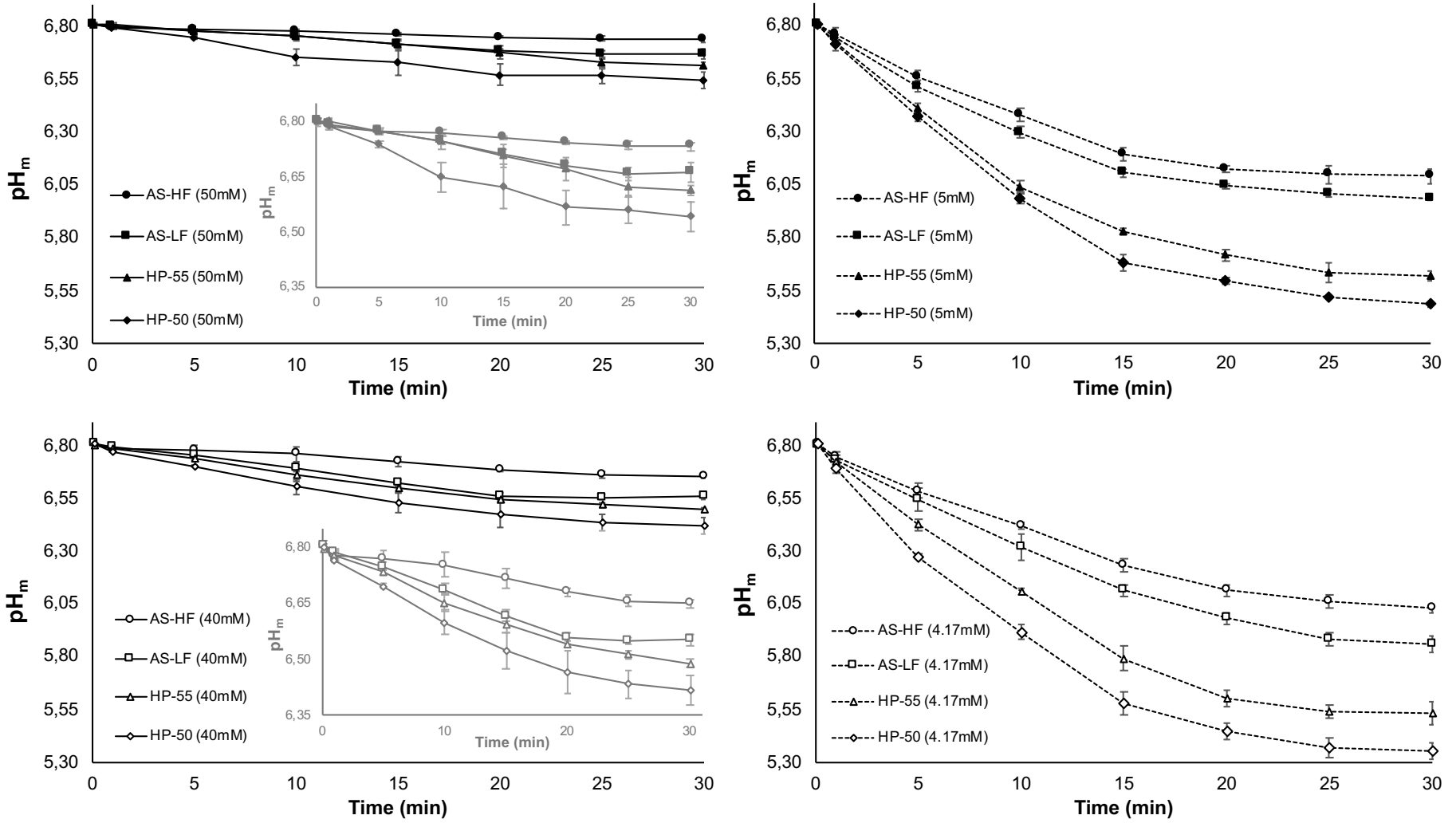

Figure 4.6: Measurement of the microenvironmental pH (pH_m) of the tested polymers under phosphate (filled symbols) or bicarbonate (empty symbols) buffers at high (solid lines) and low (dashed lines) buffer capacity.

Measurement of the pH near the surface of dissolving enteric polymers has been reported using a fluorimetric technique (Harianawala et al., 2002). The study was performed on HP-50 and HP-55 with stirred and unstirred conditions, and the media were 50 mM phosphate buffers at pH 6.5 and 7.0. Although the buffers do not exactly match those in the present work, there is a similarity which allows for comparison of some data. In Harianawala's study, the fall in pH near the polymer surface was higher for HP-50 than for HP-55, which correlates with the data obtained in this thesis. Furthermore, at pH 6.5, after 30 min the surface pH for HP-50 fell to ~6.1 and for HP-55 to ~6.3, which are much lower than the obtained in this work. These differences could be due to the method used to determine pH.

The smallest fall in pHm was for AS-HF. As discussed before in section 4.3.3, AS-HF was also the polymer with the lowest dissolution rate. The reported dissolution pH threshold for AS-HF is 6.8, the highest threshold amongst the tested polymers and the same pH at which the test takes place. This may explain the smaller changes in pH_m and also the smallest variation in the dissolution rate. When using a buffer with high buffer capacity (e.g. 50 mM phosphate buffer), the pH near the polymer surface will remain very close to the dissolution pH threshold of this polymer, however never surpassing it. So, at a pH near 6.8, AS-HF will dissolve, albeit much slower than the other tested polymers which have much lower dissolution pH thresholds. When the buffer capacity is decreased (e.g. 5 mM phosphate buffer), the generated H^+ are removed from the boundary layer more slowly, causing the pH_m to drop, thus hampering its already slow dissolution. With a lower dissolution rate, less H^+ are produced, and eventually the buffer restores the equilibrium between produced and removed H^+ ions at a pH near 6.

4.3.5. Contact angle measurements

Contact angles were measured using different concentrations of phosphate and bicarbonate buffer as probes. The results are summarised in Figure 4.7, showing observable differences between the polymer/buffer systems. Additionally, an image analysis was performed where the droplets were measured and their volume and basal area were calculated as reported by Farris et al,.(2011). Figure 4.8 – 4.11 show the evolution of the volume and the basal area of the droplet over the period of time tested for the different polymers.

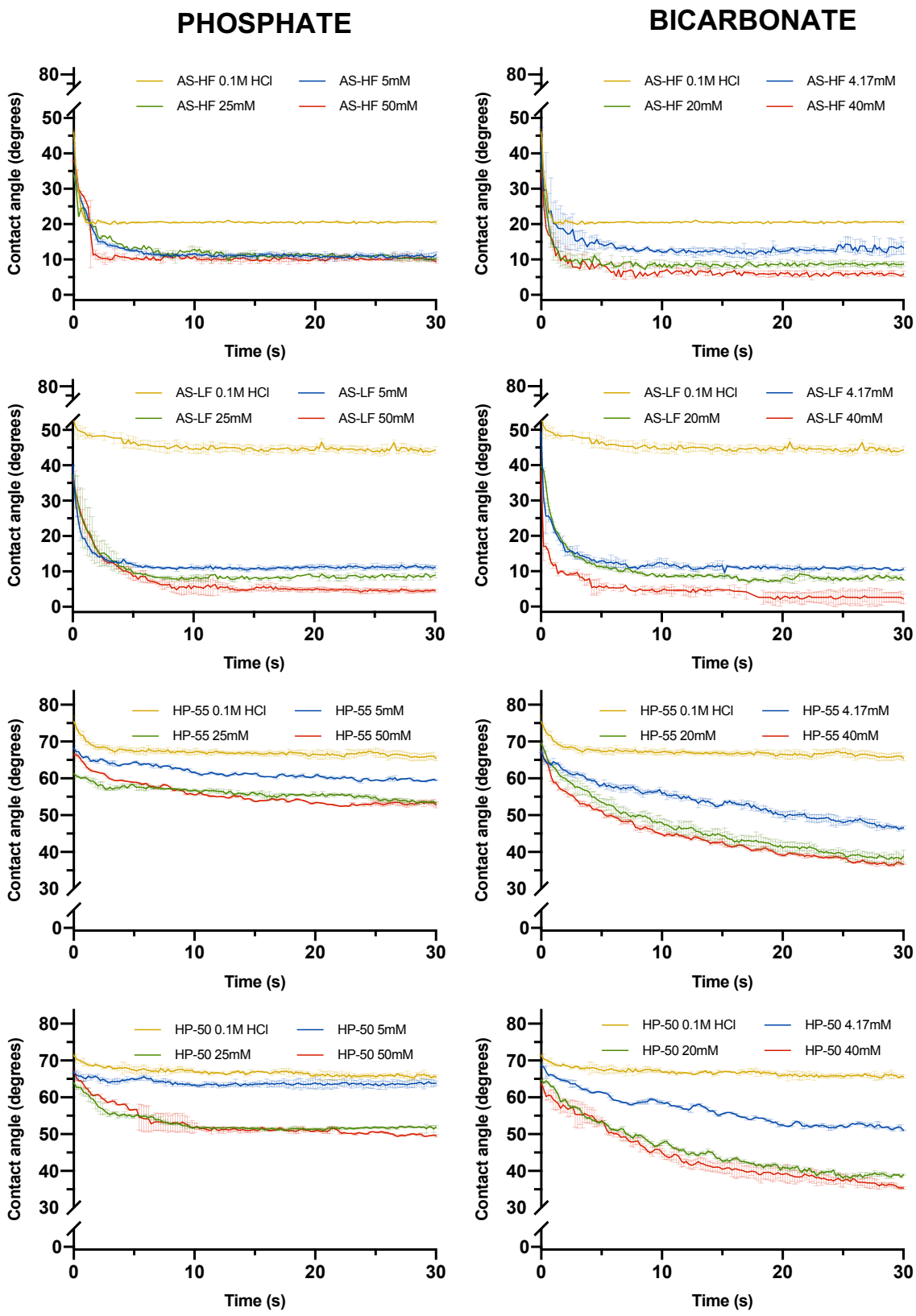

Figure 4.7: Contact angle determination for the tested polymers (AS-HF, AS-LF, HP-55 AND HP-50) using 0.1 M HCl, phosphate (left) and bicarbonate (right) buffers at different concentrations.

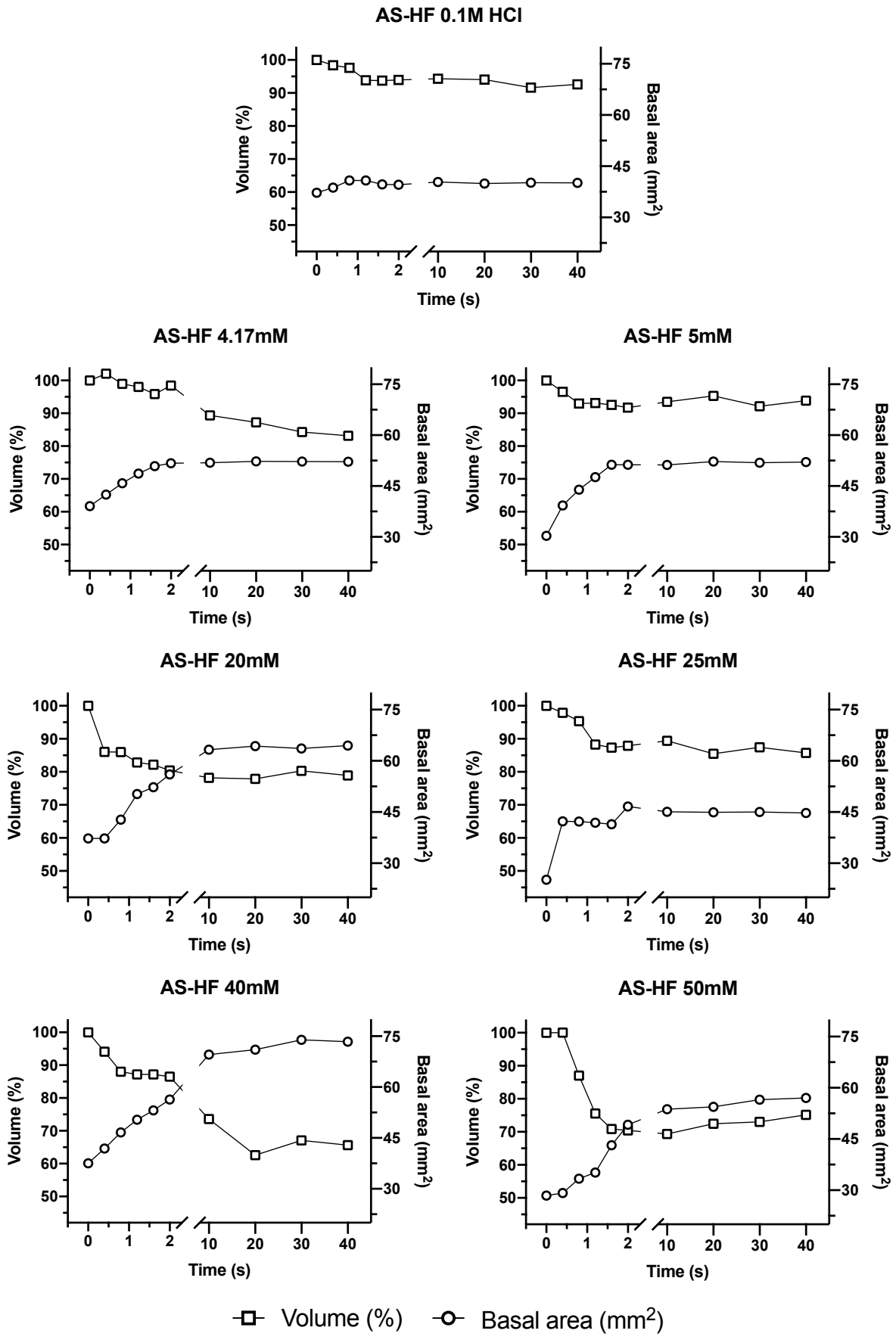

Figure 4.8: Variation of volume and basal area of the droplets during contact angle measurements of AS-HF using different concentrations of bicarbonate (left) and phosphate (right) buffers.

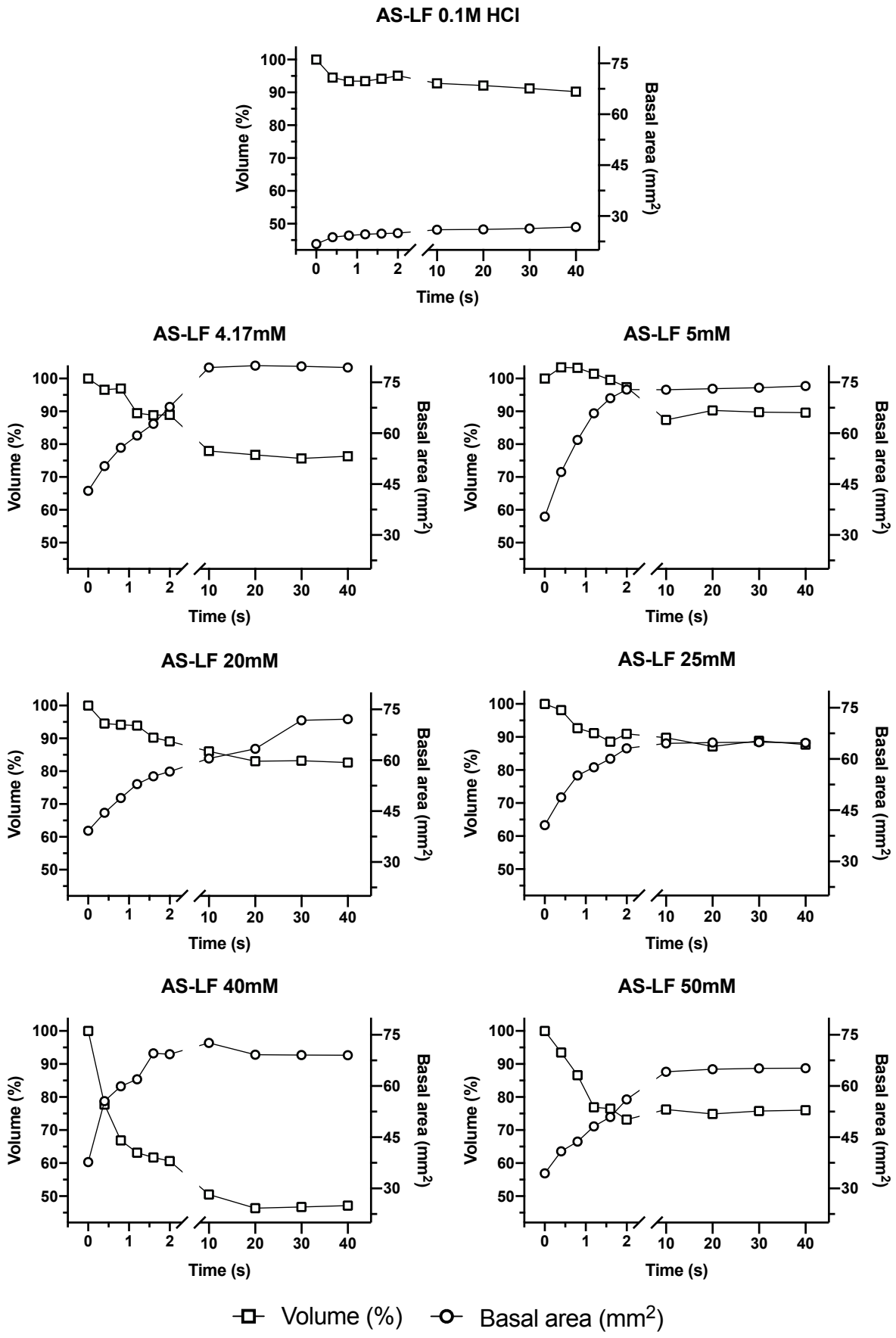

Figure 4.9: Variation of volume and basal area of the droplets during contact angle measurements of AS-LF using different concentrations of bicarbonate (left) and phosphate (right) buffers.

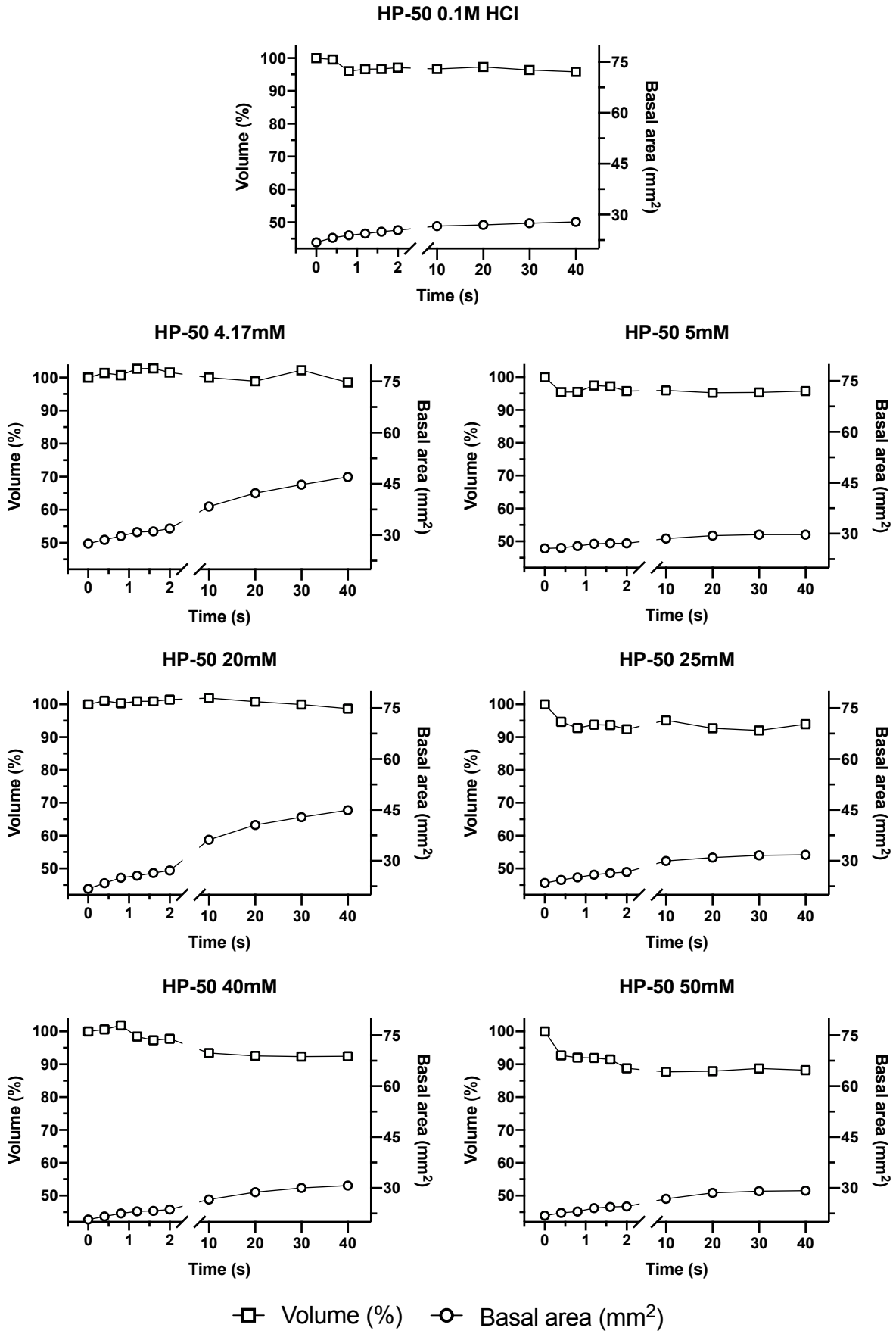

Figure 4.10: Variation of volume and basal area of the droplets during contact angle measurements of HP-50 using different concentrations of bicarbonate (left) and phosphate (right) buffers.

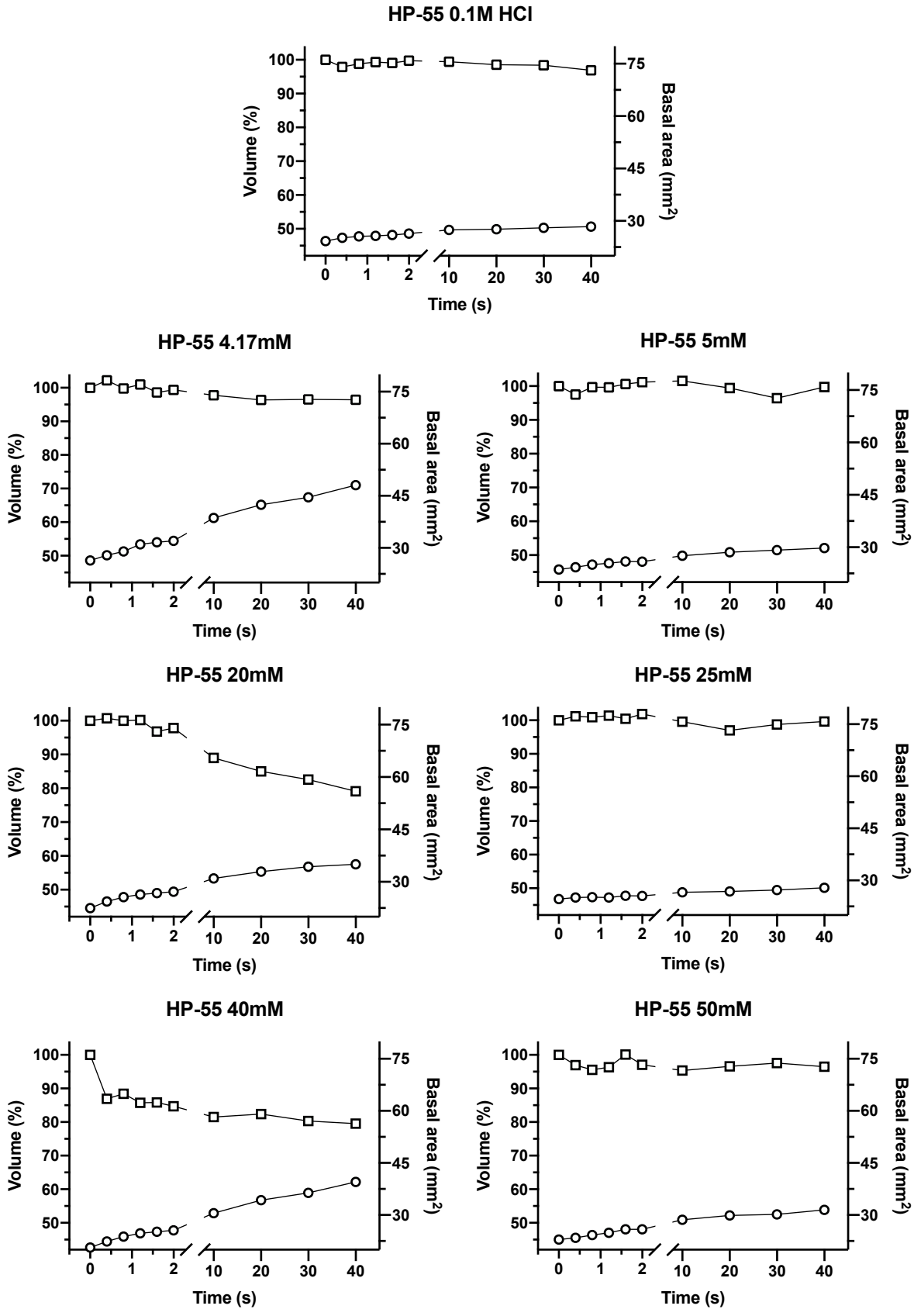

Figure 4.11: Variation of volume and basal area of the droplets during contact angle measurements of HP-55 using different concentrations of bicarbonate (left) and phosphate (right) buffers.

4.3.5.1. Influence of buffer concentration

Buffer concentration directly influences β, contributing to buffer systems more capable of countering small additions of acids or bases, thus maintaining the desired pH of the medium. In this experiment, buffer concentration (and thus buffer capacity) has shown to affect the contact angle, and therefore the wettability of the studied polymers. Figure 4.4 and Table 4.8 show that in all tested polymers, using both types of buffer, an increase in buffer concentration was translated to a decrease of the contact angle. In Table 4.8 the initial contact angle (i.e. the contact angle at the time of first contact between the droplet and the polymer(θ_0)) and the contact angle after 30 seconds (θ_{30}) is shown. For all polymers, the θ_0 and θ_{30} were the highest when using 0.1M HCl, and in general θ_0 and θ_{30} decrease with increasing concentration of buffer. The probes in this test were aqueous solutions, therefore a decrease in the contact angle indicates an increased hydrophilicity of the tested surfaces. As the polymers are not soluble in 0.1M HCl, a higher hydrophobicity is expected using this medium, as no ionisation of the polymeric chains is occurring. However, when using the buffers as the testing media polymer ionisation occurs, and as seen before, higher buffer capacities translate to higher dissolution rates, caused by the increased capacity of the buffer to remove the ions from the boundary layer. Higher dissolution rates indicate a higher generation of H^+ ions, and therefore an increased hydrophilicity. During the sessile drop test, only a small volume of buffer is placed onto the polymeric surface, thus the removal of protons to the bulk solution is somewhat more limited, due to the reduced volume and lack of agitation. Nonetheless, although there is diminished removal of the generated H^+ ions, a buffer with higher β is more capable of countering the change in pH, maintaining the pH_m stable for longer. This leads to more extensive ionisation of the polymeric chains, increasing its hydrophilicity, thus decreasing contact angle.

Additionally, from Figure 4.8 – 4.11, it is possible to observe that with higher concentrations of buffer, higher losses in volume occur. This drop in volume is explained by the absorption of the buffer by the film. With higher concentrations, higher dissolution rates are observed, indicating a possible higher rate of diffusion of the buffer, which leads to to higher volume losses. Also, when

using 0.1M HCl an insignificant loss of volume occurs, indicating that there is little absorption of this media, correlating with the non-dissolution of the polymers in acidic environment.

Table 4.8: Obtained contact angles for the tested polymers at the initial time of contact (θ_0) and after 30 seconds of contact (θ_{30}).

	HCl	Phosphate			Bicarbonate		
		5mM	25mM	50mM	4.17mM	20mM	40mM
AS-LF	θ_0 53.75 ± 5.84 θ_{30} 44.70 ± 1.03	θ_0 49.37 ± 1.80 θ_{30} 11.19 ± 0.48	θ_0 39.68 ± 1.99 θ_{30} 8.96 ± 0.75	θ_0 38.52 ± 4.93 θ_{30} 4.54 ± 0.44	θ_0 39.96 ± 0.08 θ_{30} 10.36 ± 0.20	θ_0 37.38 ± 0.16 θ_{30} 7.97 ± 0.07	θ_0 36.22 ± 0.55 θ_{30} 2.11 ± 1.24
AS-HF	θ_0 46.12 ± 0.73 θ_{30} 20.53 ± 0.54	θ_0 42.24 ± 0.67 θ_{30} 10.72 ± 1.20	θ_0 34.06 ± 1.00 θ_{30} 10.37 ± 0.24	θ_0 38.07 ± 0.16 θ_{30} 9.50 ± 0.56	θ_0 40.98 ± 6.38 θ_{30} 13.68 ± 1.73	θ_0 38.4 ± 1.18 θ_{30} 8.76 ± 1.73	θ_0 35.53 ± 0.97 θ_{30} 5.69 ± 0.76
HP-50	θ_0 71.38 ± 0.38 θ_{30} 65.60 ± 0.42	θ_0 66.73 ± 0.25 θ_{30} 63.83 ± 0.61	θ_0 64.03 ± 1.38 θ_{30} 51.92 ± 0.42	θ_0 67.09 ± 0.73 θ_{30} 49.56 ± 0.35	θ_0 68.76 ± 0.57 θ_{30} 51.04 ± 0.11	θ_0 64.69 ± 0.26 θ_{30} 39.01 ± 0.23	θ_0 63.83 ± 1.04 θ_{30} 35.39 ± 0.35
HP-55	θ_0 75.46 ± 1.50 θ_{30} 65.42 ± 0.71	θ_0 68.19 ± 0.55 θ_{30} 59.50 ± 0.05	θ_0 61.27 ± 1.96 θ_{30} 53.38 ± 0.30	θ_0 66.48 ± 0.63 θ_{30} 52.74 ± 0.81	θ_0 67.45 ± 0.49 θ_{30} 46.61 ± 0.43	θ_0 69.54 ± 0.51 θ_{30} 38.89 ± 1.56	θ_0 67.27 ± 0.23 θ_{30} 36.71 ± 0.07

4.3.5.2. Influence of polymer type

Contact angle is influenced by the type of surface that is being tested, with higher angles occurring for more hydrophobic surfaces, and lower angles for more hydrophilic ones. Therefore, the type of polymer being tested will influence the corresponding contact angle of a drop on its surface due to the differences in their constitution. The four polymers tested share a similar structure (HPMC), differing in their specific functional groups which provides them with different characteristics, of most importance in this case, their dissolution pH. HPMC-P (HP50 and HP-55 in this study) contains phthalate groups (vide Table 3.4), whereas HPMC-AS contains acetyl and succinoyl groups, with the latter being the ionisable group, as acetate only contains one -COOH group which is bonded to the polymer backbone and thus not available for further ionisation. As mentioned, the contact angle of a drop on a surface depends on the hydrophobicity/hydrophilicity, which is influenced by the functional groups present in the material, in this case a polymer. Phthalate and

succinate have very different Log P values (0.73 and -0.59, respectively (Hansch et al., 1995)), which indicates different hydrophilicity of these polymers, with phthalate being more hydrophobic than succinate. This would lead to higher contact angle values for HP-50 and HP-55 than for AS-LF and AS-HF, which is indeed reported in Figure 4.7 and Table 4.4. For the same buffer type and concentration, HP-50 and HP-55 have higher contact angles than AS-LF and HF, in agreement with the above-mentioned chemistry of these polymers.

Regarding the shape of the droplets, Figure 4.8 – 4.11 show that for HPMC-AS a higher variation of the basal area occurs, indicating a much higher spreading of the droplet than for HPMC-P, correlating to the observed higher contact angles for HPMC-AS polymers. The increasing basal area and the lower loss of volume observed for HPMC-P polymers indicates that more spreading and lower absorption is occurring in these polymers when compared to HPMC-AS polymers. Higher volumes losses are seen for HPMC-AS polymers, indicating a higher absorption of the droplets by these polymers. This may be related to possible differences in the porosity of the films (which was not measured), but may also be explained by a higher diffusion of the buffer for HPMC-AS. Due to the chemical differences of the two groups of polymers (HPMC-AS and HPMC-P), a higher affinity of these aqueous solutions for HPMC-AS is possible, as explained before.

When comparing two polymers of the same type (HP-50 and HP-55 or AS-LF and AS-HF) for the same buffer species, interestingly there seems to be no significant differences in contact angle between HP-50 and HP-55s but AS-HF shows higher contact angles than AS-LF. The similarity in contact angle between HP-50 and HP-55 may be related to the number and the chemistry of the phthalyl functional groups. HP-55 contains the most groups (27.0-35.0%, vs. 21.0-27.0% for HP-50, vide Table 3.4), and since phthalyl is a more hydrophobic group, a higher percentage should lead to higher hydrophobicity, and thus higher contact angle. However, this is not the case, as seen the obtained contact angles are very similar between the polymers. With a higher number of ionisable groups, HP-55 generates a higher charge on the surface of the polymer, as mentioned in Chapter 3 (vide Table 3.4), and therefore this increased charge translates in an increased hydrophilicity. A possibility for the similarity between these two polymers may thus lay on the balance between number of hydrophobic groups and generated surface charge.

In the case of AS polymers, the difference also arises due to the number and type of functional group present, but in this case the functional group (succinoyl) is hydrophilic. Therefore, as AS-LF contains a higher % of succinoyl groups (14-18%, vs. 4-8% for AS-HF, vide Table 3.4), a more hydrophilic surface should be expected for this polymer, leading to lower contact angles. The observed values for contact angle also correlate with the $Zeta_{max}$ values obtained, with AS-HF having shown lower charge than AS-LF (-8.76mV and -15.41mV, respectively). The nearly 2-fold higher charge shown by AS-LF will also contribute to the increased hydrophilicity of this polymer, and the lower recorded contact angle.

4.3.6. Influence of buffer type

During contact angle measurements, clear differences were seen when using phosphate or bicarbonate buffers. In general, tests using bicarbonate yielded lower contact angles than when using phosphate buffers. Following the same rationale as above, lower contact angles indicate higher hydrophilicity, potentially indicating a higher degree of ionisation. Additionally, higher volume losses and increased spreading (higher basal area) are observed when using bicarbonate buffers (Figure 4.8 – 4.11). These results are in accordance with the obtained dissolution rates for these polymers under the tested conditions. In bicarbonate, all polymers have an increased dissolution rate, indicating a higher extent of ionisation, leading to a more hydrophilic surface, therefore decreasing the contact angle. The reasons for the increased dissolution rate were already discussed in the section 4.3.3.

Worthy of remark is the lack of significant difference in the observed contact angle for AS-HF when in contact with different concentrations of phosphate buffer, whereas AS-LF shows lower contact angle values with increasing concentration of this buffer. Again, the dissolution rate could play a role in this matter, with AS-HF still having a much lower dissolution rate than AS-LF, even with phosphate buffer at 50mM. The low dissolution rate would thwart the generation of protons (i.e. the ionisation of further functional groups). Contact angle may be affected by the charged functional groups, and at higher buffer capacities the generation of protons will be increased. However, the increase in the number of protons occurs at a scale that allows for the increased buffer capacity to neutralise the generated ions. This would cause minimum changes in the

experienced contact angle, causing a minimum limit for contact angle to be reached. This minimum seems to have been reached for this polymer during this test as observed in Figure 4.7. This is not the case for AS-LF, where a more significant increase in the dissolution rate is observable with the increase in buffer concentration (Table 4.5), which would encompass more deprotonated ionisable groups. Again, a higher quantity of ionised groups instigated by higher buffer concentrations suggests higher hydrophilicity, and therefore lower contact angles.

Additionally, the buffer chemistry may also pose an effect with these polymers, with different substances reacting differently to each buffer species. In Sheng's and colleagues (2009) work, indomethacin and ketoprofen responded differently to phosphate and bicarbonate buffers, requiring reduction in phosphate molarity to manifest the same intrinsic dissolution rate as in 15mM bicarbonate buffer. Moreover, the concentration of phosphate buffer used for indomethacin was much lower than for ketoprofen (3.5 mM and 13.5 mM, respectively), showing that the different drugs perform differently in the media due to, and as stated by the authors, intrinsic differences in the chemistry of the molecules.

Finally, when using the highest concentration of bicarbonate buffer, a near zero contact angle was registered for AS-LF. Figure 4.9 shows that when using 40mM bicarbonate buffer, there is approx. 60% of volume loss, with the basal area of the droplet greatly increasing as well. The very low contact angle can be thus explained by the absorption of the droplet occurring for AS-LF. The analysis of the volume of the droplets show that for HPMC-AS, a higher volume loss occurs when using bicarbonate buffer then when using phosphate buffer. These polymers may be reacting with more affinity to bicarbonate buffer, which by generating higher dissolution rates, allows a higher diffusion of the buffer through the gel-layer of the polymer, leading to higher volume losses, i.e. higher absorption. Additional explanations may be related to the porosity of the polymeric film (which was not measured) with high porosity causing the higher absorption of the droplet.

4.3.7. Acid uptake: insights from contact angle kinetics

The contact angle kinetics provides useful insights into how a fluid interacts at the surface of a polymeric film and can deliver useful clues into acid uptake and gastroresistance exhibited by various polymers. Conventionally, acid uptake is evaluated in gastroresistant dosage forms to

access how much acid diffuses through the enteric polymeric film during the acid stage of the compendial dissolution test. This test is conducted by weighing the tested tablets before and after 2h in 0.1M HCl and the acid uptake is given as a percentage of the weight gained during this period.

The contact angle kinetics of various polymers were studied in 0.1M HCl and provide palpable information on wettability of the polymeric films in acidic environment of the stomach. As mentioned, the obtained contact angle for all polymers was highest when using acid than in buffers, however, after analysing the obtained images and calculating the volumes changes during the test, it can be seen that a small percentage of acid was absorbed through these films which can be seen by the reduction of the drop volume on surface of the polymeric film with time (Figure 4.12). Since the fluid contact area with the film did not change significantly during this period, this confirms that the loss of volume is not mainly due to the spreading of the droplet over the film surface but as a result of absorption/penetration into the films.

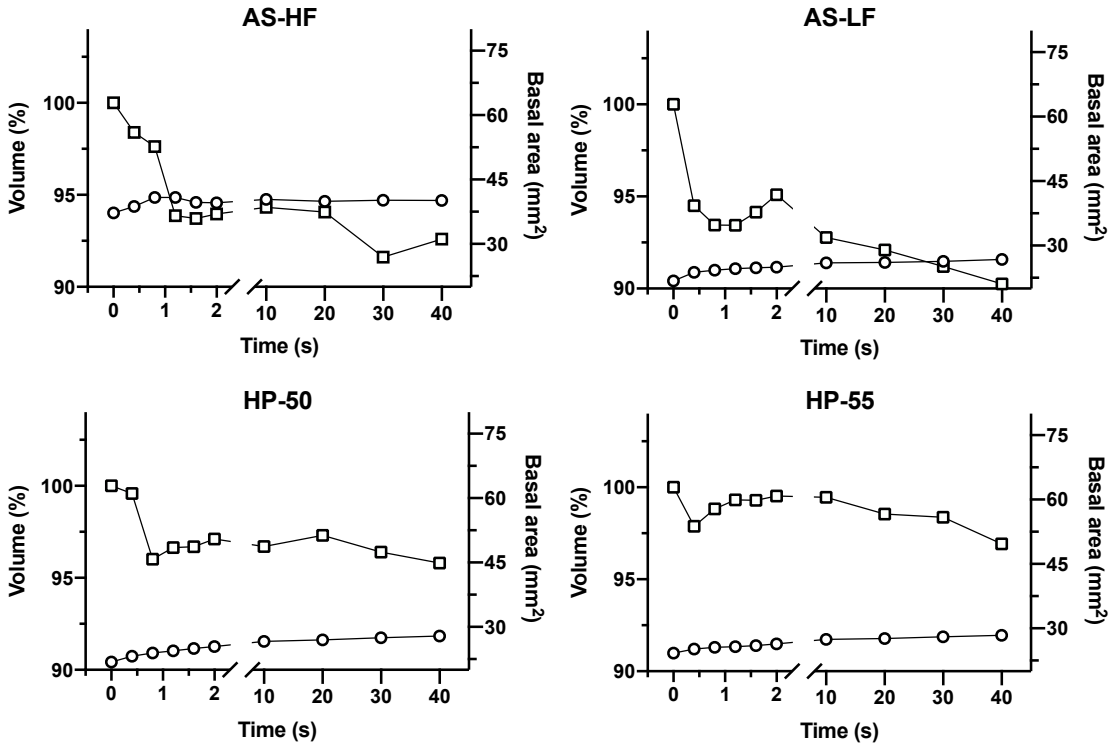

Figure 4.12: Variation of volume during contact angle measurements using 0.1M HCl as testing medium.

The acid uptake of these polymers has been previously studied by Liu and colleagues (2011) and interestingly the results correlate with the variations in volumes obtained during contact angle

kinetics. In Liu's study, HPMC-P had a lower acid uptake than HPMC-AS, and a similar trend can be seen in Figure 4.12, with HP-50 and HP-55 showing a less volume variation than AS-LF and AS-HF. Additionally, HP-55 has shown a lesser loss in volume than HP-50, which is also in agreement with Liu's findings where HP-55 exhibited less acid uptake than the HP-50 (2.1 and 2.8%, respectively). Similarly, Liu et al., (2011) also reported that a higher acid uptake occurs with AS-LF which corresponds to a higher decrease in volume in our studies. Therefore, the contact angle kinetics can be a useful tool to study the acid uptake from pH responsive polymeric films employed in modified release dosage forms. Future experiments should aim to directly relate the acid uptake of these polymers on coated tablets in relation to the contact angle kinetics on tablet surface and implications in subsequent drug release in acid and buffer.

4.4. Conclusion

The effect of buffer capacity on the dissolution of different polymers was investigated. For this, an adaptation of the previously reported PSA quantification technique was developed for the direct quantification of HPMC-based polymers, more specifically those employed in enteric coatings. This technique was used to assess the dissolution rate of some of these polymers, and it will allow for the direct quantification of dissolving coatings from enteric dosage forms during dissolution tests. Additionally, the effect of the buffer capacity in the regulation of the microenvironmental pH surrounding a dissolving polymer was shown to directly dictate the dissolution rate of acidic polymers, by actively regulating the pH_m and influencing its dissolution. The dissolution of polymeric materials is a complex process ruled not only by the ionisation of their functional groups, but also by their nature and possible interactions. Knowledge of the pK_a value of these polymers may be useful when studying dissolution behaviour, however it is necessary to know the nature and the number of functional groups to accurately predict their ionisation and applicability in gastroresistant dosage forms.

Chapter 5

SUMMARY AND FUTURE WORK

5.1. Deciphering the challenge: mechanistic insights into polymer dissolution and subsequent drug release

After examining and discussing the obtained results in detail for the dissolution rate, microenvironmental pH and contact angle for all polymers, a broader discussion is needed covering all aspects of the tests and correlating these with other properties of the polymers, such as their constitution, estimated pK_a and DpHT. Ultimately, the goal is to understand the factors governing polymer dissolution. Contact angle kinetics has provided insight into hydrophilicity of the polymeric surface and corroborated the results obtained for the pH_m and the polymer dissolution rate.

It would be acceptable to assume that polymer dissolution is directly linked to the extent of ionisation of an enteric polymer, but other factors also play a role and the relationship is not as straightforward as usually perceived. Using HP-50 and HP-55 in low buffer capacity bicarbonate buffer as an example, the first has a higher dissolution rate (0.220±0.023 mg/min/cm^2 vs. 0.134±0.009 mg/min/cm^2, vide Table 4.5). The above-mentioned rationale would lead to the conclusion that HP-50 is more extensively ionised than HP-55. However, at the tested pH, both of these polymers should attain the same degree of ionisation, as they are more than 2 units above their estimated pK_a (vide Figure 1.6 and Table 5.1). They are also well above their reported DpHT, therefore the difference in dissolution rate ought not to be related to a possible effect of the pH of the media.

Regarding the pH_m, HP-50 has a lower value after 30 minutes, reinforcing that ionisation was more extensive for HP-50, producing more H^+ ions which would accumulate at the diffusion layer. Ultimately, a contradiction seems to arise: the extent of ionisation ought to be the same since both polymers are more than 2 units above the pKa, yet it is not, as shown by the difference in pH_m.

A possible explanation could reside in the percentage of functional groups each polymer contains, whereby a polymer with more ionisable groups should produce more protons when fully ionised. Nonetheless, this explanation is not viable as HP-50 has fewer groups (HP-50: 21.0-27.0%; HP-55: 27.0-35.0%) therefore fewer protons would be produced, which is not the case as a higher number of protons are indeed being produced by HP-50. An additional and more plausible

explanation lies with the type of functional groups in these materials. Phthalate (the substituent present in HP-50 and HP-55) contains an aromatic ring. This group is prone to interact with other intra- and inter-molecular rings by π-π stacking, hindering the disentanglement of the polymeric chains during dissolution (López-Barrón and Zhou, 2017). During polymer dissolution, the medium diffuses through the polymer, creates a gel layer through which produced protons diffuse towards the bulk solution and where the disentanglement of the polymeric chains occurs (more details in Figure 1.7). A delay in the disentanglement caused by a higher presence of phthalate groups (such as in case of HP-55) leads to a slower dissolution (i.e. a slower production of protons), meaning a higher pH_m after the 30 min of the test.

A different story unfolds for AS-LF and AS-HF regarding the effect of the number and type of functional groups affecting the polymer dissolution. For these polymers, a higher dissolution rate was obtained for AS-LF, which also had a lower pH_m. However, the % of functional groups is higher for AS-LF than for AS-HF (14.0-18.0% vs. 4.0-8.0%). This behaviour is contrary to that of HP, where the polymer with lowest % of functional groups had the highest dissolution rate and the lowest pH_m. The obtained results are explained by the type of functional group and are in agreement with the pK_a values, DpHT and obtained pH_m for these polymers (Table 5.1).

Firstly, in the case of AS-LF and AS-HF the difference in DpHT is much more than between HP-50 and HP-55. AS-LF dissolves above pH 5.5, whereas AS-HF dissolves above pH 6.8 which immediately causes a distinction; for HPMC-AS it is the polymer with the highest % of functional groups which dissolves at lower pH values, to the opposite of HPMC-P. This issue has been addressed and the reason for this difference is discussed in more detail in Section 2.3.6.

Secondly, it is also important to consider the pH at which all tests were conducted (pH 6.8), which corresponds to the DpHT of AS-HF. During polymer dissolution protons accumulate at the surface of the dissolving polymer, steadily decreasing the pH. For AS-HF even small increases in H^+ can drop the pH below its DpHT, hindering its dissolution. As fewer protons are produced due to a lower dissolution rate, the equilibrium between generated and removed protons is eventually re-established, and the pH_m of the dissolving polymer stabilises, causing a higher pH_m than for AS-LF. The estimated pK_a values for these polymers are very similar (AS-LF: 4.8; AS-HF 4.85), which

indicates that both these polymers should be nearly completely ionised at the pH used. However, the number of ionisable groups greatly differs between them, showing that, in the absence of additional hindering effects such as in the case of HP, more ionised groups lead to higher dissolution rates. The presence of more ionisable groups may increase the polymer's hydrophilicity, as demonstrated by lower contact angle values for AS-LF, which in turn increases the affinity of the media to the polymer, improving wettability and causing higher dissolution rates. Results from pH_m and dissolution rate measurements clearly demonstrate the importance not only of the buffer concentration, but of the buffer type and capacity.

Table 5.1: Comparative table of measured parameters of importance in regulating polymer dissolution.

Polymers	**% ionsable groups**	**pK_a**	**DpHT**	**pH_m**			
				Phosphate		Bicarbonate	
				5mM	50mM	4.17mM	40mM
HP-50	21-27% (phthalyl) [1]	3.99 ± 0.09	≥ 5.0 [1]	5.48 ± 0.01	6.54 ± 0.04	5.35 ± 0.04	6.42 ± 0.04
HP-55	27-35% (phthalyl) [1]	3.54 ± 0.20	≥ 5.5 [1]	5.61 ± 0.03	6.61 ± 0.02	5.53 ± 0.05	6.49 ± 0.01
HPMC **AS-LF**	14-18% (succinoyl) [2]	4.80 ± 0.20	≥ 5.5 [2]	5.98 ± 0.01	6.66 ± 0.03	5.86 ± 0.04	6.55 ± 0.02
HPMC **AS-HF**	4-8% (succinoyl) [2]	4.85 ± 0.16	≥ 6.8 [2]	6.09 ± 0.04	6.73 ± 0.01	6.02 ± 0.02	6.65 ± 0.01

***DpHT**: Dissolution pH threshold; **pH_m**: Microenvironmental pH*
1: Shin-Etsu Chemical Co. (2002)*; 2: Shin-Etsu Chemical Co.* (2018)

5.2. Future Works: New answers create new questions

The use of dynamic light scattering allowed for the measurement of the pK_a of different polymers, both natural and synthetic. The developed work showed how this technique can be used to study the ionisation behaviour of multiple polymers. Understanding how these polymers behave under different conditions would be the next step in this work, with both phosphate and bicarbonate buffers being the media to test. These two media types were tested throughout this thesis, with clear differences occurring with the two buffer types in polymer dissolution rates, microenvironmental pH, contact angles, among others. Therefore, it is important to address how these buffers influence the ionisation behaviour and ultimately the polymer dissolution.

The reported studies further demonstrated the complexity of polymer dissolution under different conditions; yet, it was only applied to selected polymers. When these polymers are used, they are coated onto an oral solid dosage form, where the drug and other excipients are also present. It has been previously demonstrated that the acidity or alkalinity of a tablet core can have significant effect on the dissolution of the enteric coating. This can be the case with high dose weakly acidic or basic drugs (Dangel et al., 2001; Dressman and Amidon, 1984; Ozturk et al., 1988a) or due to the presence of buffers or pH responsive excipients in the core which may modulate the dissolution of the coating both *in-vitro* (Liu et al., 2009) and *in-vivo* (Liu and Basit, 2010). These studies have demonstrated that the core is fully capable of buffering the polymeric layer, with more acidic cores leading to longer disintegration times of the coating (Dangel et al., 2001; Ozturk et al., 1988a) and less acidic cores leading to quicker drug releases (Liu et al., 2009). Therefore, future investigations aiming to directly study the dissolution of enteric coatings should consider the dissolution of both polymer and drug in the same system. Ultimately, a broader study of different polymer types (including acrylic enteric polymers) should be included to allow a better understanding of how and what affects polymer dissolution.

Parallelly to different polymer types, the study of the effect of different types of drugs (acidic, basic or non-ionisable) on the pH_m of dissolving polymers present in enteric solid dosage forms under biologically relevant conditions would present even deeper insights regarding polymer and drug dissolution *in-vivo*. To understand how the drug, the polymeric layer, the ionic strength, buffer type

and capacity of the medium affect the pHm and, indisputably, the dissolution of the polymer would be the apogee of decades of studies and would finally permit the design of the quintessential gastroresistant drug delivery system.

The capsules produced in this thesis may very well be applied to such studies, facilitating the process of sample preparation, where a drug or excipients to be tested may be directly added to the capsule, ready for further studies in a very short time. As shown, the drug release from AS-LF and HP-55 capsules is in accordance with the dissolution rates obtained for these polymers, showing the reliability of these formulations for future studies. A process of tablet manufacturing and coating is thus avoided, and variables may be more easily controlled. Moreover, the enteric capsules can be further optimised to manipulate the drug release and target various pH thresholds by using a blend of multiple enteric polymers. The capsule size and shape can also be optimised for various age groups in clinic or for animal species used in drug delivery research or for veterinary applications.

The next step in the productions of these capsules is to understand how different storage conditions may affect their stability and their enteric performance. A low water content may yield the capsules too brittle to handle or possibly excessive water may cause changes in the drug release profile due to enhanced diffusion. Additionally, it is important to also understand how the polymer type affects the formation of the capsules, and if polymers with different molecular weight would produce capsules with different properties. The final step would be assuring the scalability of this technology. Although the mechanics of the capsule formation are different from traditional gelatine capsules, the capsule production method is very similar, with the same dipping and drying steps. The key difference in this case would be to optimise drying conditions, to assure the polymeric film formation occurs at appropriate temperatures (accounting for the glass transition temperature of the polymer) and during an appropriate time while in the conveyor belts.

REFERENCES

Abrahamsson, B., Alpsten, M., Jonsson, U.E., Lundberg, P.J., Sandberg, A., Sundgren, M., Svenheden, A., Tölli, J., 1996. Gastro-intestinal transit of a multiple-unit formulation (metoprolol CR/ZOK) and a non-disintegrating tablet with the emphasis on colon. Int. J. Pharm. 140, 229–235. https://doi.org/10.1016/0378-5173(96)04604-2

Aduba, D.C., An, S.S., Selders, G.S., Yeudall, W.A., Bowlin, G.L., Kitten, T., Yang, H., 2019. Electrospun gelatin–arabinoxylan ferulate composite fibers for diabetic chronic wound dressing application. Int. J. Polym. Mater. Polym. Biomater. 68, 660–668. https://doi.org/10.1080/00914037.2018.1482466

Al-Gousous, J., Penning, M., Langguth, P., 2015. Molecular insights into shellac film coats from different aqueous shellac salt solutions and effect on disintegration of enteric-coated soft gelatin capsules. Int. J. Pharm. 484, 283–291. https://doi.org/10.1016/j.ijpharm.2014.12.060

Al-Gousous, J., Ruan, H., Blechar, J.A., Sun, K.X., Salehi, N., Langguth, P., Job, N.M., Lipka, E., Loebenberg, R., Bermejo, M., Amidon, G.E., Amidon, G.L., 2019. Mechanistic analysis and experimental verification of bicarbonate-controlled enteric coat dissolution: Potential in vivo implications. Eur. J. Pharm. Biopharm. 139, 47–58. https://doi.org/10.1016/j.ejpb.2019.03.012

Al-Saidan, S.M., Krishnaiah, Y.S.R., Patro, S.S., Satyanaryana, V., 2005. In vitro and in vivo evaluation of guar gum matrix tablets for oral controlled release of water-soluble diltiazem hydrochloride. AAPS PharmSciTech 6, E14–E21. https://doi.org/10.1208/pt060105

Albertini, B., Vitali, B., Passerini, N., Cruciani, F., Di Sabatino, M., Rodriguez, L., Brigidi, P., 2010. Development of microparticulate systems for intestinal delivery of Lactobacillus acidophilus and Bifidobacterium lactis. Eur. J. Pharm. Sci. 40, 359–366. https://doi.org/10.1016/j.ejps.2010.04.011

Ali-Merchant, R.H., Kulkarni, M., Alkademi, Liu, F., Basit, A.W., 2009. Efficacy of an enteric coating system suitable for nutraceutical applications (Nutrateric®). 2009 AAPS Annu. Meet. Expo.

Ali, A., Ahmed, S., 2018. A review on chitosan and its nanocomposites in drug delivery. Int. J. Biol. Macromol. 109, 273–286. https://doi.org/10.1016/j.ijbiomac.2017.12.078

Alvarez-Lorenzo, C., Blanco-Fernandez, B., Puga, A.M., Concheiro, A., 2013. Crosslinked ionic polysaccharides for stimuli-sensitive drug delivery. Adv. Drug Deliv. Rev. 65, 1148–1171. https://doi.org/10.1016/j.addr.2013.04.016

Alvarez-Manceñido, F., Landin, M., Lacik, I., Martínez-Pacheco, R., 2008. Konjac glucomannan and konjac glucomannan/xanthan gum mixtures as excipients for controlled drug delivery systems. Diffusion of small drugs. Int. J. Pharm. 349, 11–18. https://doi.org/10.1016/j.ijpharm.2007.07.015

Anton Paar GmbH, 2020. Basics of rheology :: Anton Paar Wiki. https://wiki.anton-paar.com/en/basics-of-rheology/ (Last accessed: 2020-01-28).

Arroyo-Maya, I.J., McClements, D.J., 2015. Biopolymer nanoparticles as potential delivery systems for anthocyanins: Fabrication and properties. Food Res. Int. 69, 1–8. https://doi.org/10.1016/j.foodres.2014.12.005

Aunins, J.G., Southard, M.Z., Myers, R.A., Himmelstein, K.J., Stella, V.J., 1985. Dissolution of carboxylic acids III: The effect of polyionizable buffers. J. Pharm. Sci. 74, 1305–1316. https://doi.org/10.1002/jps.2600741212

Bagheri, L., Madadlou, A., Yarmand, M., Mousavi, M.E., 2014. Spray-dried alginate microparticles carrying caffeine-loaded and potentially bioactive nanoparticles. Food Res. Int. 62, 1113–1119. https://doi.org/10.1016/j.foodres.2014.05.040

Barbosa, J.A.C., Al-Kauraishi, M.M., Smith, A.M., Conway, B.R., Merchant, H.A., 2019. Achieving gastroresistance without coating: Formulation of capsule shells from enteric polymers. Eur. J. Pharm. Biopharm. 144, 174–179. https://doi.org/10.1016/j.ejpb.2019.09.015

Barbosa, J.A.C., Conway, B.R., Merchant, H.A., 2017. Going Natural: Using polymers from nature for gastroresistant applications. Br. J. Pharm. 2, 14–30. https://doi.org/10.5920/bjpharm.2017.01

Benameur, H., 2015. Capsule technology: Enteric Capsule Drug Delivery Technology – Achieving Protection Without Coating. Drug Dev. Deliv. 15.

Beneke, C.E., Viljoen, A.M., Hamman, J.H., 2009. Polymeric plant-derived excipients in drug delivery. Molecules 14, 2602–2620. https://doi.org/10.3390/molecules14072602

BioCaps, 2019. Acid Resistant Vegetable Capsules Bio-VXR. Https://Biocaps.Net/Portfolio/Acid-Resistant-Vegetable-Capsules/.

Bogner, R.H., LaPorte, S.L., Hartz, B.M., Albanese, D.L., Bradley, M., 1997. Experimental evidence for the development of a microviscous layer near the surface of dissolving polyethylene glycol. Int. J. Pharm. 151, 155–164. https://doi.org/10.1016/S0378-5173(97)04878-3

Brophy, C.M., Moore, J.G., Christian, P.E., Egger, M.J., Taylor, A.T., 1986. Variability of gastric emptying

measurements in man employing standardized radiolabeled meals. Dig. Dis. Sci. 31, 799–806. https://doi.org/10.1007/bf01296046

Burke, S.E., Barrett, C.J., 2003. Acid-base equilibria of weak polyelectrolytes in multilayer thin films. Langmuir 19, 3297–3303. https://doi.org/10.1021/la026500i

Campbell, G.M., Čukelj Mustač, N., Alyassin, M., Gomez, L.D., Simister, R., Flint, J., Philips, D.J., Gronnow, M.J., Westwood, N.J., 2019. Integrated processing of sugarcane bagasse: Arabinoxylan extraction integrated with ethanol production. Biochem. Eng. J. 146, 31–40. https://doi.org/10.1016/j.bej.2019.03.001

Capsugel®, 2019. CAPSUGEL® Coni-Snap® Capsule size information. https://www.capsugel.com/knowledge-center/coni-snap-capsule-size-information (Last accessed: 02/02/2020).

Capsugel, 2019a. Functional Capsules. Https://Www.Capsugel.Com/Product-Suites/Functional-Capsules.

Capsugel, 2019b. enTRinsic™ DDT. https://www.capsugel.com/biopharmaceutical-technologies/entrinsic-ddt (Last accessed: 27/10/2019).

Capsugel, 2013. Capsugel® VCaps® Capsule size information. https://www.capsugel.com/knowledge-center/vcaps-capsule-size-information (Last accessed: 13/01/2020).

Cerea, M., Foppoli, A., Maroni, A., Palugan, L., Zema, L., Sangalli, M.E., 2008. Dry coating of soft gelatin capsules with HPMCAS. Drug Dev. Ind. Pharm. 34, 1196–1200. https://doi.org/10.1080/03639040801974360

Chang, R.-J., Wu, C.-J., Lin, Y.-H., 2015. Acid resistant capsule shell composition, acid resistant capsule shell and its preparing process - Google Patents. Patent number: US9452141B1.

Chen, L., Subirade, M., 2009. Elaboration and characterization of soy/zein protein microspheres for controlled nutraceutical delivery. Biomacromolecules 10, 3327–3334. https://doi.org/10.1021/bm900989y

Chourasia, M.K., Jain, S.K., 2004. Potential of guar gum microspheres for target specific drug release to colon. J. Drug Target. 12, 435–442. https://doi.org/10.1080/10611860400006604

Chow, P.S., Landhäusser, S.M., 2004. A method for routine measurements of total sugar and starch content in woody plant tissues. Tree Physiol. 24, 1129–1136. https://doi.org/10.1093/treephys/24.10.1129

Chuang, J.J., Huang, Y.Y., Lo, S.H., Hsu, T.F., Huang, W.Y., Huang, S.L., Lin, Y.S., 2017. Effects of pH on the Shape of Alginate Particles and Its Release Behavior. Int. J. Polym. Sci. 2017, 9. https://doi.org/10.1155/2017/3902704

Chung, Tze Wen, Lu, Y.F., Wang, S.S., Lin, Y.S., Chu, S.H., 2002. Growth of human endothelial cells on photochemically grafted Gly-Arg-Gly-Asp (GRGD) chitosans. Biomaterials 23, 4803–4809. https://doi.org/10.1016/S0142-9612(02)00231-4

Chung, Taek Woong, Yang, J., Akaike, T., Cho, K.Y., Nah, J.W., Kim, S. Il, Cho, C.S., 2002. Preparation of alginate/galactosylated chitosan scaffold for hepatocyte attachment. Biomaterials 23, 2827–2834. https://doi.org/10.1016/S0142-9612(01)00399-4

Cole, E.T., Scott, R.A., Connor, A.L., Wilding, I.R., Petereit, H.U., Schminke, C., Beckert, T., Cadé, D., 2002. Enteric coated HPMC capsules designed to achieve intestinal targeting. Int. J. Pharm. 231, 83–95. https://doi.org/10.1016/S0378-5173(01)00871-7

Colorcon®, 2019. Nutrateric® Nutritional Enteric Coating System. Http://Www.Colorcon.Com/Products-Formulation/All-Products/Nutritional-Coatings/Enteric-Release/Nutrateric.

Czarnocka, J.K., Alhnan, M.A., 2015. Gastro-resistant characteristics of GRAS-grade enteric coatings for pharmaceutical and nutraceutical products. Int. J. Pharm. 486, 167–174. https://doi.org/10.1016/j.ijpharm.2015.03.039

D'Haens, G.R., Sandborn, W.J., Zou, G., Stitt, L.W., Rutgeerts, P.J., Gilgen, D., Jairath, V., Hindryckx, P., Shackelton, L.M., Vandervoort, M.K., Parker, C.E., Muller, C., Pai, R.K., Levchenko, O., Marakhouski, Y., Horynski, M., Mikhailova, E., Kharchenko, N., Pimanov, S., Feagan, B.G., 2017. Randomised non-inferiority trial: 1600 mg versus 400 mg tablets of mesalazine for the treatment of mild-to-moderate ulcerative colitis. Aliment. Pharmacol. Ther. 46, 292–302. https://doi.org/10.1111/apt.14164

Dangel, C., Kolter, K., Reich, H.B., Schepky, G., 2001. Aqueous enteric coatings with methacrylic acid copolymer type C on acidic and basic drugs in tablets and pellets, Part II: Dosage forms containing indomethacin and diclofenac sodium. Pharm. Technol. Eur. 13, 36/42.

Davis, M., Ichikawa, I., Williams, E.J., Banker, G.S., 1986. Comparison and evaluation of enteric polymer properties in aqueous solutions. Int. J. Pharm. 28, 157–166. https://doi.org/10.1016/0378-5173(86)90241-3

Davis, S.S., Hardy, J.G., Taylor, M.J., Whalley, D.R., Wilson, C.G., 1984. The effect of food on the gastrointestinal transit of pellets and an osmotic device (Osmet). Int. J. Pharm. 21, 331–340. https://doi.org/10.1016/0378-5173(84)90191-1

De Barros, J.M.S., Lechner, T., Charalampopoulos, D., Khutoryanskiy, V. V., Edwards, A.D., 2015. Enteric coated spheres produced by extrusion/spheronization provide effective gastric protection and efficient release of live therapeutic bacteria. Int. J. Pharm. 493, 483–494. https://doi.org/10.1016/j.ijpharm.2015.06.051

De Carvalho, R.A., Grosso, C.R.F., 2006. Properties of chemically modified gelatin films. Brazilian J. Chem. Eng.

23, 45–53. https://doi.org/10.1590/s0104-66322006000100006

Dickhaus, B.N., Priefer, R., 2016. Determination of polyelectrolyte pKa values using surface-to-air tension measurements. Colloids Surfaces A Physicochem. Eng. Asp. 488, 15–19. https://doi.org/10.1016/j.colsurfa.2015.10.015

Dimantov, A., Greenberg, M., Kesselman, E., Shimoni, E., 2004. Study of high amylose corn starch as food grade enteric coating in a microcapsule model system. Innov. Food Sci. Emerg. Technol. 5, 93–100. https://doi.org/10.1016/j.ifset.2003.11.003

Dionísio, M., Grenha, A., 2012. Locust bean gum: Exploring its potential for biopharmaceutical applications. J. Pharm. Bioallied Sci. 4, 175–185. https://doi.org/10.4103/0975-7406.99013

Doherty, C., York, P., 1989. Microenvironmental pH control of drug dissolution. Int. J. Pharm. 50, 223–232. https://doi.org/10.1016/0378-5173(89)90126-9

Dornez, E., Gebruers, K., Delcour, J.A., Courtin, C.M., 2009. Grain-associated xylanases: occurrence, variability, and implications for cereal processing. Trends Food Sci. Technol. https://doi.org/10.1016/j.tifs.2009.05.004

Dressman, J.B., Amidon, G.L., 1984. Radiotelemetric method for evaluating enteric coatings in vivo. J. Pharm. Sci. 73, 935–938. https://doi.org/10.1002/jps.2600730718

Dressman, J.B., Amidon, G.L., Reppas, C., Shah, V.P., 1998. Dissolution testing as a prognostic tool for oral drug absorption: Immediate release dosage forms. Pharm. Res. 15, 11–22. https://doi.org/10.1023/A:1011984216775

Du, J., Dai, J., Liu, J.L., Dankovich, T., 2006. Novel pH-sensitive polyelectrolyte carboxymethyl Konjac glucomannan-chitosan beads as drug carriers. React. Funct. Polym. 66, 1055–1061. https://doi.org/10.1016/j.reactfunctpolym.2006.01.014

Dubois, M., Gilles, K.A., Hamilton, J.K., Rebers, P.A., Smith, F., 1956. Colorimetric Method for Determination of Sugars and Related Substances. Anal. Chem. https://doi.org/10.1021/ac60111a017

Evonik, 2015. EUDRAGIT ® E 100, EUDRAGIT ® E PO and EUDRAGIT ® E 12,5. Evonik Tech. Inf. 1–6.

Evonik Industries, 2019. EUDRAGIT® product brochure. https://healthcare.evonik.com/product/health-care/downloads/evonik-eudragit-brochure.pdf (Last access: 17/10/2019).

Evonik Industries, 2018. Technical Information: EUDRAGIT® L 100-55. https://oncare.evonik.com/media/?file=868_evonik_specification_and_test_methods_eudragit_l_100_55.pdf (Last accessed: 16/01/2020).

Evonik Industries, 2012. Technical Information EUDRAGIT® L 100 and EUDRAGIT® S 100. Evonik Ind. AG 1–7.

Evonik Industries AG, 2018. EUDRAGUARD® product brochure - Advanced functional coating solutions for nutraceuticals. Https://Healthcare.Evonik.Com/Product/Health-Care/Downloads/Evonik-Eudraguard-Brochure.Pdf.

Fagron, 2019. Entericaps®. https://fagron.com/sites/default/files/fagron/iberica/pdf/ENTERICAPS%20Folleto%20BR.pdf (last accessed: 11/02/2020).

Fan, J., Wang, K., Liu, M., He, Z., 2008. In vitro evaluations of konjac glucomannan and xanthan gum mixture as the sustained release material of matrix tablet. Carbohydr. Polym. 73, 241–247. https://doi.org/10.1016/j.carbpol.2007.11.027

Farag Badawy, S.I., Hussain, M.A., 2007. Microenvironmental pH modulation in solid dosage forms. J. Pharm. Sci. 96, 948–959. https://doi.org/10.1002/jps.20932

Farris, S., Introzzi, L., Biagioni, P., Holz, T., Schiraldi, A., Piergiovanni, L., 2011. Wetting of biopolymer coatings: Contact angle kinetics and image analysis investigation. Langmuir 27, 7563–7574. https://doi.org/10.1021/la2017006

Future Market Insights, 2016. Empty Capsule Market: Increased demand for vegetarian empty capsules in developing markets to create significant revenue traction : Global Industry Analysis and Opportunity Assessment, 2016 - 2026. Http://Www.Futuremarketinsights.Com/Reports/Empty-Capsules-Market.

Galia, E., Nicolaides, E., Hörter, D., Löbenberg, R., Reppas, C., Dressman, J.B., 1998. Evaluation of various dissolution media for predicting In vivo performance of class I and II drugs. Pharm. Res. 15, 698–705. https://doi.org/10.1023/A:1011910801212

Garbacz, G., Wedemeyer, R.S., Nagel, S., Giessmann, T., Mönnikes, H., Wilson, C.G., Siegmund, W., Weitschies, W., 2008. Irregular absorption profiles observed from diclofenac extended release tablets can be predicted using a dissolution test apparatus that mimics in vivo physical stresses. Eur. J. Pharm. Biopharm. 70, 421–428. https://doi.org/10.1016/j.ejpb.2008.05.029

Gerchakov, S.M., Hatcher, P.G., 1972. Improved Technique for Analysis of Carbohydrates in Sediments. Limnol. Oceanogr. 17, 938–943. https://doi.org/10.4319/lo.1972.17.6.0938

Ghanam, D., Kleinebudde, P., 2011. Suitability of κ-carrageenan pellets for the formulation of multiparticulate tablets with modified release. Int. J. Pharm. 409, 9–18. https://doi.org/10.1016/j.ijpharm.2011.02.016

Ghori, M.U., Ginting, G., Smith, A.M., Conway, B.R., 2014. Simultaneous quantification of drug release and erosion from hypromellose hydrophilic matrices. Int. J. Pharm. 465, 405–412. https://doi.org/10.1016/j.ijpharm.2014.02.028

Giunchedi, P., Conte, U., Chetoni, P., Saettone, M.F., 1999. Pectin microspheres as ophthalmic carriers for piroxicam: Evaluation in vitro and in vivo in albino rabbits. Eur. J. Pharm. Sci. 9, 1–7. https://doi.org/10.1016/S0928-0987(99)00023-8

Goyanes, A., Hatton, G.B., Merchant, H.A., Basit, A.W., 2015. Gastrointestinal release behaviour of modified-release drug products: Dynamic dissolution testing of mesalazine formulations. Int. J. Pharm. 484, 103–108. https://doi.org/10.1016/j.ijpharm.2015.02.051

Hansch, C., Leo, A., Hoekman, D., 1995. Hydrophobic, electronic, and steric constants, ACS Professional Reference Book, ACS professional reference book. American Chemical Society.

Harianawala, A.I., Bogner, R.H., Bradley, M., 2002. Measurement of pH near dissolving enteric coatings. Int. J. Pharm. 247, 139–146. https://doi.org/10.1016/S0378-5173(02)00404-0

Hodsdon, A.C., Mitchell, J.R., Davies, M.C., Melia, C.D., 1995. Structure and behaviour in hydrophilic matrix sustained release dosage forms: 3. The influence of pH on the sustained-release performance and internal gel structure of sodium alginate matrices. J. Control. Release 33, 143–152. https://doi.org/10.1016/0168-3659(94)00076-7

Hu, Q., Li, B., Wang, M., Shen, J., 2004. Preparation and characterization of biodegradable chitosan/hydroxyapatite nanocomposite rods via in situ hybridization: A potential material as internal fixation of bone fracture. Biomaterials 25, 779–785. https://doi.org/10.1016/S0142-9612(03)00582-9

Ibekwe, V.C., Fadda, H.M., Parsons, G.E., Basit, A.W., 2006. A comparative in vitro assessment of the drug release performance of pH-responsive polymers for ileo-colonic delivery. Int. J. Pharm. 308, 52–60. https://doi.org/10.1016/j.ijpharm.2005.10.038

Imai, T., Shiraishi, S., Otagiri, M., 2000. A strategy for the immediate-release of indomethacin from a sustained-release preparation using a chitosan hydrolysate. S.T.P. Pharma Sci. 10, 57–62.

Jain, V., Karibasappa, G., Dodamani, A., Mali, G., 2017. Estimating the carbohydrate content of various forms of tobacco by phenol-sulfuric acid method. J. Educ. Health Promot. 6, 90. https://doi.org/10.4103/jehp.jehp_41_17

Jantratid, E., Janssen, N., Reppas, C., Dressman, J.B., 2008. Dissolution media simulating conditions in the proximal human gastrointestinal tract: An update. Pharm. Res. 25, 1663–1676. https://doi.org/10.1007/s11095-008-9569-4

Karkossa, F., Klein, S., 2017. Assessing the influence of media composition and ionic strength on drug release from commercial immediate-release and enteric-coated aspirin tablets. J. Pharm. Pharmacol. 69, 1327–1340. https://doi.org/10.1111/jphp.12777

Kawakami, T., Antoh, M., Hasegawa, H., Yamagishi, T., Ito, M., Eda, S., 1992. Experimental study on osteoconductive properties of a chitosan-bonded hydroxyapatite self-hardening paste. Biomaterials 13, 759–763. https://doi.org/10.1016/0142-9612(92)90014-F

Kesavan, K., Nath, G., Pandit, J.K., 2010. Sodium alginate based mucoadhesive system for gatifloxacin and its in vitro antibacterial activity. Sci. Pharm. 78, 941–957. https://doi.org/10.3797/scipharm.1004-24

Khoshakhlagh, P., Johnson, R., Langguth, P., Nawroth, T., Schmueser, L., Hellmann, N., Decker, H., Szekely, N.K., 2015. Fasted-State Simulated Intestinal Fluid “faSSIF-C”, a Cholesterol Containing Intestinal Model Medium for in Vitro Drug Delivery Development. J. Pharm. Sci. 104, 2213–2224. https://doi.org/10.1002/jps.24470

Khutoryanskiy, V. V., 2015. Supramolecular materials: Longer and safer gastric residence. Nat. Mater. https://doi.org/10.1038/nmat4432

Klein, S., 2010. The use of biorelevant dissolution media to forecast the in vivo performance of a drug. AAPS J. https://doi.org/10.1208/s12248-010-9203-3

Klein, S., Dressman, J.B., Butler, J., Hempenstall, J.M., Reppas, C., 2004. Media to simulate the postprandial stomach I. Matching the physicochemical characteristics of standard breakfasts. J. Pharm. Pharmacol. 56, 605–610. https://doi.org/10.1211/0022357023367

Krieg, B.J., Taghavi, S.M., Amidon, G.L., Amidon, G.E., 2014. In vivo predictive dissolution: Transport analysis of the CO2, bicarbonate in vivo buffer system. J. Pharm. Sci. 103, 3473–3490. https://doi.org/10.1002/jps.24108

Kumar, P.T.S., Abhilash, S., Manzoor, K., Nair, S. V., Tamura, H., Jayakumar, R., 2010. Preparation and characterization of novel β-chitin/nanosilver composite scaffolds for wound dressing applications. Carbohydr. Polym. 80, 761–767. https://doi.org/10.1016/j.carbpol.2009.12.024

Kuntz, T., 2016. EUDRAGUARD® World - The Next Level in Nutraceutical Delivery. Evonik Workshop - Advances in nutraceuticals through functional ingredients and targeted delivery.

Kushwaha, S.C., Kates, M., 1981. Modification of phenol-sulfuric acid method for the estimation of sugars in lipids. Lipids 16, 372–373. https://doi.org/10.1007/BF02534965

Lambert, J.M., Weinbreck, F., Kleerebezem, M., 2008. In vitro analysis of protection of the enzyme bile salt hydrolase against enteric conditions by whey protein-gum arabic microencapsulation. J. Agric. Food Chem. 56, 8360–8364. https://doi.org/10.1021/jf801068u

Lennernäs, H., Abrahamsson, B., 2005. The use of biopharmaceutic classification of drugs in drug discovery and development: current status and future extension. J. Pharm. Pharmacol. 57, 273–285. https://doi.org/10.1211/0022357055263

Leong, K.H., Chung, L.Y., Noordin, M.I., Mohamad, K., Nishikawa, M., Onuki, Y., Morishita, M., Takayama, K., 2011. Carboxymethylation of kappa-carrageenan for intestinal-targeted delivery of bioactive macromolecules. Carbohydr. Polym. 83, 1507–1515. https://doi.org/10.1016/j.carbpol.2010.09.062

Li, L., Ni, R., Shao, Y., Mao, S., 2014. Carrageenan and its applications in drug delivery. Carbohydr. Polym. 103, 1–11. https://doi.org/10.1016/j.carbpol.2013.12.008

Li, X.N., Guo, H.X., Heinamaki, J., 2010. Aqueous coating dispersion (pseudolatex) of zein improves formulation of sustained-release tablets containing very water-soluble drug. J. Colloid Interface Sci. 345, 46–53. https://doi.org/10.1016/j.jcis.2010.01.029

Limmatvapirat, S., Panchapornpon, D., Limmatvapirat, C., Nunthanid, J., Luangtana-Anan, M., Puttipipatkhachorn, S., 2008. Formation of shellac succinate having improved enteric film properties through dry media reaction. Eur. J. Pharm. Biopharm. 70, 335–344. https://doi.org/10.1016/j.ejpb.2008.03.002

Liu, F., Basit, A.W., 2010. A paradigm shift in enteric coating: Achieving rapid release in the proximal small intestine of man. J. Control. Release 147, 242–245. https://doi.org/10.1016/j.jconrel.2010.07.105

Liu, F., Lizio, R., Meier, C., Petereit, H.U., Blakey, P., Basit, A.W., 2009. A novel concept in enteric coating: A double-coating system providing rapid drug release in the proximal small intestine. J. Control. Release 133, 119–124. https://doi.org/10.1016/j.jconrel.2008.09.083

Liu, F., Merchant, H.A., Kulkarni, R.P., Alkademi, M., Basit, A.W., 2011. Evolution of a physiological pH 6.8 bicarbonate buffer system: Application to the dissolution testing of enteric coated products. Eur. J. Pharm. Biopharm. 78, 151–157. https://doi.org/10.1016/j.ejpb.2011.01.001

López-Barrón, C.R., Zhou, H., 2017. Extensional Strain Hardening Induced by π-π Interactions in Barely Entangled Polymer Chains: The Curious Case of Poly(4-vinylbiphenyl). Phys. Rev. Lett. 119. https://doi.org/10.1103/PhysRevLett.119.247801

Lu, E.X., Jiang, Z.Q., Zhang, Q.Z., Jiang, X.G., 2003. A water-insoluble drug monolithic osmotic tablet system utilizing gum arabic as an osmotic, suspending and expanding agent. J. Control. Release 92, 375–382. https://doi.org/10.1016/S0168-3659(03)00371-7

Luo, Y., Pan, K., Zhong, Q., 2015. Casein/pectin nanocomplexes as potential oral delivery vehicles. Int. J. Pharm. 486, 59–68. https://doi.org/10.1016/j.ijpharm.2015.03.043

Luxbacher, T., 2014. The zeta potential for solid surface analysis, 1st Editio. ed. Anton Paar GmbH, Austria.

Ma, Q., Ren, Y., Wang, L., 2017. Investigation of antioxidant activity and release kinetics of curcumin from tara gum/ polyvinyl alcohol active film. Food Hydrocoll. 70, 286–292. https://doi.org/10.1016/j.foodhyd.2017.04.018

Madhumathi, K., Sudheesh Kumar, P.T., Abhilash, S., Sreeja, V., Tamura, H., Manzoor, K., Nair, S. V., Jayakumar, R., 2010. Development of novel chitin/nanosilver composite scaffolds for wound dressing applications. J. Mater. Sci. Mater. Med. 21, 807–813. https://doi.org/10.1007/s10856-009-3877-z

Mahdavinia, G.R., Etemadi, H., Soleymani, F., 2015. Magnetic/pH-responsive beads based on caboxymethyl chitosan and κ-carrageenan and controlled drug release. Carbohydr. Polym. 128, 112–121. https://doi.org/10.1016/j.carbpol.2015.04.022

Mahdi, H.J., 2015. Eudragit L-100 for enteric coating of hard gelatine capsules: Formulation and evaluation. Issues Biol. Sci. Pharm. Res. 3, 14–20. https://doi.org/10.15739/ibspr.008

Maiti, S., Singha, K., Ray, S., Dey, P., Sa, B., 2009. Adipic acid dihydrazide treated partially oxidized alginate beads for sustained oral delivery of flurbiprofen Oxidized alginate beads of flurbiprofen S. Maiti et al. Pharm. Dev. Technol. 14, 461–470. https://doi.org/10.1080/10837450802712658

Malvern Instruments Ltd, 2005. Automated Protein Characterization With The MPT-2 Autotitrator: Zetasizer Nano Application note.

Marzorati, M., Possemiers, S., Verhelst, A., Cadé, D., Madit, N., Van de Wiele, T., 2015. A novel hypromellose capsule, with acid resistance properties, permits the targeted delivery of acid-sensitive products to the intestine. LWT - Food Sci. Technol. 60, 544–551. https://doi.org/10.1016/j.lwt.2014.08.040

Masuko, T., Minami, A., Iwasaki, N., Majima, T., Nishimura, S.I., Lee, Y.C., 2005. Carbohydrate analysis by a phenol-sulfuric acid method in microplate format. Anal. Biochem. 339, 69–72. https://doi.org/10.1016/j.ab.2004.12.001

Mattioli-Belmonte, M., Gigante, A., Muzzarelli, R.A.A., Politano, R., De Benedittis, A., Specchia, N., Buffa, A., Biagini, G., Greco, F., 1999. N,N-dicarboxymethyl chitosan as delivery agent for bone morphogenetic protein in the repair of articular cartilage. Med. Biol. Eng. Comput. 37, 130–134. https://doi.org/10.1007/BF02513279

McConnell, E.L., Fadda, H.M., Basit, A.W., 2008. Gut instincts: Explorations in intestinal physiology and drug delivery. Int. J. Pharm. https://doi.org/10.1016/j.ijpharm.2008.05.012

Meghal, A.K., Chaudhari, P.S., Mathur, V.B., 2011. Formulation and evaluation of enteric coated HPMC capsule of diclofenac sodium. Res. J. Pharm. Biol. Chem. Sci. 2, 790–797.

Mehuys, E., Remon, J.P., Vervaet, C., 2005. Production of enteric capsules by means of hot-melt extrusion. Eur. J. Pharm. Sci. 24, 207–212. https://doi.org/10.1016/j.ejps.2004.10.011

Mendis, M., Simsek, S., 2014. Arabinoxylans and human health. Food Hydrocoll. 42, 239–243. https://doi.org/10.1016/j.foodhyd.2013.07.022

Merchant, H.A., 2012. In-vitro, in-vivo and in-silico models in oral drug delivery and their relevance to human gastrointestinal physiology (PhD Thesis). UCL School of Pharmacy, University College London.

Merchant, H.A., Frost, J.A., Basit, A.W., 2013. Apparatus and methods for testing medicaments. Patent number: WO2013164629A1.

Merchant, H.A., Goyanes, A., Parashar, N., Basit, A.W., 2014. Predicting the gastrointestinal behaviour of modified-release products: Utility of a novel dynamic dissolution test apparatus involving the use of bicarbonate buffers. Int. J. Pharm. 475, 585–591. https://doi.org/10.1016/j.ijpharm.2014.09.003

Miller-Chou, B.A., Koenig, J.L., 2003. A review of polymer dissolution. Prog. Polym. Sci. https://doi.org/10.1016/S0079-6700(03)00045-5

Murachanian, D., 2010. Two-Piece Hard Capsules for Pharmaceutical Formulations. J. GXP Compliance 14, 2013.

Musabayane, C.T., Munjeri, O., Matavire, T.P., 2003. Transdermal delivery of chloroquine by amidated pectin hydrogel matrix patch in the rat. Ren. Fail. 25, 525–534. https://doi.org/10.1081/JDI-120022543

Nature's Way Products, 2011a. ProbioticPearls™ Why Pearls. http://www.pearlsprobiotics.com/Why-Pearls.

Nature's Way Products, 2011b. All about Acidophilus Pearls. https://www.supersupps.com/downloads/product_files/228/All%20about%20Acidophilus%20Pearls.pdf.

Nguyen, D.A., Fogler, H.S., 2005. Facilitated diffusion in the dissolution of carboxylic polymers. AIChE J. 51, 415–425. https://doi.org/10.1002/aic.10329

Niño-Medina, G., Carvajal-Millán, E., Rascon-Chu, A., Marquez-Escalante, J.A., Guerrero, V., Salas-Muñoz, E., 2010. Feruloylated arabinoxylans and arabinoxylan gels: Structure, sources and applications. Phytochem. Rev. https://doi.org/10.1007/s11101-009-9147-3

Oliveira, H.V.A., Peixoto, M.P.G., Tacon, L.A., Freitas, L.A.P., 2013. Enteric coating of hard gelatin capsules by the spouted bed process. J. Appl. Pharm. Sci. 3, 57–63. https://doi.org/10.7324/JAPS.2013.3810

Ozturk, S.S., Palsson, B.O., Donohoe, B., Dressman, J.B., 1988a. Kinetics of Release from Enteric-Coated Tablets. Pharm. Res. An Off. J. Am. Assoc. Pharm. Sci. 5, 550–565. https://doi.org/10.1023/A:1015937912504

Ozturk, S.S., Palsson, B.O., Dressman, J.B., 1988b. Dissolution of Ionizable Drugs in Buffered and Unbuffered Solutions. Pharm. Res. An Off. J. Am. Assoc. Pharm. Sci. 5, 272–282. https://doi.org/10.1023/A:1015970502993

Park, H.J., 2009. Film-Forming composition for hard capsules comprising fish gelatin and its preparation method. Patent number: WO2007/123350Al.

Patel, S., 2012. Therapeutic importance of sulfated polysaccharides from seaweeds: updating the recent findings. 3 Biotech 2, 171–185. https://doi.org/10.1007/s13205-012-0061-9

Picker, K.M., 1999. Matrix tablets of carrageenans. II. Release behavior and effect of added cations. Drug Dev. Ind. Pharm. 25, 339–346. https://doi.org/10.1081/DDC-100102179

Podczeck, F., Jones, B.E., 2004. Manufacture and properties of two-piece hard capsules, in: Podczeck, Fridrun, Jones, Brian E (Eds.), Pharmaceutical Capsules. Pharmaceutical Press, pp. 79–100.

Prajapati, V.D., Jani, G.K., Moradiya, N.G., Randeria, N.P., 2013. Pharmaceutical applications of various natural gums, mucilages and their modified forms. Carbohydr. Polym. 92, 1685–1699. https://doi.org/10.1016/j.carbpol.2012.11.021

Qualicaps, 2019. Qualicaps Capsules. https://qualicaps.com/en/Capsules/pharma.

Quinteros, D.A., Manzo, R.H., Allemandi, D.A., 2011. Interaction between Eudragit® E100 and anionic drugs: Addition of anionic polyelectrolytes and their influence on drug release performance. J. Pharm. Sci. 100, 4664–4673. https://doi.org/10.1002/jps.22651

Rahman Bhuiyan, M.A., Hossain, M.A., Zakaria, M., Islam, M.N., Zulhash Uddin, M., 2017. Chitosan Coated Cotton Fiber: Physical and Antimicrobial Properties for Apparel Use. J. Polym. Environ. 25, 334–342. https://doi.org/10.1007/s10924-016-0815-2

Rajabi-siahboomi, A.R., Rane, M., 2018. Medicines Complete: Polyvinyl Acetate Phthalate. https://www.medicinescomplete.com/#/content/excipients/1001944009 (Last accessed: 15/01/2020).

Rajsharad, C., Kamble, S., Pareek, S., 2005. Aqueous film coating composition containing sodium alginate and preparation thereof. Patent number: US8123849B2.

Ramtoola, Z., Corrigan, O.I., 1989. Influence of the buffering capacity of the medium on the dissolution of drug-excipient mixtures. Drug Dev. Ind. Pharm. 15, 2359–2374. https://doi.org/10.3109/03639048909052535

Rasool, B.K.A., Fahmy, S.A., Galeel, O.W.A., 2012. Impact of Chitosan as a disintegrant on the bioavailability of furosemide tablets: In vitro evaluation and in vivo simulation of novel formulations. Pak. J. Pharm. Sci. 25, 815–822.

Ravi, V., Siddaramaiah, Pramod Kumar, T.M., 2008. Influence of natural polymer coating on novel colon targeting drug delivery system. J. Mater. Sci. Mater. Med. 19, 2131–2136. https://doi.org/10.1007/s10856-007-3155-x

Reis, A. V., Guilherme, M.R., Cavalcanti, O.A., Rubira, A.F., Muniz, E.C., 2006. Synthesis and characterization of pH-responsive hydrogels based on chemically modified Arabic gum polysaccharide. Polymer (Guildf). 47, 2023–2029. https://doi.org/10.1016/j.polymer.2006.01.058

Reix, N., Guhmann, P., Bietiger, W., Pinget, M., Jeandidier, N., Sigrist, S., 2012. Duodenum-specific drug delivery: In vivo assessment of a pharmaceutically developed enteric-coated capsule for a broad applicability in rat studies. Int. J. Pharm. 422, 338–340. https://doi.org/10.1016/j.ijpharm.2011.10.017

Riedel, A., Leopold, C.S., 2005. Degradation of omeprazole induced by enteric polymer solutions and aqueous dispersions: HPLC investigations. Drug Dev. Ind. Pharm. 31, 151–160. https://doi.org/10.1081/DDC-200047787

Roxlor, 2019. Roxlor Capsules. Http://Www.Roxlor.Com/Products.Php.

Rutz, J.K., Zambiazi, R.C., Borges, C.D., Krumreich, F.D., Da Luz, S.R., Hartwig, N., Da Rosa, C.G., 2013. Microencapsulation of purple Brazilian cherry juice in xanthan, tara gums and xanthan-tara hydrogel matrixes. Carbohydr. Polym. 98, 1256–1265. https://doi.org/10.1016/j.carbpol.2013.07.058

Sansone, F., Mencherini, T., Picerno, P., D'Amore, M., Aquino, R.P., Lauro, M.R., 2011. Maltodextrin/pectin microparticles by spray drying as carrier for nutraceutical extracts. J. Food Eng. 105, 468–476. https://doi.org/10.1016/j.jfoodeng.2011.03.004

Schmidt-Mende, T., 2001. Freisetzung aus magensaftresistent überzogenen Arzneiformen (PhD Thesis). Heinrich-Heine-Universität Düsseld. 1–198.

Shalumon, K.T., Binulal, N.S., Selvamurugan, N., Nair, S. V., Menon, D., Furuike, T., Tamura, H., Jayakumar, R., 2009. Electrospinning of carboxymethyl chitin/poly(vinyl alcohol) nanofibrous scaffolds for tissue engineering applications. Carbohydr. Polym. 77, 863–869. https://doi.org/10.1016/j.carbpol.2009.03.009

Sheng, J.J., McNamara, D.P., Amidon, G.L., 2009. Toward an In Vivo dissolution methodology: A comparison of phosphate and bicarbonate buffers. Mol. Pharm. 6, 29–39. https://doi.org/10.1021/mp800148u

Shi, J., Alves, N.M., Mano, J.F., 2008. Chitosan coated alginate beads containing poly(N-isopropylacrylamide) for dual-stimuli-responsive drug release. J. Biomed. Mater. Res. - Part B Appl. Biomater. 84, 595–603. https://doi.org/10.1002/jbm.b.30907

Shi, L.E., Li, Z.H., Li, D.T., Xu, M., Chen, H.Y., Zhang, Z.L., Tang, Z.X., 2013. Encapsulation of probiotic lactobacillus bulgaricus in alginate'milk microspheres and evaluation of the survival in simulated gastrointestinal conditions. J. Food Eng. 117, 99–104. https://doi.org/10.1016/j.jfoodeng.2013.02.012

Shi, L.E., Zheng, W., Zhang, Y., Tang, Z.X., 2016. Milk-alginate microspheres: Protection and delivery of Enterococcus faecalis HZNU P2. LWT - Food Sci. Technol. 65, 840–844. https://doi.org/10.1016/j.lwt.2015.08.071

Shin-Etsu Chemical Co., 2018. AQOAT® - For Pharmaceutical: Shin-Etsu Cellulose. http://www.elementoorganika.ru/files/aqoat (Last accessed: 05/01/2020).

Shin-Etsu Chemical Co., 2002. Hydroxypropyl Methylcellulose Phthalate - HPMCP: Technical information. http://www.metolose.ru/files/hpmcp.pdf (Last accessed: 09/01/2020).

Siepe, S., Lueckel, B., Kramer, A., Ries, A., Gurny, R., 2006. Strategies for the design of hydrophilic matrix tablets with controlled microenvironmental pH. Int. J. Pharm. 316, 14–20. https://doi.org/10.1016/j.ijpharm.2006.02.021

Smith, A.M., Ingham, A., Grover, L.M., Perrie, Y., 2010. Polymer film formulations for the preparation of enteric pharmaceutical capsules. J. Pharm. Pharmacol. 62, 167–172. https://doi.org/10.1211/jpp.62.02.0003

Smith, R., 2019. Medicines Complete: Cellulose Acetate Phthalate. https://www.medicinescomplete.com/#/content/excipients/1001935793 (Last accessed: 16/01/2020).

Söderlind, E., Karlsson, E., Carlsson, A., Kong, R., Lenz, A., Lindborg, S., Sheng, J.J., 2010. Simulating fasted human intestinal fluids: Understanding the roles of lecithin and bile acids. Mol. Pharm. 7, 1498–1507. https://doi.org/10.1021/mp100144v

Spitael, J., Kinget, R., 1977. Factors affecting the dissolution rate of enteric coatings. Pharm. Ind. 39, 502–505.

Sriamornsak, P., Sungthongjeen, S., Puttipipatkhachorn, S., 2007. Use of pectin as a carrier for intragastric floating drug delivery: Carbonate salt contained beads. Carbohydr. Polym. 67, 436–445. https://doi.org/10.1016/j.carbpol.2006.06.013

Taniguchi, C., Kawabata, Y., Wada, K., Yamada, S., Onoue, S., 2014. Microenvironmental pH-modification to

improve dissolution behavior and oral absorption for drugs with pH-dependent solubility. Expert Opin. Drug Deliv. 11, 505–516. https://doi.org/10.1517/17425247.2014.881798

Torpac®, 2016a. Torpac® - Capsules Pharma Use / Rat & Guinea pig. https://www.torpac.com/ (Last accessed: 10/02/2020).

Torpac®, 2016b. Torpac ® - A dispensing & dosing aid for veterinarians. https://www.torpac.com/ (Last accessed: 10/02/2020).

Tran, P.H.L., Tran, H.T.T., Lee, B.J., 2008. Modulation of microenvironmental pH and crystallinity of ionizable telmisartan using alkalizers in solid dispersions for controlled release. J. Control. Release 129, 59–65. https://doi.org/10.1016/j.jconrel.2008.04.001

Tulain, U.R., Ahmad, M., Rashid, A., 2018. Development, in vitro and in vivo evaluation of hydrogel based system of carboxymethyl arabinoxylan for controlled delivery of rabeprazole sodium. Polym. - Plast. Technol. Eng. 57, 1771–1783. https://doi.org/10.1080/03602559.2018.1434668

Unna, 1884. Keratinirte Pillen. Pharm. Zentrahlle 25.

Vácha, R., Horinek, D., Berkowitz, M.L., Jungwirth, P., 2008. Hydronium and hydroxide at the interface between water and hydrophobic media. Phys. Chem. Chem. Phys. 10, 4975–4980. https://doi.org/10.1039/b806432f

Vandamme, T.F., Lenourry, A., Charrueau, C., Chaumeil, J.C., 2002. The use of polysaccharides to target drugs to the colon. Carbohydr. Polym. 48, 219–231. https://doi.org/10.1016/S0144-8617(01)00263-6

Varum, F.J.O., Merchant, H.A., Basit, A.W., 2010. Oral modified-release formulations in motion: The relationship between gastrointestinal transit and drug absorption. Int. J. Pharm. 395, 26–36. https://doi.org/10.1016/j.ijpharm.2010.04.046

Varum, F.J.O., Merchant, H.A., Goyanes, A., Assi, P., Zboranová, V., Basit, A.W., 2014. Accelerating the dissolution of enteric coatings in the upper small intestine: Evolution of a novel PH 5.6 bicarbonate buffer system to assess drug release. Int. J. Pharm. 468, 172–177. https://doi.org/10.1016/j.ijpharm.2014.04.019

Vertzoni, M., Dressman, J., Butler, J., Hempenstall, J., Reppas, C., 2005. Simulation of fasting gastric conditions and its importance for the in vivo dissolution of lipophilic compounds. Eur. J. Pharm. Biopharm. 60, 413–417. https://doi.org/10.1016/j.ejpb.2005.03.002

Vertzoni, M., Fotaki, N., Nicolaides, E., Reppas, C., Kostewicz, E., Stippler, E., Leuner, C., Dressman, J., 2004. Dissolution media simulating the intralumenal composition of the small intestine: physiological issues and practical aspects. J. Pharm. Pharmacol. 56, 453–462. https://doi.org/10.1211/0022357022935

Villena, M.J.M., Lara-Villoslada, F., Martínez, M.A.R., Hernández, M.E.M., 2015. Development of gastro-resistant tablets for the protection and intestinal delivery of Lactobacillus fermentum CECT 5716. Int. J. Pharm. 487, 314–319. https://doi.org/10.1016/j.ijpharm.2015.03.078

Wang, J., Liu, C., Shuai, Y., Cui, X., Nie, L., 2014. Controlled release of anticancer drug using graphene oxide as a drug-binding effector in konjac glucomannan/sodium alginate hydrogels. Colloids Surfaces B Biointerfaces 113, 223–229. https://doi.org/10.1016/j.colsurfb.2013.09.009

Wang, X., Yan, Y., Lin, F., Xiong, Z., Wu, R., Zhang, R., Lu, Q., 2005. Preparation and characterization of a collagen/chitosan/heparin matrix for an implantable bioartificial liver. J. Biomater. Sci. Polym. Ed. 16, 1063–1080. https://doi.org/10.1163/1568562054798554

Williams, P.A., Phillips, G.O., 2003a. GUMS | Properties of Individual Gums, in: Caballero, B. (Ed.), Encyclopedia of Food Sciences and Nutrition. Academic Press, Oxford, pp. 2992–3001. https://doi.org/10.1016/b0-12-227055-x/00573-3

Williams, P.A., Phillips, G.O., 2003b. GUMS | Food Uses, in: Caballero, B. (Ed.), Encyclopedia of Food Sciences and Nutrition. Academic Press, Oxford, pp. 3001–3007. https://doi.org/10.1016/b0-12-227055-x/00574-5

Wong, T.W., Colombo, G., Sonvico, F., 2011. Pectin matrix as oral drug delivery vehicle for colon cancer treatment. AAPS PharmSciTech 12, 201–214. https://doi.org/10.1208/s12249-010-9564-z

Wu, Q.X., Xu, X., Xie, Q., Tong, W.Y., Chen, Y., 2016. Evaluation of chitosan hydrochloride-alginate as enteric micro-probiotic-carrier with dual protective barriers. Int. J. Biol. Macromol. 93, 665–671. https://doi.org/10.1016/j.ijbiomac.2016.09.034

Yin, H., Lu, T., Liu, L., Lu, C., 2015. Preparation, characterization and application of a novel biodegradable macromolecule: Carboxymethyl zein. Int. J. Biol. Macromol. 72, 480–486. https://doi.org/10.1016/j.ijbiomac.2014.08.025

Young, C., Dietzsch, C., Fegely, K., Rajabi-siahboomi, A.R., 2006. The Influence of a pH Dependent Pore Former on Acid Protection from Tablets Coated with an Aqueous Ethylcellulose Barrier Membrane. Coating.

Young, V., Fraser, J., 2010. A ' true enteric ', food grade , coating suitable for both nutraceutical and pharmaceutical applications. Encap Drug Deliv. A Poster Present. Morial Conv. Center, New Orleans, Louisiana, USA, Booth 2742.

Yuan, Q., Shah, J., Hein, S., Misra, R.D.K., 2010. Controlled and extended drug release behavior of chitosan-based nanoparticle carrier. Acta Biomater. 6, 1140–1148. https://doi.org/10.1016/j.actbio.2009.08.027

Zeng, H., Moroni, A., Baichwal, A.R., Goliber, P.A., Ketsela, S., Mcnamara, D.P., 2005. Controlled-release emulsion compositions. Patent number: WO2007056424.

Zhang, Y., Gong, J., Yu, H., Guo, Q., Defelice, C., Hernandez, M., Yin, Y., Wang, Q., 2014. Alginate-whey protein dry powder optimized for target delivery of essential oils to the intestine of chickens. Poult. Sci. 93, 2514–2525. https://doi.org/10.3382/ps.2013-03843

Zhu, J., Ma, Y., Yang, Q., Chow, K.Y., Lam, H.C., 2019. Method for Dry Powder Coating Capsules. Patent number: US20190099378 A1.

Ziessman, H.A., Chander, A., Clarke, J.O., Ramos, A., Wahl, R.L., 2009. The added diagnostic value of liquid gastric emptying compared with solid emptying alone. J. Nucl. Med. 50, 726–731. https://doi.org/10.2967/jnumed.108.059790